The Glutaredoxin-like Cysteine-rich family of genes, *Grxcr1* and *Grxcr2,* in stereocilia development and function

by

Matthew R. Avenarius

A dissertation submitted in partial fulfillment
of the requirements for the degree of
Doctor of Philosophy
(Human Genetics)
in The University of Michigan
2012

Doctoral committee:

Associate Professor David C. Kohrman, Chair
Professor Sally Ann Camper
Professor Yehoash Raphael
Professor Lois S. Weisman
Associate Professor Thomas M. Glaser

To: The people who supported me

ACKNOWLEDGEMENTS

First and foremost, I would like to acknowledge my parents Dixie and Dennis Avenarius for their unconditional love and support through my academic endeavors. You have made personal sacrifices that have allowed me to pursue higher education and for that I am eternally grateful. I also thank you for raising me to understand the importance of hard work and believing in myself.

I would also like to acknowledge Dr. Richard Smith, my undergraduate mentor. My experience in your lab taught me the foundations of my genetics knowledge base and fueled my excitement for science. Your positive attitude towards life and excitement about science continues to inspire me. I thank you for believing in me and providing me with opportunities I never would have imagined possible.

Lastly, I would like to acknowledge my PhD mentor, Dr. David Kohrman. I am grateful for the outstanding projects you allowed me to work on in your lab. I am appreciative for your excellent mentoring, patience, guidance, and support throughout my graduate career. Your willingness to drop everything to discuss results, review my writing, and listen and help with problems I've encountered is very much appreciated and will not be forgotten. My experience in your lab has taught me about being a thorough and rigorous scientist and the importance of

being a kind and patient mentor.

TABLE OF CONTENTS

LIST OF FIGURES

Figure

ABSTRACT

The Glutaredoxin-like Cysteine-rich family of genes, *Grxcr1* and *Grxcr2*, in stereocilia development and function

by

Matthew R. Avenarius

Chair: David C. Kohrman

Grxcr1 encodes an evolutionarily conserved cysteine-rich protein with sequence similarity to the glutaredoxin family of proteins. Mutations in this *Grxcr1* are associated with deafness and vestibular dysfunction in the pirouette mouse, a model for human deafness segregating at the *DFNB25* locus. In this thesis, I characterize spontaneous loss of function mutations in *Grxcr1* and a paralogous gene, *Grxcr2*, *in vivo*, and explore structure-function relationships between genes to provide insight into their functions in the inner ear. Mice homozygous for null alleles of *Grxcr1* exhibit abnormally thin stereocilia on the apical surface of sensory cells in the inner ear, indicating a role for this gene in the control of stereocilia dimensions. Despite defects in stereocilia maturation, sensory hair cells exhibit relatively normal mechanotransduction at early postnatal time points. The vertebrate specific paralog, *Grxcr2*, encodes a protein

that is localized to stereocilia of sensory cells in the cochlea and vestibular organs, similar to GRXCR1. Generation and analysis of a targeted mutation of mouse *Grxcr2* indicated a similar requirement for this gene in the normal maturation of stereocilia bundles and in auditory function. Mice homozygous for the *Grxcr2* mutation exhibited severe hearing loss associated with abnormal stereocilia bundle orientation and organization. Later onset hearing loss in mice homozygous for the *Grxcr2* hypomorphic allele suggests that this gene may also be required to maintain auditory function in the mature cochlea. The different stereocilia morphologies identified in *Grxcr1* and *Grxcr2* mutants and the lack of an overt vestibular phenotype in *Grxcr2* mutants, are consistent with distinct roles for these genes during inner ear development. Structure-function analysis of GRXCR1 and GRXCR2 indicated a conserved role for the N-terminus in localization of these proteins to actin filament-rich structures and for the C-terminal Cysteine-rich domain in mediating multimer formation. These studies suggest a model in which multimeric complexes of GRXCR1 and GRXCR2 play a local role to coordinate proper stereocilia development.

CHAPTER 1

Introduction

The anatomical structures and physiological basis of hearing

The ear is divided into three principal components; the outer, middle, and inner ear (Figure 1.1A). Chiefly, the outer ear acts to collect sound waves from the environment and delivers them to the middle ear by way of the external auditory canal. The vibration of sound waves against the tympanic membrane cause the bones of the middle ear (incus, malleus, and stapes) to pivot. The stapes, the medial most bone, articulates the oval window of the cochlea allowing airborn sound waves to be transduced to the fluid-filled cochlea (Figure 1.1B).

The cochlea functions by transducing sound energy into neuronal signals. This occurs as sound waves, traveling through the cochlea, physically displace stereocilia, the hair-like structures on the apical surface of sensory hair cells. The deflection of the stereocilia causes opening of transduction channels, that demonstrate putative localization to the tips of stereocilia, results in rapid hair cell depolarization and synaptic transmission to the auditory nerve (Figure 1.1C). Neuronal signals are carried to the Central Nervous System (CNS) for higher order processing that ultimately allows for the perception of auditory stimuli.

Cochlear hair cells are divided into two cell types based on morphology and function. A single row of inner hair cells and three rows of outer hair cells are arrayed along the cochlear spiral (Figure 1.1C & Figure 1.2A). Inner hair cells synapse directly to the auditory nerve (afferent) and serve as the primary sensory cell of the auditory system. This is in contrast with outer hair cells that synapse primarily with efferent neurons and function to amplify responses to sound detected by the inner hair cells. The configuration of cochlear hair cells allows for detection of sound in a frequency-specific manner. This is achieved by the tonotopic organization of the cochlea in which basal sensory cells are more responsive to high frequency sound while more apical sensory cells are more responsive to lower frequencies (Figure 1.2B).

The five vestibular organs (utricle, saccule, and three ampullae) are also housed in the inner ear and collectively cooperate to give cues about body position relative to space (Figure 1.3A). More specifically, the utricle and saccule function to detect linear acceleration whereas the three ampullae of the semicircular canals detect angular acceleration. The vestibular organs also have sensory hair cells and are found in patches rather than an organized spiral like that seen in the cochlea. Additionally, sensory hair cells of the vestibular system have apical stereocilia that morphologically share some, but not all features with those of cochlear hair cells (Figure 1.3A). Despite these differences, vestibular hair cells fundamentally respond to stimuli much like cochlear hair cells: deflection of stereocilia causes opening of transduction channels that leads to hair cell depolarization and neural responses in the vestibular nerve.

Stereocilia development

Early studies using a Scanning Electron Microscopy (SEM) approach and later analysis of deaf mice with defects in stereocilia maturation defined the developmental stages and the regulatory molecules involved in determining proper bundle morphology (Zine, 1996, Chacon-Heszele, 2009). Initially the cochlear sensory epithelium lacks the characteristic pattern of 1 row of inner hair cells and 3 rows of outer hair cells between E13 and E14 (Chacon-Heszele, 2009). At this time sensory cells exhibit a single, centrally located kinocilium, a microtubule based structure, which is surrounded by numerous microvilli (shorter actin filament based projections). From E15 – E18 a transition takes place where planar cell polarity (PCP) proteins, including VANGL2, provide directional cues to the kinocilium (discussed later) by asymmetrically localizing to the apical surfaces of sensory hair cell. This defines an apparent polarized axis that will become important for the correct localization of the kinocilium to the lateral side (portion of cell closest to lateral wall) of the apical surface of hair cells (Yamamoto, 2008).

Near birth, cochlear sensory cells exhibit a subset of microvilli that are in a semi-circular shape and that are beginning to form a graded staircase pattern, allowing them to be distinguished as nascent stereocilia (Zine, 1996). Also at this time, the cellular axis set up by VANGL2 and other PCP genes, has directed the kinocilium toward the lateral side of the apical surface of sensory cells where it eventually marks the vertices of the bundles (Chacon-Heszele, 2009). The distinct staircase configuration of the bundle is well defined and the surrounding

microvilli have begun to resorb. One week after birth the kinocilium is also resorbed, suggesting a transient developmental role for this structure in orienting the bundles.

After development, the mature bundles contain 50 to 300 stereocilia that are connected to one another by an assortment of links located along their lateral surfaces that act to form and preserve their rigid 'V' shape and staircase-like morphology (Lim, 1985, Goodyear, 2005). Molecular genetic studies have identified various facets of stereocilia development, including the maturation of stereocilia dimensions and proper bundle orientation and organization (Petit, 2009). These studies will be discussed in more detail in later sections.

Inner ear dysfunction results in deafness

The onset of hearing loss may occur throughout the lifetime of a person. Hearing loss acquired prior to the development of speech is referred to as prelingual while later onset hearing loss is described as postlingual. Patients with genetic forms of hearing loss may present with nonsyndromic hearing loss, which indicates that hearing impairment is the sole clinical manifestation, while others present with syndromic hearing loss referring to hearing loss along with other clinical phenotypes. The hearing pathology may be due to defects in conducting sound waves into the inner ear (conductive hearing loss) or to defects of the sensory or neural cells (sensorineural hearing loss)

The degree of hearing loss patients experience can range from mild to profound. A multitude of etiological factors may contribute to the severity of hearing loss including environmental factors such as age-related effects,

ototoxicity due to certain pharmacologic agents, noise exposure, or inherited genetic lesion(s) that either cause or increase the susceptibility to hearing loss. To distinguish genetic cases from non-genetic cases it is important to obtain a comprehensive family history and, ideally, pursue molecular genetic testing. Retrospective analyses has identified congenital deafness as the most prevalent sensory deficit, affecting nearly 1 in every 1,000-2,000 live births with approximately 50% of the cases due to genetic aberrations (Kochhar, 2007).

Several modes of inheritance have been observed in pedigrees segregating hearing loss, including autosomal dominant, autosomal recessive, X-linked, mitochondrial, and complex inheritance. After initial mapping studies localized mutant deafness genes to many different locations in the human genome, the heterogeneity of human hearing loss became apparent (Dror, 2009). Auditory geneticists organized the loci by designating the first dominant locus as 'DFNA1' and assigning each newly identified dominant locus a successive number (DFNA2, DFNA3, DFNA4, etc…). A similar designation is used for recessive loci, only 'DFNB' is used as the prefix. Information regarding these loci, along with the nearly 70 deafness-causing genes that have been identified to date, are managed on the Hereditary Hearing Loss website: http://hereditaryhearingloss.org/.

In nearly all cases human deafness-causing genes have been identified through traditional linkage analysis of large families. In the case of recessive deafness, consanguineous pedigrees segregating regions of homozygosity by descent have often been identified and mutation screening of candidate genes

within this region has uncovered the genetic lesion underlying hearing loss in the families. In many cases, identification of deafness-causing genes in mouse has facilitated human geneticists through screening orthologous genes in their candidate intervals (Mitchem, 2002, Naz, 2002).

Genetic studies have demonstrated multiple examples of syndromic and non-syndromic deafness that are associated with allelic heterogeneity, i.e. alternative mutations in the same gene. For example, different mutations in *CDH23* have been associated either with patients segregating deafness at the DFNB12 locus or with the pleiotropic effects in the visual and auditory system observed in patients diagnosed with Usher Syndrome 1D (USH1D) (Bork, 2001). The cases of allelic heterogeneity between Usher syndrome and nonsyndromic deafness have demonstrated that patients with Usher syndrome segregate nonsense or frameshift mutations while nonsyndromic deafness patients segregate missense mutations. As *Cdh23* is expressed in both sensory hair cells in the inner ear and in photoreceptors in the retina (Lagziel, 2009), this appears to reflect tissue specific splicing or a greater tolerance of hypomorphic mutations in photoreceptors.

Utilizing the mouse as a model organism to study deafness and stereocilia development

The mouse is a highly relevant organism to study the genetics of auditory development and furthermore serves as an excellent model of human hearing pathologies. The cochlear and vestibular organs in the two species exhibit the remarkably organized arrangement of sensory neuroepithelium typical of

mammals. Although the number of turns in the spiral cochlea differs between the two species (2.75 in human, ~ 1.5 in mouse), both exhibit the conserved mammalian organization of the sensory neuroepithelium of the cochlea, with a single row of inner hair cells and three rows of outer hair cell that extend along the entire length of the cochlea (Keen, 1939). Both species also have sensory hair cells with apical stereocilia, the highly specialized structure required for mechanosensory transduction.

The high relative sequence conservation of genes between humans and mouse makes this organism appealing in a genetic context. The existence of inbred mouse strains with isogenic backgrounds is a strong advantage of using the mouse as a model system. This nearly eliminates the possibility of experimental variability attributed to genetic background. In addition, the ability to rear mice in defined conditions permits control of potential environmental components that may impact auditory function. The auditory physiology of many inbred strains are also well characterized and provides important baseline information about hearing abilities.

The lack of high-resolution technologies to image the human ear, especially during its prenatal developmental state, hampers evaluation of inner ear pathology associated with particular mutant genes. The auditory research community therefore relies heavily on mouse models to understand the pathological outcome of deafness mutations. The ability to target specific genes and to custom design alleles (e.g., deletions, knock-in of orthologous human mutations, and temporally or spatially conditional mutations) is possible in mouse

and transgenesis remains an extremely valued approach to study the effect of a gene(s) on biological processes. The success of targeting genes in the mouse, in part, has been facilitated by the availability of the fully sequenced and annotated mouse genome.

Despite the similarities between the mouse and human inner ear the correlation of mutation and phenotype is not always translatable. It is sometimes the case that vestibular phenotypes are observed in mouse models of deafness and not always in patients with conserved mutations (Mitchem, 2002, Naz, 2002). Reciprocally, retinal phenotypes observed in patients with Usher syndrome, a syndromic form of hearing loss, are often absent in mouse models (Geller, 2009). These differences likely reflect the functional ability of species to compensate for a pathogenic mutation in a cell-type specific manner.

The molecular genetics of stereocilia development

Many of the studies aimed at determining the genetic mechanisms that underlie hearing and deafness have been performed in mouse. Characterization of spontaneously arising and targeted mutant alleles resulting in inner ear dysfunction have revealed defects in sensory hair cells of the auditory and vestibular system and more specifically have been associated with defects of the stereocilia on the apical surfaces of these cells. Collectively the identification, localization, and functional analysis of deafness-causing genes have distinguished three biological processes required for the proper development of stereocilia: organization, orientation, and dimension. Genes implicated in stereocilia development encode a diverse range of proteins, including myosin

motors, actin binding proteins, and protein with putative roles in metabolic processes (Probst, 1998, Zheng, 2000, Du, 2008).

Stereocilia bundle organization

Mouse models of genes associated with Usher Syndrome (deafness and retinitis pigmentosa) such as *Cdh23*, *Pcdh15*, *Myo7a*, *Ush1C*, *Sans,* and *Vlgr1* all exhibit early defects in stereocilia bundle organization (Lefevre, 2008). The cohesive, organized nature of the bundle appears to depend upon an assortment of links that form at the base (ankle links), transiently throughout the lateral surface (top connectors), and at the tips (tip links) of stereocilia. Developmentally, ankle links and top connectors counteract the mechanical forces that displace the stereocilia bundles by collectively holding together stereocilia bundles and reinforcing the structure to maintain bundle integrity (Muller, 2008). Tip links are also associated with maintaining stereocilia structure but are also thought to associate and modulate the mechanotransduction channel complex at the tips of stereocilia (Pickles, 1984, Pickles, 1989, Schwander, 2009). The majority of Usher genes encode proteins that directly comprise the links themselves such as CDH23 and PCDH15 or proteins that interact through intracellular contacts with the links such as USH1C and MYOVIIA (Lefevre, 2008).

Significant effort has been put forth to understand the mechanism by which these genes function to build cohesive stereocilia bundles. One important set of experiments defined the localization of Usher proteins throughout the stereocilia bundles early on in development (E16.5) (Boeda, 2002, Grillet, 2009).

During the first week of postnatal development the Usher gene products seem to preferentially localize towards the tips of the stereocilia (Boeda, 2002, Grillet, 2009). In most cases Usher proteins persist in the adult stereocilia where they complex at the tip links or upper tip link densities (Grillet, 2009, Kazmierczak, 2007).

Strong evidence points toward CDH23 and PCDH15, two Usher I proteins, as the molecular constituents of stereocilia links including the tip links. Detailed immunolocalization studies of CDH23 and PCDH15 demonstrated these proteins along the length of stereocilia during late embryogenesis and early postnatal time points but specifically at the tips of stereocilia at the onset of hearing (Kazmierczak, 2007, Lagziel, 2005, Michel, 2005, Rzadzinska, 2005, Siemens, 2004). Several *in vivo* and *in vitro* experiments established the direct interaction of these proteins through their extracellular domains in a Ca^{2+} dependent manner. Further studies utilizing a mouse mutant with a point mutation (E737V) in *Cdh23* demonstrated normal development of bundle morphology but had defects in mechanotransduction and progressive hair cell loss associated with degeneration of the tip links (Schwander, 2009). In contrast, waltzer and Ames waltzer mice, with null mutations in *Cdh23* and *Pcdh15* respectively, demonstrated early stereocilia organization defects consistent with early disruption of stereocilia links. The differences in phenotypic onset between these mouse models illuminate the importance of early developmental molecules in later maintenance processes.

Studies using an assortment of experimental approaches including Yeast-two-hybrid (Y2H), co-localization, co-immunoprecipitation, and glutathione S-transferase (GST) pull downs have identified an Usher protein interaction complex. Broadly, the interpretation of these interactions suggests a model in which cytoskeletal adaptor proteins (Harmonin, SANS, and Myosin VIIa) localize to densities along the stereocilia and complex with the actin core of stereocilia to anchor PCDH15 and CDH23, the primary molecules that comprise stereocilia links (Senften, 2006; Weil, 2003; Boeda, 2002; Adato, 2005; Kazmierczak, 2007). The intact Usher complex allows for the proper establishment of linkages between stereocilia and therefore cohesive and organized stereocilia bundles. In the context of tip links, the Usher complex appears to play an additional role in maintaining tension on the mechanotransduction apparatus at the tips of stereocilia.

Stereocilia bundle orientation

Normal auditory function relies on the establishment of proper stereocilia orientation to permit uniform stimulation of the bundles throughout the length of the cochlea. The precise placement of stereocilia vertices pointing towards the periphery of the cochlear spiral is achieved in part by early signals from the planar cell polarity (PCP) pathways (Chacon-Heszele, 2009). These pathways operate in many tissues to regulate uniform, 2-dimensional positioning of epithelial cells and associated organelles (Fanto, 2004). Previous studies have identified the essential PCP genes *Vangl2, Scrb1,* and *Celsr1* as critical regulators of bundle orientation. Mice carrying mutations in these genes exhibit

deafness and vestibular dysfunction associated with randomly oriented bundles. In addition, *Vangl2* and *Scrb1* mouse mutants show shortened cochleae, implicating these genes in a process known as convergent extension to regulate the orderly migration of epithelial cells of the growing cochlear duct (Montcouquiol, 2003; Curtin, 2003).

Study of several mouse models of Bardet-Biedl Syndrome (Bbs) and a recent mouse model with a mutation in *Ift88* have uncovered a second but closely related group of mutants exhibiting similar stereocilia orientation defects (Jones, 2008; Ross, 2005). In the case of mice with mutations in *Bbs* genes, the kinocilium shows apparent dissociation from the stereocilia bundles, whereas the conditional null allele of *Ift88* demonstrates complete loss of the kinocilium along with misoriented hair bundles, directly implicating the kinocilium in bundle orientation.

These mice show overt defects in stereocilia orientation much like that observed in the core PCP mutants (*Vangl2*, *Scrb1*, and *Celsr1*). However, the failure of the kinocilium to track with the bundle or complete absence of this structure points towards a kinociliary defects rather than appropriate definition of the cellular axis. Furthermore, these mouse mutants strongly suggest a requirement for the kinocilium in receiving and responding to PCP cues that result in the directed movement of the kinocilia and associated bundles into the proper orientation. This is thought to occur through the dynamic rearrangement of the cytoskeleton, with respect to the kinocilium, exerted by membrane-associated PCP complexes (Chacon-Heszele, 2009).

There has also been evidence for the Usher family of proteins, traditionally thought to play a developmental role in stereocilia organization, in impacting the orientation of bundles. Mouse models of Usher syndrome also show defects in stereocilia orientation at late embryonic ages (E18.5) consistent with a role for Usher proteins in the proper orientation of stereocilia bundles (Lefevre, 2008). The orientation defects in mouse models of Usher syndrome indicate that links between stereocilia that are established by the Usher proteins are required for the successful lateral movement and orientation of stereocilia bundles.

Stereocilia bundle dimensions

Another critical aspect of stereocilia development is regulation of proper stereocilia dimensions. Tilney and colleagues provided elegant descriptions of the early formation of stereocilia through analysis of sectioned chick cochleae, indicating growth occurred through alternating increases in length and diameter (Tilney, 1986; Tilney, 1986; Tilney, 1986). This group also provided evidence that an increase in stereocilia diameter is associated with the addition of actin filaments to the core of the stereocilia (Tilney, 1986). Similar results were shown in the hamster, although elongation and diameter appeared to occur simultaneously (Kaltenbach, 1994).

More recent studies involving transfection of actin-GFP into sensory cells in explant cultures indicated addition of actin monomers at the tips of stereocilia (Schneider, 2002), the location of the barbed ends of actin filaments and the typically preferred site for filament growth (Tilney, 1986; Tilney, 1986). The actin addition rate appears to be highest for the tallest stereocilia and lower in

stereocilia in shorter rows (Rzadzinska, 2005). These studies are consistent with the addition of actin monomers at the tips of stereocilia as the driver of stereocilia elongation

The characterization of deaf mouse mutants such as deaf-jerker, shaker 2, whirler, and pirouette defined a subset of genes involved in establishing stereocilia dimensions. The short and thin stereocilia observed in deaf-jerker mice, for the first time, associated the functional role of Espin in establishing stereocilia dimensions (Zheng, 2000). The ability of Espins to facilitate the bundling of actin filaments is consistent with the notion that actin filaments are added to stereocilia cores to achieve proper diameter. Furthermore, a more recent study demonstrates a role of espin in lengthening the stereocilia bundle through a proximal-to-distal direction that is consistent with a barbed-end elongation mechanism in a concentration dependent manner (Sekerkova, 2011).

Analysis of two other deaf strains of mutant mice, shaker-2 and whirler have led to the identification of additional genes required for normal maturation of stereocilia length. Mutations of *Myo15a* in shaker2 mice and *whirlin* in whirler mice result in remarkably similar, short stereocilia in the cochlea and in vestibular organs. Molecular studies confirmed that MYO15A, an unconventional myosin motor protein, transports whirlin to the tips of stereocilia, where the two proteins are presumably required for barbed-end addition of actin monomers to the elongating filament core.

Pirouette is a mouse model for nonsyndromic hearing loss associated with the DFNB25 locus

The pirouette mouse (*pi*) is a spontaneously arising mouse mutant that was discovered within a colony of C3H mice in 1943. Pirouette mice are profoundly deaf and exhibit circling behaviors and hyperactivity consistent with vestibular defects (Dickie, 1946). Traits exhibited by *pi* mice demonstrate a recessive mode of inheritance and were linked to a single locus on chromosome 5 (Lane, 1967). Histological analysis determined that pirouette mice exhibit overall normal inner ear development with progressive sensory cell degeneration, a common finding in many deaf mouse strains (Deol, 1956).

Since the origin of the original pirouette allele, five additional alleles have been genetically characterized, all of which are likely to be null in nature (Erven, 2002; Odeh, 2004; Odeh, 2010; Avenarius M, 2011). Evaluation of *pi* inner ear morphology by SEM at early postnatal time points indicated a qualitative reduction in stereocilia diameter in cochlear and vestibular hair cells that was associated with early profound hearing loss and vestibular dysfunction. Later experiments by Erven and colleagues made precise measurements at several developmental time points to quantitatively demonstrate decreased stereocilia diameter in inner and outer hair cells (Erven, 2002).

The inner ear phenotype in affected pirouette mice was recently associated with mutations in *Glutaredoxin-like cysteine rich protein 1* (*Grxcr1)* (Odeh, 2010). Experiments interrogating the original *pi* locus identified a large 700 kb genomic inversion, the centromeric breakpoint of which is within the first

intron of *Grxcr1,* effectively preventing production of a normal transcript. The other *pi* alleles were found to have similar transcriptional defects as in *Grxcr1*, due either to transgene insertions or genomic deletions.

Grxcr1 is an evolutionarily conserved gene with homologs present in a wide range of vertebrate and invertebrate metazoan organisms, as well as in plants. The central domain of the protein encoded by *Grxcr1* shows sequence similarity to the glutaredoxin family of proteins. Classic glutaredoxins function as enzymes that act to reduce oxidized cysteines of cellular proteins using glutathione as an electron donor. The N-terminal domain of GRXCR1 does not show significant sequence similarity to other known proteins, while the C-terminus contains two groups of four cysteine residues arranged in a putative zinc finger configuration.

Expression of *Grxcr1* was specifically detected in the inner ear by RT-PCR and in sensory hair cells as determined by *in situ* hybridization (Odeh, 2010). Using a specific, affinity-purified antibody, GRXCR1 protein was detected along the entire length of stereocilia in the cochlea at early postnatal time points (P1-P5) as well as in the mature, adult ear. GRXCR1 was also localized within the short apical microvilli of maturing hair cells in the early postnatal cochlea (Odeh, 2010).

Ectopic expression of *Grxcr1* in heterologous cell types (COS-7 fibroblasts, CL4 epithelial cells, and cultured explants) demonstrated localization of GFP-tagged hybrid proteins to actin-filament-rich structures such as dorsal filopodia and apical microvilli, as well as to stereocilia in sensory hair cells. In

non-sensory cells of cultured explants, *Grxcr1* over-expression induced substantial elongation of actin-rich microvilli, apparently independent of a direct actin interaction (Odeh, 2010; Avenarius, 2011). The observation that GRXCR1 localizes to actin-filament rich structures in a variety of cell types and has the ability to modify the lengths of these structures suggests GRXCR1 influences the dynamics of actin polymerization.

In parallel with the genetic characterization of the pirouette mouse, Odeh and colleagues pursued a collaborative effort to screen the human GRXCR1 ortholog located on chromosome 4p in patients segregating recessive, congenital deafness. This study resulted in the identification of three novel variants segregating in two pedigrees. An affected member in the first family (Family A) harbors two missense variants identified in the homozygous state: p.G64S (c.190G>A) located in the N-terminal coding region and p.F153V (c.457T>G), located in the glutaredoxin-related, central domain of GRXCR1 (Odeh, 2010). An affected member of the second family (Family B) harbors the missense variant p.P38L (c.113C>T), located in the N-terminus, also identified in the homozygous state (Odeh, 2010). Concurrently, Schraders and colleagues utilized homozygosity mapping and subsequent candidate gene screening to identify mutations in *GRXCR1* in an additional four pedigrees segregating autosomal recessive deafness. The identified mutations include two splice site mutations, a missense mutation, and a nonsense mutation (Schraders, 2010). Collectively these studies have successfully associated mutations in the human gene

GRXCR1 with autosomal recessive, nonsyndromic deafness at the *DFNB25* locus.

A paralogous gene, *Grxcr2*, as a candidate for inner ear development and function

A second glutaredoxin-like cysteine rich family member, *Grxcr2*, is located on mouse chromosome 18 in a region paralogous to the *Grxcr1* locus. *Grxcr2* homologs, unlike *Grxcr1*, are found only in vertebrate genomes. GRXCR1 and GRXCR2 exhibit approximately 30% amino acid identity with absolute conservation of the bipartite cysteine motif ($CX_2CX_7CX_2CX_{20}CX_2CX_7C$). A considerable degree of sequence similarity between these proteins is also observed at the N termini, while sequence comparisons across species shows a more divergent central domain between the two paralogs.

The work conducted in my doctoral research is aimed at characterizing genes involved in auditory development and function. The central hypothesis of the first aim of my thesis is that *Grxcr2* is required for normal stereocilia development and normal auditory and vestibular function. A targeted mutation in the mouse *Grxcr2* gene was generated and characterized to test the requirement for its function in inner ear development. Mice homozygous for the *Grxcr2* mutation exhibit significantly elevated hearing threshold shifts, although they retain behavioral characteristics consistent with normal vestibular function. The stereocilia orientation and organization defects observed in *Grxcr2* mutants are morphologically distinct from those observed in pirouette mice, suggesting that

while both paralogs are required for auditory function each have a biochemically distinct role.

In a second aim of my thesis, I conducted additional studies to characterize an additional mutant allele (*pi*^{4J}) of *Grxcr1* that harbors a ~200 kB deletion similar to that observed in the *pi*^{2J} and *pi*^{3J} alleles. Morphological analysis of *pi*^{4J} demonstrates the hallmark reduction in stereocilia diameter much like that seen in other *pi* alleles. Collaborative efforts demonstrated that, despite morphological defects, stereocilia bundles in affected *pi* mice are capable of relatively normal mechanotransduction at early postnatal time points.

My final research aim was to understand the biochemical role of GRXCR1 and GRXCR2 in stereocilia development and maintenance. In these experiments I used a structure-function approach to define the domains of GRXCR1 and GRXCR2 that are necessary and sufficient for localization to actin-rich structures, dorsal filopodia of COS-7 cells or microvilli of CL4 or nonsensory cells. I also identified putative homodimerization and heterodimerization interactions of GRXCR1 and GRXCR2 that are mediated by the C-terminal cysteine-rich motif. Current biochemical studies focusing on GRXCR2 are being conducted to determine the role of these proteins in actin binding, putative glutaredoxin activity, chaperone activity, and zinc binding activity. Correlation of these individual biochemical properties with effects of the proteins in sensory cells will provide important information about the biological role of GRXCR1 and GRXCR2 in stereocilia development.

CHAPTER 2

Expression and functional analysis of sensory hair cells in *Grxcr1* deafness mutants

Matthew R. Avenarius[1,2], Gwenaëlle S. G. Géléoc[4], Kristina L. Hunker[1], Tzy Wen Gong[1], Leona H. Gagnon[3], Kenneth R. Johnson[3], and David C. Kohrman[1,2]

[1]Department of Otolaryngology/Kresge Hearing Research Institute and [2]Department of Human Genetics, University of Michigan Medical School, Ann Arbor, Michigan 48109, USA; [3]The Jackson Laboratory, Bar Harbor, Maine 04609, USA; [4]Departments of Neuroscience and Otolaryngology, University of Virginia, Charlottesville, Virginia 22908, USA

Avenarius Contribution: Southern blot (Figure 2.2 B), PCR assay (Figure 2.2 C), SEM analysis (Figure 2.3), GRXCR1/Acetylated α-tubulin immunostaining (Figure 2.4)

ABSTRACT

Mutations in *Grxcr1* are responsible for hearing loss and vestibular dysfunction in mice and in humans and are associated with defects in stereocilia bundle development in the inner ear. In the current study, we use genetic and molecular analyses to identify a new spontaneous recessive allele (pi^{4J}) of *Grxcr1*. The pi^{4J} allele contains a large genomic deletion that includes exon 1 andfails to express full-length *Grxcr1* transcript or protein. The inner ear dysfunction exhibited by mice homozygous for this allele is associated with morphologically thin stereocilia at early postnatal ages, similar to other mutant *Grxcr1* alleles. We also demonstrate that, despite lack of wild type Grxcr1 expression, sensory cells from a null mutant exhibit relatively normal mechanotransduction at early postnatal time points. Mechanical weakness of stereocilia bundles together with sensory cell loss are likely to underlie the loss of auditory responses to sound stimuli.

INTRODUCTION

Characterization of mutant mouse models with hearing loss and vestibular defects has provided insight into genes that are required for development, maturation and maintenance of sensory function in the inner ear (Petit, 2009). These genes are expressed in a variety of sensory and nonsensory cell types and encode proteins with a wide range of known or predicted biochemical activities. Many of the proteins are required for normal development of specialized structures known as stereocilia that are located on the apical surface of sensory cells in the cochlea and in vestibular organs. Bundles of 50 to 300 stereocilia are organized in

a staircase arrangement, with multiple fine connections along their lengths that link neighboring stereocilia with one another (Goodyear, 2005). The core of each stereocilium is composed of tightly packed bundles of uniformly polarized actin filaments (Flock, 1977). Deflection of bundles in response to auditory or vestibular stimuli, and the associated gating of cation channels in the plasma membrane near the tip of individual stereocilium, plays an essential role in mechanotransduction and subsequent sensory perception (Gillespie, 2009). Mutations in genes required for inner ear development, including those necessary for stereocilia maturation and function, also underlie many forms of syndromic and nonsyndromic hearing loss in humans (Dror, 2009).

Null mutations in *Grxcr1* result in vestibular dysfunction and profound deafness in the mouse pirouette (*pi*) strain (Odeh, 2010). Similarly, mutations in human *GRXCR1* are associated with early onset, moderate to profound hearing loss as well as vestibular abnormalities (Schraders, 2010; Odeh, 2010). *Grxcr1* is expressed in sensory hair cells in the inner ear and the GRXCR1 protein is localized to stereocilia in the cochlea and vestibular sensory organs of normal mice in the early postnatal period and at maturity (Odeh, 2010). Cochlear stereocilia in early postnatal *pi* mutants fail to reach a normal diameter during development and become disorganized during the second postnatal week, indicating that *Grxcr1* is necessary for processes that regulate stereocilia dimensions and organization during maturation (Beyer, 2000;Odeh, 2004;Erven, 2002). Similar developmental defects in stereocilia have also been observed in vestibular organs of *Grxcr1* mutant mice (Erven, 2002). GRXCR1 expressed in cultured cell lines and in inner

ear tissue explants localizes to actin filament-rich structures at the cell periphery or apical surface and depending upon cell type, induces structures with greater actin filament content and/or increased lengths (Odeh, 2010).

In the current study, we present a new spontaneous mouse mutant that exhibits profound hearing loss and behavioral defects indicative of vestibular dysfunction. These phenotypes are due to a large deletion that includes exon 1 of *Grxcr1* and results in a null allele. We used this mutant to further investigate the effects of loss of *Grxcr1* function on stereocilia development and on *Grxcr1* expression. In addition, we use a similar null mutant strain to evaluate the effects of loss of function on sensory cell mechanotransduction at early postnatal time points.

MATERIALS AND METHODS

Mice. The original *pi* mutation arose spontaneously on a C3H strain of mice (Woolley, 1945) and was maintained by repeated backcrossing to C57BL/6J mice. The resulting congenic strain (B6.C3-*Grxcr1*^{piJ}; referred to hereafter as *pi*) was obtained from the cryopreservation laboratory at The Jackson Laboratory (Bar Harbor, ME) and maintained by mating heterozygous *pi* mice with homozygous *pi* mice. A new *pi* mutation (*nm3050*) arose spontaneously on a mixed NZB/BlNJ and NZW/LacJ genetic background at The Jackson Laboratory. This line was also backcrossed for over 10 generations to C57BL/6J mice, and is now referred to as B6.Cg-*Grxcr1*^{pi4J}. Each of the *Grxcr1* mutant strains was maintained by homozygote to heterozygote matings. C57BL/6J mice were obtained from The Jackson Laboratory (Bar Harbor, ME)

and were maintained by brother-sister matings. All mice were cared for in accordance with protocol number 08234 approved by the University of Michigan.

Linkage and molecular analysis of a new Grxcr1 mutant allele. A genome-wide linkage analysis was performed on genomic DNA from 55 F2 progeny of a (B6.Cg-*Grxcr1*^{pi4J} X CAST-EiJ) F1 intercross according to published methods (Johnson, 2003). Total RNA from cochleae was reverse transcribed with random hexamers, then amplified with either *Grxcr1* primers (exon 1: 5'-CTGTGGCAAGGGGGATGAACT-3'; exon 4: 5'-TTATCCTTTGTTTAATGAAATGAGGCTTT-3') or *Gapdh* primers (5'-GCATGGCCTTCCGTGTTCCTAC-3'; 5'-CCTGTTATTATGGGGGTCTGGGAT-3'). For Southern blot analysis, genomic DNA derived from control +/*pi*^{4J} and affected mutant *pi*^{4J}/*pi*^{4J} mice were digested with one of three restriction enzymes, separated by agarose gel electrophoresis, stained with ethidium bromide (bottom panel) and transferred to Zetaprobe membrane (Biorad, Hercules, CA). The Southern membrane was hybridized with a radiolabeled DNA fragment encompassing exon 1 of *Grxcr1*, washed stringently and exposed to X-ray film.

GRXCR1 antibodies and tissue immunocytochemistry. Peptides designed from the primary sequence of mouse GRXCR1 (N-NEQEKDQDNLLVLART-C) were covalently linked to KLH and injected into New Zealand rabbits (Proteintech Group, Inc.; Chicago, IL). Antiserum was purified using an affinity column containing full-length recombinant GRXCR1, using previously described methods (Bartles, 1996). Cochleae were dissected and

fixed in 4% paraformaldehyde for 0.5 – 1 hour, washed in PBS, permeabilized for 10 min in 0.2 % Triton X-100 and pre-treated with 5% goat serum in PBS. Samples were then treated with anti-GRXCR1 antiserum and the monoclonal antibody to acetylated α-tubulin (Sigma Cat # T7451), washed in PBS, and incubated with Alexa 555 conjugated anti-mouse or Alexa 488-conjugated anti-rabbit secondary antibodies (Molecular Probes). After washing in PBS, samples were mounted in Prolong Gold (Molecular Probes) and analyzed by a Leica SPX5 2-photon laser-scanning confocal microscope. Images were processed using Adobe Photoshop.

Scanning electron microscopy (SEM). Inner ear tissue was dissected in PBS from mice at postnatal day 7 and fixed in 2.5 % glutaraldehyde and 0.15 cacodylate buffer. Cochleae were processed using the OTOTO method as previously described (Osborne, 1991; Beyer, 2000), and were analyzed using a Amray 1910 scanning electron microscope. Two homozygous affected and two heterozygous control mice were analyzed.

ABR. Anesthetized mice were placed in a sound proof chamber for auditory brain stem recording procedure. Electrodes were inserted sub-dermal at the vertex and ventrolaterally to each ear. Presentation of stimuli, ABR physiological recordings, and data acquisition were coordinated by the computerized Intelligent Hearing Systems (HIS; Miami, FL, USA). Acoustic stimuli, including clicks, and 8, 16, and 32 kHz tone-bursts were generated by two high frequency transducers and relayed into the animal's ear. The electrophysiological responses were averaged and thresholds were obtained for

each stimulus by reducing the sound pressure level (SPL) at 10 dB steps or until the lowest dB level at which an ABR signal could be recognized (Johnson, 2003).

Electrophysiology. Utricles were dissected from *+/pi^{4J}* and *pi^{4J}/pi^{4J}* mice between P0 and P7, then mounted and cultured as previously described (Geleoc, 2003). Hair cells were viewed from the apical surface using an upright microscope (Axioskop FS, Zeiss, Oberkochen, Germany) equipped with a 63X water immersion objective with differential interference contrast optics. Mechanical stimuli to stereocilia bundles were transmitted using a stiff glass probe mounted on a one-dimensional piezoelectric bimorph element and hair cell currents were recorded under whole-cell, voltage-clamp at room temperature (22-24 °C) using an Axopatch multiclamp 700A (Axon Instruments, Foster City, CA) as detailed previously (Geleoc, 2003). Results are presented as means ± S.D and a second order Boltzmann equation of the form I = Imax × [1 + ea2(d2–x)(1 + ea1(d1–x))]–1 was used to fit current-displacement relationships.

RESULTS

A new *Grxcr1^{pi}* mutant allele. Recently, we identified a mouse strain (*nm3050*) that exhibited circling and head shaking behaviors, which are often indicative of dysfunction in vestibular organs of the inner ear. Mice with these defects exhibited a reduced startle response to sound, suggesting that cochlear function was also abnormal. To further evaluate hearing, we determined auditory brainstem responses (ABR), a measure of the synchronous output of the auditory system in response to sound. At 6 weeks of age, *nm3050* mice with behavioral defects and reduced startle responses also required a large increase in sound

levels to produce threshold ABRs in response to a range of pure tones (8-32 kHZ) and to click stimuli, relative to littermate controls (Fig. 1).

The inner ear phenotypes resulted from a spontaneous recessive mutation on a mixed NZB/BlNJ and NZW/LacJ genetic background. The mutation was genetically mapped to chromosome 5 between markers *D5Mit182* and *D5Mit355*, a region coincident with the map position of *Grxcr1*. In order to evaluate allelism, we performed a complementation test by mating an *nm3050* heterozygous female to a male carrying a known homozygous null mutation of *Grxcr1* (pi^{3J}/pi^{3J}) (Odeh, 2010). Of 22 total progeny, 13 exhibited circling and head shaking behaviors and lacked a startle reflex, consistent with non-complementation of the two mutations. Together with the coincident map positions, this indicated allelism of *nm3050* and *pi* (Odeh, 2010). The new pi allele is designated pi^{4J} and is the sixth allele of pirouette to be described.

Molecular analysis of the *Grxcr1*^{pi4J} allele. RT-PCR analysis indicated that affected pi^{4J}/pi^{4J} mice do not express full-length transcripts of *Grxcr1* in the cochlea (Fig. 2A). Southern blot analysis of genomic DNA indicated that the pi^{4J}/pi^{4J} chromosome carries a deletion that includes exon 1 (Fig. 2B). Genomic PCR analysis indicated the centromeric edge of the deletion is located approximately 120 kb upstream of exon 1 and the telomeric edge is within intron 1, near the 5' end of exon 2 (Figure 2C). These deletion borders are very similar to those previously defined for null *Grxcr1* alleles in independently arising pi^{2J} and pi^{3J} mutant (Odeh, 2010) and again suggests nonhomologous recombination between large arrays of L1 repeat elements near the centromeric and telomeric

deletion breakpoints as a likely deletion mechanism.

Cochlear and vestibular pathology in *Grxcr1* mutants. We and others have previously identified early stereocilia pathology in the sensory cells of pirouette mutant alleles (Beyer, 2000;Odeh, 2004;Erven, 2002). Sensory and supporting cells in the cochleae of pi^{4J}/pi^{4J} mice at P4 were arranged in a uniform mosaic pattern like that observed in control $+/pi^{4J}$ mice (Fig. 3A,B). Developing stereocilia bundles were present on the apical surfaces of inner and outer hair cells in the mutant mice and were arranged in bundles shaped similarly to bundles in control mice. The bundles on inner hair cells in the mutants (Fig. 3D), however, were less densely packed than those in controls (Fig. 3C) and individual stereocilia were notably thinner. Stereocilia on outer hair cells in mutants (Fig. 3B) also appeared thinner than those on control hair cells (Fig. 3A).

Expression pattern of GRXCR1 in developing stereocilia bundles. In earlier expression studies, we observed localization of GRXCR1 to stereocilia bundles by P1 and further note GRXCR1 immunoreactivity in kinocilia, a microtubule-based structure that lacks actin filaments (Odeh, 2010). The kinocilia is present on the apical surfaces of developing sensory cells in the cochlea and in both developing and mature vestibular sensory cells. This reactivity, while significantly diminished in inner ear tissue from a *Grxcr1* mutant, was not completely abolished. The *Grxcr1* mutant analyzed in the previous study (pi^{tde}), although lacking expression of a full-length *Grxcr1* transcript, does produce low levels of a short transcript that is capable of encoding the N-terminal portion of the protein (Odeh, 2010). Since this N-terminal region contains the

epitope used for production of the anti-GRXCR1 antisera, the low level of immunoreactivity observed in kinocilia may have derived from such a truncated protein. We reexamined this reactivity in cochleae from *pi*^{4J}/*pi*^{4J} mice, which lack exon 1 and therefore do not encode the epitope to the GRXCR1 antibody. In surface preparations of cochleae from +/*pi*^{4J} control mice, immunoreactivity with the anti-GRXCR1 antisera was observed kinocilia that were stained with an antibody against acetylated α-tubulin (Fig. 4A-C). While immunoreactivity with the anti-GRXCR1 antisera was absent from stereocilia bundles of cochleae from *pi*^{4J}/*pi*^{4J} mice, co-localization with α-tubulin-positive kinocilia was still observed (Fig. 4D-F). This result, together with the inconsistent staining in control mice, indicates that this signal is non-specific and does not represent localization of GRXCR1 protein in kinocilia.

Mechanotransduction in *Grxcr1* mutant hair cells. We have demonstrated profound hearing loss in all known *Grxcr1* mutant alleles, including the *pi*^{4J}/*pi*^{4J} mice described here. Although progressive loss of sensory cells in the cochleae of *Grxcr1* mutants may underlie loss of function at later postnatal time points (Odeh, 2004), the functional status of the altered stereocilia bundles at earlier time points in these mutants has not been evaluated. In order to determine the mechanotransduction ability of mutant bundles, we measured receptor potentials in response to step deflections of bundles from sensory tissue explanted from early postnatal *pi* mutants and control mice. Bundles of utricular sensory cells from pi mutants responded to deflections with transduction currents very similar to those of control wild type cells (Fig. 6). Notably, attempts to

measure transduction currents in sensory cells from *pi* mutants older than P5 were unsuccessful due to mechanical breakage of the stereocilia bundles by the stimulus pipette. This presumably resulted from an increase in fragility of the thin stereocilia in these null mutants.

DISCUSSION

The current study indicates that *pi*^{4J} represents a new recessive mutant allele of *Grxcr1*. This conclusion is based upon four lines of evidence. First, this mutation exhibits profound hearing loss and vestibular dysfunction associated with morphological defects in stereocilia that are typical of other known *Grxcr1* mutants at the *pi* locus (Odeh, 2010). Second, the mutation genetically maps to central chromosome 5 coincident with the *Grxcr1* locus. Third, the mutation fails to complement inner ear dysfunction in crosses with another known *Grxcr1* mutation. Finally, we have identified a large deletion of approximately 175 kb that spans the region upstream of *Grxcr1* exon 1 and most of intron 1 of the gene. This deletion is very similar to that found in two other independent *Grxcr1* mutant alleles (*pi*^{4J} and *pi*^{4J}) and likely arose through a common nonhomologous recombination mechanism. As in the previously identified deletion alleles, *pi*^{4J} fails to express full-length transcripts and lacks immunoreactivity to GRXCR1 protein in stereocilia. Analysis of the new *pi*^{4J} mutant strain also indicates that GRXCR1 is unlikely to be present in microtubule-associated kinocilia. Finally, we also demonstrate that, despite lack of wild type *Grxcr1* expression, sensory cells in the cochlea and in vestibular organs from a null mutant nevertheless exhibit relatively normal mechanotransduction at early postnatal time points.

The phenotypes we observed in *pi*^{4J} mutants are similar to that previously identified in other likely null mutant *pi* alleles (Beyer, 2000;Erven, 2002;Odeh, 2004). In addition to circling and head shaking behavioral anomalies, *pi*^{4J} mutants exhibit comparable pathology in the inner ear. Here we demonstrated the presence of thin and disorganized stereocilia by P4 in sensory cells of the cochleae in *pi*^{4J} mice. These pathologies are associated with substantial elevated auditory brainstem thresholds in the homozygous mutants and, together with the lack of expression of normal *Grxcr1* transcript and protein, indicate that *pi*^{4J} is also likely to be a null allele. We demonstrated somewhat better hearing (approximately 50 dB threshold shifts) in 6 week old mutants homozygous for the *pi*^{4J} allele than has been observed in other *pi* alleles, including the original pirouette (*pi*) allele (Beyer, 2000), as well as the *pi*^{tde} (Erven, 2002) and *pi*^{tg370} (Odeh, 2004) alleles, which typically exhibit shifts of at least 60 dB at multiple frequencies. Differences in the severity of hearing loss may be attributable to genetic background differences, a common feature of inherited hearing loss in mice (Johnson, 2006). Most of the *pi* alleles are on *C57BL/6J*-derived backgrounds, with the exception of the *pi*^{4J} allele, which was on a *NZB/NZW* mixed background at the time of ABR testing. The *C57BL/6J* strain carries a number of variant loci that contribute to an early onset, age-related hearing loss (ARHL) (Noben-Trauth, 2009) and may thus contribute to more severe loss of function in many of the *pi* alleles. The *NZB/NZW* strain does not carry a major susceptibility variant for ARHL (Noben-Trauth, 2003) and so may not have such an effect on the *pi*^{4J} allele.

We have demonstrated that despite the abnormal thin structure of stereocilia in *pi* mutants, bundles in the cochlea and utricle are capable of relatively normal transduction in early postnatal mutants, indicating that at least initially, components of the mechanotransduction apparatus undergo normal assembly. Relatively normal mechanotransduction in early postnatal life has also been demonstrated in other mutants that effect stereocilia bundle maturation, including *Myo15A* mutants that have severely shortened stereocilia (Stepanyan, 2006) and conditional *Rac1* mutants, in which bundles are disorganized (Grimsley-Myers, 2009). This suggests that assembly of the mechanotransduction apparatus is relatively independent of many processes involved in structural development of stereocilia. The behavioral dysfunction and severe reduction in hearing that is observed in *pi* mutants indicates that mechanotransduction is likely reduced at later ages when more severe structural deterioration of the stereocilia may occur as suggested by the breakage of bundles upon experimental deflection.

The thin stereocilia observed in *Grxcr1* mutant mice indicate a critical role for GRXCR1 in growth of stereocilia during development. Molecular genetic studies have indicated that a large number of other proteins are also critical for normal stereocilia growth and bundle maturation. These include proteins localized to the tips of stereocilia, the position of the barbed ends of actin filaments and the preferred end for addition of actin monomers (Schneider, 2002). Loss of the unconventional myosin Myo15a (Beyer, 2000;Probst, 1998), the adaptor protein whirlin (Holme, 2002;Mburu, 2003), or the actin regulatory

protein Eps8 (Manor, 2011) results in shortened stereocilia, indicating that these proteins normally promote length increases during development. Other tip proteins also appear to play a role in modulating actin filament growth at this site, including the actin capping protein twinfilin (Peng, 2009;Rzadzinska, 2009) and the actin binding protein gelsolin (Mburu, 2010).

Proteins present in the actin filament core itself have also been implicated in stereocilia growth and maturation, including the non-muscle β and γ actin monomer proteins. Mice carrying inner ear-specific homozygous null mutations in genes encoding both of these proteins fail to develop stereocilia, although the genes are individually dispensable for the initial maturation of the bundle (Perrin, 2010). Both actin genes are required to maintain the normal length and function of stereocilia in the adult (Perrin, 2010). The actin bundling protein espin, present throughout the filament core (Zheng, 2000), is also required for normal development of length and width of stereocilia (Zheng, 2000;Sekerkova, 2011;Rzadzinska, 2005). We have previously demonstrated that espin and plastin 1 (fimbrin), a second actin-bundling protein normally present in stereocilia bundles (Flock, 1982;Daudet, 2002), are also present in stereocilia of affected pirouette mice, indicating that gross alterations in the expression levels or localization of these two proteins do not appear to be involved in the pirouette pathology (Odeh, 2004).

During sensory cell development, increases in stereocilia dimensions require elongation of existing actin filaments, nucleation of additional filaments and incorporation of these filaments into their cores (Tilney, 1986;Tilney,

1986;Tilney, 1986). The failure of *Grxcr1* mutants to achieve normal stereocilia diameters suggests a direct impact of GRXCR1 on actin filament architecture or dynamics. Our demonstration of an ability of GRXCR1 to induce dimensional changes of microvilli, principally elongation (Odeh, 2010), suggests that it may act to enhance actin polymerization of new filaments in stereocilia during development. Interestingly, *in vitro* assays with purified recombinant protein demonstrated that Thrumin1, an *Arabadopsis thaliana* homolog of GRXCR1, possesses actin filament binding and bundling activity. Mutations in *Thrumin1* result in defects in light-mediated chloroplast movement *in vivo* (Whippo, 2011), a process which appears to require actin filament reorganization at the plasma membrane (Kadota, 2009;Suetsugu, 2010). Thrumin1 is likely to directly regulate filament reorganization through direct actin interactions. Attempts to purify recombinant full-length GRXCR1 have so far been unsuccessful. We have purified an N-terminal fragment of GRXCR1, however, that is both necessary and sufficient for localization of hybrid proteins to actin filament-rich structures in transfected cells (unpublished data). This N-terminal fragment lacks actin filament binding ability, suggesting that GRXCR1 may affect actin in stereocilia by influencing other actin binding proteins.

CHAPTER 3

Determinants of localization and induction of actin filament-rich structures by the stereocilia protein GRXCR1

Matthew R. Avenarius[1,2], Kristina L. Hunker[1], Lili Zheng[3], Tzy Wen Gong[1], Yehoash Raphael[1], James R. Bartles[3], and David C. Kohrman[1,2]

[1]Department of Otolaryngology/Kresge Hearing Research Institute and [2]Department of Human Genetics, University of Michigan Medical School, Ann Arbor, Michigan 48109, USA; [3]Department of Cell and Molecular Biology, Feinberg School of Medicine, Northwestern University, Chicago, IL 60611, USA

Avenarius Contribution: Confocal imaging of COS-7 cell transfections (Figure 3.4), Sensory and nonsensory cell transfections (Figure 3.5)

ABSTRACT

The GRXCR1 protein is localized to stereocilia, specialized actin filament-rich structures on the apical surface of sensory cells in the inner ear that are essential for hearing and vestibular function. Mutations in the *GRXCR1* gene are responsible for deafness and vestibular defects in mice and in humans and are associated with the failure of stereocilia to attain normal dimensions during

development. GRXCR1 is composed of an evolutionarily divergent N-terminal domain, along with central glutaredoxin-like and C-terminal Cys-rich domains that are conserved in all known family members. In order to determine the functional roles of these domains, we transfected GFP-tagged expression constructs into cultured cell lines and inner ear tissue explants and evaluated fusion protein localization and effects on cell morphology in general and actin filament-rich structures in particular. We demonstrated that the divergent N-terminal domain is a novel element sufficient to drive fusion protein localization to a diverse set of actin filament-rich structures, including sensory cell stereocilia. The N-terminus, plus additional conserved domains of GRXCR1, is required for the elongation of selected actin filament-rich structures.

INTRODUCTION

In the normal inner ear, sensory cells in the cochlea and in vestibular organs contain specialized, actin filament-rich structures on their apical surfaces that are known as stereocilia and that are essential for detection of auditory and vestibular stimuli (Gillespie, 2009). Bundles containing 50 to 300 stereocilia are organized in a staircase arrangement, with multiple fine connections along their lengths that link neighboring stereocilia with one another (Goodyear, 2005). The core of each stereocilium is composed of tightly packed bundles of actin filaments of the same relative orientation (Flock, 1977), similar to the cores of other actin filament-rich structures such as filopodia and microvilli that are present on the surface of many cell types.

Characterization of mutant mouse models with hearing loss and/or vestibular defects have provided insight into genes that are required for development, maturation and maintenance of stereocilia in the inner ear (Petit, 2009). Null mutations in *Grxcr1* result in vestibular dysfunction and profound deafness in the mouse pirouette (*pi*) strain (Odeh, 2010). Similarly, mutations in human *GRXCR1* are associated with early onset, moderate to profound hearing loss as well as vestibular abnormalities (Odeh, 2010;Schraders, 2010). *Grxcr1* is expressed in sensory hair cells in the inner ear and the GRXCR1 protein is localized to stereocilia in the cochlea and vestibular sensory organs of normal mice in the early postnatal period and at maturity (Odeh, 2010). Cochlear stereocilia in early postnatal *pi* mutants fail to reach a normal diameter during development and become disorganized during the second postnatal week, indicating that *Grxcr1* is necessary for processes that regulate stereocilia dimensions and organization during maturation (Beyer, 2000;Odeh, 2004 ;Erven, 2002). Similar developmental defects in stereocilia have also been observed in vestibular organs of *Grxcr1* mutant mice (Erven, 2002). GRXCR1 expressed in cultured cell lines and in inner ear tissue explants localizes to actin filament-rich structures at the cell periphery or apical surface and depending upon cell type, induces structures with greater actin filament content and/or increased lengths (Odeh, 2010).

Sequence analysis indicated GRXCR1 possesses a central domain related to glutaredoxin proteins, which typically exhibit reduction/oxidation (redox) activity (Holmgren, 2000), and a cysteine-rich C-terminus arranged in a putative

zinc finger configuration (Odeh, 2010). Proteins implicated in stereocilia maturation include those that are required for normal polarity of the bundle, for bundle organization and cohesion, and for appropriate growth of individual stereocilia (Petit, 2009). The majority of these proteins are localized within stereocilia indicating that they act locally to influence bundle morphogenesis. Although a growing body of evidence supports a role for unconventional myosins in protein trafficking to and within stereocilia (Schwander, 2010), intrinsic determinants for stereocilia localization are unclear. In order to investigate the domain requirements of GRXCR1 for localization and for its effects on actin filament-rich structures, we analyzed transfected cells in culture that express either wild type or mutant GFP fusion proteins. We demonstrate the importance of the evolutionarily divergent N-terminus of this protein for localization to actin filament-rich structures. In addition, we provide evidence that the C-terminal, deeply conserved domains of GRXCR1 are also involved in stereocilia localization and in pathways that control the dimensions of actin filament-rich structures.

MATERIAL AND METHODS

Mice. C57BL/6J mice were obtained from The Jackson Laboratory (Bar Harbor, ME) and were maintained by brother-sister matings. All mice were cared for in accordance with protocol number 08234 approved by the University Committee on Use and Care of Animals at the University of Michigan.

Protein sequence analysis. Sequence comparisons to protein databases were performed using the BLAST-PSI algorithm (Altschul, 1997). Multiple

sequence alignments were made using the CLUSTALW algorithm (version 1.83), with MacVector 11.0.1 software (MacVector, Inc.; Cary, NC, USA) and the following multiple alignment parameters: Open Gap Penalty = 10.0; Extend Gap Penalty = 0.1; Delay Divergent = 40%; Gap Distance = 8; and Similarity Matrix: Blosum.

Grxcr1 Fusion Constructs. The entire 870 bp open reading frame of *Grxcr1*, plus partial 5' and 3' UTR sequences, was amplified from inner ear cDNA and cloned into the EcoRI and BamHI sites of pEGFP-N1, upstream of and in-frame with the coding region for green fluorescent protein (GFP) (BD Biosciences, Palo Alto, CA, USA). Overlap PCR was used to amplify subregions of the wild type cDNA that corresponded precisely with the exon borders of the gene in order to generate mutant constructs that lacked: exon 1 (Δ-N-terminus); exons 2 and 3 (Δ-Grx), and exon 4 (Δ-Cys-rich). The first exon alone was similarly amplified to generate the N-terminal only insert. All of these mutant inserts were similarly cloned into the EcoRI and BamHI sites of pEGFP-N1, upstream of and in-frame with the coding region for GFP.

Cell Culture and Expression Studies. COS-7 cells were obtained from the American Type Culture Collection (Manassas, VA). COS-7 cells were transfected at subconfluency on glass coverslips with a GRXCR1-GFP constructs or a control pEGFP-N1 vector, using the *Trans*IT-COS transfection kit (Mirus; Madison, WI). Cells were fixed 20 hours after transfection, permeabilized, and incubated with an antibody specific for GFP (Chemicon; Temecula, CA, USA), secondary anti-rabbit IgG antibodies conjugated to Alexa 488 (Molecular

Probes; Eugene, OR, USA), and rhodamine-phalloidin (Molecular Probes; Eugene, OR, USA). Differentiated LLC-PK1-CL4 (CL4) epithelial cells were originally derived from pig kidney LLC–PK1 cells (Amsler, 1985). This cell line was helpfully provided by Dr. Mark S. Mooseker (Department of Molecular, Cellular, and Developmental Biology, Yale University, New Haven, CT) (Tyska, 2002). CL4 cells were transfected with a Grxcr1-GFP construct, fixed, permeabilized and incubated with Texas Red-phalloidin (Loomis, 2003). CL4 cells were analyzed with a Zeiss LSM 510 confocal microscope and COS7 cells were analyzed with a Leica TCS SP5 X confocal microscope.

Inner Ear Explant Studies. For explant studies, utricles were dissected from C57BL/6J mice at between postnatal day 4 (P4) and P8, cultured for 1 to 2 days in Dulbecco's modified Eagle's medium supplemented with 7% fetal bovine serum, transfected with a Helios gene gun (Biorad; Hercules, CA, USA) with the GFP fusion constructs coupled to 1.0 mm gold particles (Biorad), and processed for immunohistochemistry 24 hr later and analyzed with an Olympus FV-500 confocal microscope, as previously described (Belyantseva, 2003). The images from explant transfections are representative of GRXCR1-GFP expression data from three independent experiments (total number of expressing cell types: 6 vestibular hair cells and more than 14 nonsensory epithelial cells). Sensory cells and nonsensory cells were identified by the presence or absence, respectively, of stereocilia bundles, and by cell morphologies.

RESULTS

Evolutionary conservation of GRXCR1. A database sequence comparison of mouse GRXCR1 indicated significant similarity throughout its full length to a large number of vertebrate orthologs. Amino acid alignments of the mouse protein with human, chicken and zebrafish orthologs are shown in Figure 1. Proteins from non-vertebrate species also exhibit similarity to GRXCR1 (Fig. 1), including the plant protein THRUMIN1, which was recently identified as a critical component of the chloroplast movement response to light in *A. thaliana* (Whippo, 2011). The similarity in these non-vertebrate homologs extends generally throughout the central glutaredoxin (Grx)-like region, including a conserved Cys in a putative Grx active site and the two $CX_2CX_7CX_2C$ motifs arranged in a putative zinc finger configuration in the C-terminus of GRXCR1. Interestingly, the N-terminal regions of the non-vertebrate proteins differ greatly in length and exhibit limited similarity with GRXCR1, suggesting different molecular activities for this region in the divergent proteins. Our previous studies indicated that full-length, wild type GRXCR1 expressed in cultured cell lines and in inner ear tissue explants localized to actin filament-rich structures at the cell periphery or apical surface and depending upon cell type, induced structures with greater actin filament content and/or increased lengths (Odeh, 2010). In order to determine the potential roles of the N-terminal, Grx-like, and Cys-rich domains in these processes, we evaluated subcellular localization, cell morphology and actin filament-rich structures in cells transfected with a series of constructs (Fig. 2) that express C-terminal GFP fusion proteins carrying single domains of GRXCR1 or

single deletions of each of the domains.

Role of the N-terminus in subcellular localization to microvilli of cultured epithelial cells. The LLC–PK1–CL4 epithelial cell line (CL4) is derived from pig kidney and exhibits several properties that are useful for study of epithelial cell properties in culture, including the production of actin filament-rich microvilli on their apical surfaces and sorting of cellular proteins to appropriate *in vivo* locations (Tyska, 2002;Zheng, 2010). The actin filaments in the core of apical microvilli are bundled into parallel arrays, similar to filaments in stereocilia (Loomis, 2003). CL4 cells have been used to evaluate the cellular targeting requirements and activities of a number of proteins expressed in sensory hair cells (Loomis, 2003; Zheng, 2010). Transfection of a construct expressing wild type GRXCR1 into CL4 cells indicated primary localization of the protein in apical microvilli (Fig. 3A). Mutant proteins that lacked the central Grx domain (Fig. 3B) or the C-terminal Cys-rich (Fig. 3C) domain of GRXCR1 were capable of microvilli localization, albeit at slightly reduced efficiencies relative to wild type protein. Mutant protein lacking the N-terminus of GRXCR1, however, failed to localize to the apical surface and was present mainly in the cytoplasm and nucleus of transfected cells (Fig. 3D). A mutant protein containing only this N-terminal domain (Fig. 3E) localized to microvilli much like the wild type protein, indicating that this domain is both necessary and sufficient for microvilli localization in CL4 cells.

Role of the N-terminus in subcellular localization to filopodia of cultured fibroblast cells. Our previous transfection studies in fibroblasts indicated that wild type GRXCR1 exhibited a preference for localization to regions of the cell enriched in parallel actin filaments such as filopodia on the peripheral and dorsal surface (Odeh, 2010), similar to its localization in the apical microvilli of CL4 epithelial cells. In the present study, we observed a similar localization of wild type GRXCR1, with a substantial amount of the protein observed in dorsal filopodia (Fig. 4A). GRXCR1 deletion mutants lacking the Grx (Fig. 4B) or the Cys-rich domain (Fig. 4C) localized to dorsal filopodia in a fashion similar to wild type GRXCR1, while the N-terminal deletion mutant exhibited a diffuse cytoplasmic localization, with little or no protein observed in filopodia (Fig. 4D). This cytoplasmic localization was similar to that observed with GFP alone (Fig. 4F). The N-terminal only mutant localized to filopodial structures much like wild type GRXCR1 (Fig. 4E). These data indicate that in COS cells, an intact N-terminal domain is also necessary and sufficient for localization of GRXCR1 to structures enriched in parallel actin filaments.

Subcellular localization and microvillar elongation in inner ear cells. Previous studies of transfected inner ear explants indicated localization of wild type GRXCR1-GFP to the microvilli of nonsensory cells and to the stereocilia of sensory hair cells (Odeh, 2010). To evaluate if the determinants for localization to apical actin filament-rich structures are similar to those found in CL4 and fibroblast cells, we transfected the set of wild type and mutant GRXCR1-GFP constructs into explants derived from the postnatal mouse utricle. We observed

GFP fusion protein expression in numerous nonsensory epithelial cells, which express little or no endogenous GRXCR1 (Odeh, 2010). Similar to our previous studies, wild type GRXCR1 protein localized preferentially to the apical microvilli of nonsensory cells (Fig. 5A-C). As in CL4 cells and fibroblasts, the ∆-N-terminal mutant remained principally in the cytoplasm of nonsensory cells (Fig. 5G-H) while a protein containing only this N-terminal domain localized like wild type GRXCR1 to apical microvilli (Fig. 5M-O), indicating the necessity and sufficiency of the N-terminus for apical actin filament-rich structure localization. Our previous explant transfection studies also indicated that wild type GRXCR1 induced elongation of the microvilli of nonsensory cells in the inner ear (Odeh, 2010). We found similar results in the present study (Fig. 5A-C). The microvilli of nonsensory cells expressing wild type GRXCR1 were significantly elongated compared to neighboring untransfected cells or control cells transfected with GFP alone (Fig. 5 S-U). The N-terminal deletion mutant, which localized to the cytoplasm, failed to induce substantial microvilli elongation (Fig. 5G-I), consistent with a requirement for apical localization for this activity. Notably, while capable of microvilli localization, the N-terminal domain alone was not able to appreciably alter the dimensions of the microvilli (Fig. 5M-O), suggesting that C-terminal domains of GRXCR1 are also required for this activity.

Analysis of sensory cells expressing GRXCR1-GFP fusion proteins indicated that wild type GRXCR1 (Fig. 5D-F) as well the ∆-N-terminal (Fig. 5J-L) and the N-terminal only (Fig. 5P-R) mutants were all capable of stereocilia localization, indicating that while sufficient, the N-terminus of GRXCR1 is not

absolutely necessary for localization in this cell type. This inconsistency was rectified

Neither wild type GRXCR1 nor any of the mutants induced substantial stereocilia elongation when expressed in sensory cells, consistent with previous transfection studies of wild type GRXCR1 (Odeh, 2010).

DISCUSSION

The results of our structure-function studies indicate the importance of the N-terminal domain in subcellular localization to actin filament-rich structures and also highlight the cell type-specific qualities of GRXCR1. Transfections of GRXCR1-GFP fusion constructs into fibroblasts and nonsensory epithelial cells demonstrate the necessity and sufficiency of the N-terminus of GRXCR1 for preferential localization of the protein to actin filament-rich structures such as filopodia and microvilli. Additional domains of GRXCR1, however, are required to induce elongation of apical microvilli of nonsensory supporting cells and are likely to also contribute to stereocilia localization of the protein in sensory cells.

A shared requirement for the N-terminus of GRXCR1 for actin filament-rich localization in several different cell types is consistent with a common localization pathway. Structure-function studies of a number of stereocilia proteins suggest that actin binding ability is necessary for their appropriate localization. Mutations in the motor domain of Myo15a prevent localization of the protein to the tips of stereocilia in the inner ear (Belyantseva, 2005) or to the tips of microvilli in transfected CL4 cells in culture (Zheng, 2010), consistent with myosin 15a as a motor protein directed to the plus/barbed ends of actin

filaments. Similarly, actin filament-rich structure localization of espin and Myo3a depends upon intact actin filament binding domains (Zheng, 2010;Loomis, 2003;Les Erickson, 2003). We have not detected any known actin binding motifs in the primary amino acid sequence of GRXCR1 (Revenu, 2004) and the N-terminus of GRXCR1 does not have detectable actin filament binding activity (unpublished data), suggesting that direct affinity for actin filaments in the core of actin filament-rich structures is unlikely to be the basis for specific localization of this protein. Although the amino acid sequence of the N-terminus is conserved in GRXCR1 homologs across vertebrate species, it diverges significantly in non-vertebrate homologs such as plant THRUMIN1. Notably, the N-terminus of THRUMIN1 is also required for localization of this protein to the plasma membrane and to thick actin filaments associated with chloroplasts (Whippo, 2011). Membrane localization is dependent upon a predicted myristylation site at the extreme N-terminus of THRUMIN1, while actin filament localization appears to occur through direct interactions between the N-terminal domain and actin filaments. GRXCR1 lacks this myristylation site and has only limited N-terminal sequence similarity to the plant protein. Together with our structure-function studies with mouse GRXCR1, analysis of THRUMIN1 suggests that the divergent N-terminal domains direct localization of these proteins to species-specific subcellular locations at which each protein controls distinct cellular processes that are dependent upon dynamic changes in actin filaments.

Interestingly, our transfection experiments in inner ear explant cultures indicated that, while the N-terminal domain of GRXCR1 is sufficient to drive

localization to the stereocilia bundle in sensory cells, it is not absolutely necessary as an N-terminal deletion mutant retains localization ability. This indicates that the Grx-like and/or the Cys-rich C-terminal domains may also be involved in protein localization in sensory cells. These highly conserved domains could interact with another stereocilia protein(s) and thus appropriately target the N-terminal deletion mutant in transfected sensory cells.

The thin stereocilia with slightly shortened length in pirouette mutant mice carrying loss of function *Grxcr1* mutations indicate a critical role for GRXCR1 in growth of stereocilia during development (Odeh, 2010). In mammals, simultaneous increases in length and diameter of stereocilia occur during late embryogenesis and early postnatal life (Zine, 1996; Kaltenbach, 1994) and require elongation of existing actin filaments, nucleation of additional filaments and incorporation of these filaments into the core (Tilney, 1986;Tilney, 1986). A number of proteins in addition to GRXCR1 have been identified that are required for growth of stereocilia, including Myo15a (Probst, 1998) and the actin-bundling protein espin (Zheng, 2000). Similar to GRXCR1, these proteins also influence actin filament-rich structures on the apical surface of cells in culture. In transfected epithelial cells, espin cross-links increase the steady-state length of apical microvilli through apparent effects on the structure of the actin bundle at their core (Loomis, 2003). Espin also induces elongation of actin filament-rich structures in transfected sensory cells and supporting cells (Rzadzinska, 2005). Our transfection studies suggest a similar effect of GRXCR1 on a more limited range of cell types. Unlike espin, GRXCR1 fails to induce substantial elongation

of apical microvilli of CL4 epithelial cells, suggesting that these cells may lack critical molecular components that are necessary for activation of actin polymerization or alternatively, that these cells contain factors that can counteract or modulate such an effect of GRXCR1. This restriction is similar to that of Myo15a, which localizes to the tips of apical microvilli in transfected CL4 cells but also fails to induce elongation (Zheng, 2010). The inability of transfected GRXCR1 to substantially alter the dimensions of stereocilia of sensory hair cells in explant cultures suggests that pathways that normally regulate endogenous GRXCR1 may also limit the activity of the transfected protein. Again, this situation is similar to that found for Myo15a which, while capable of elongation of the shortened stereocilia bundles in Myo15a mutants (Belyantseva, 2005), does not appear to significantly alter bundle morphology when expressed in transfected sensory cells from normal mice (Belyantseva, 2003).

Our demonstration that transfected GRXCR1 can induce elongation of microvilli in nonsensory cells in the cochlea suggests that, in particular cellular contexts, GRXCR1 may increase net actin polymerization. The plant homolog THRUMIN1 also appears to directly alter actin filament architecture during light-induced chloroplast movement (Whippo, 2011). We have demonstrated that microvilli elongation by GRXCR1 depends upon localization of the fusion protein to these structures via its N-terminal domain. The failure of this N-terminus alone to support elongation indicates a requirement for additional C-terminal domains. Although we cannot definitively exclude direct interactions of full-length GRXCR1 with actin filaments, the apparent lack of such an interaction of the N-terminal

domain suggests that GRXCR1 alters actin filament-rich structures by instead influencing the activities of other cellular proteins required for net elongation of actin filaments. Our structure-function data suggests that these influences are likely to occur through the action of the deeply conserved Grx-like domain of GRXCR1 and/or its Cys-rich C-terminus. While glutaredoxins have been implicated in the control of actin filament distribution in the cell through redox-mediated processes (Pujol-Carrion, 2010;Wang, 2001), the relative position of the conserved Cys in the Grx-like domain of GRXCR1 suggests it may be unable to catalyze redox activity (Lillig, 2008). Notably, redox-independent function is also supported by the ability of a THRUMIN1 transgenic protein carrying a C231S mutation in the putative active site of its Grx-like domain to rescue chloroplast movement in *thrumin1* mutant plants (Whippo, 2011). Redox-independent chaperone activity has been described in several glutaredoxin-related proteins (McGee, 2006;Kern, 2003), suggesting a potential alternative role for GRXCR1 family members. Interestingly, the C-terminal domains of this family exhibit similarity to the Cys-rich zinc finger region of dnaJ proteins (data not shown), a well characterized family of chaperones (Vos, 2008). A number of chaperone proteins have been detected through proteomic studies of stereocilia bundles (Shin, 2007), suggesting that regulation of protein folding and assembly may be important for stereocilia development and homeostasis.

Further analysis of the GRXCR1 protein will be required to determine the mechanisms by which the N-terminal domain drives localization to actin filament-rich structures and the Grx and Cys-rich domains impact actin filament

distribution in the cell. Understanding these mechanisms will provide insight into normal development of stereocilia bundles and auditory function. As GRXCR1 is also expressed in the stereocilia of adult mice, such studies may also uncover processes necessary for maintenance and repair of bundles in the mature inner ear.

MATERIAL AND METHODS

Mice. C57BL/6J mice were obtained from The Jackson Laboratory (Bar Harbor, ME) and were maintained by brother-sister matings. All mice were cared for in accordance with protocol number 08234 approved by the University Committee on Use and Care of Animals at the University of Michigan.

Protein sequence analysis. Sequence comparisons to protein databases were performed using the BLAST-PSI algorithm (Altschul, 1997). Multiple sequence alignments were made using the CLUSTALW algorithm (version 1.83), with MacVector 11.0.1 software (MacVector, Inc.; Cary, NC, USA) and the following multiple alignment parameters: Open Gap Penalty = 10.0; Extend Gap Penalty = 0.1; Delay Divergent = 40%; Gap Distance = 8; and Similarity Matrix: Blosum.

Grxcr1 Fusion Constructs. The entire 870 bp open reading frame of *Grxcr1*, plus partial 5' and 3' UTR sequences, was amplified from inner ear cDNA and cloned into the EcoRI and BamHI sites of pEGFP-N1, upstream of and in-frame with the coding region for green fluorescent protein (GFP) (BD Biosciences, Palo Alto, CA, USA). Overlap PCR was used to amplify subregions of the wild type cDNA that corresponded precisely with the exon borders of the

gene in order to generate mutant constructs that lacked: exon 1 (Δ-N-terminus); exons 2 and 3 (Δ-Grx), and exon 4 (Δ-Cys-rich). The first exon alone was similarly amplified to generate the N-terminal only insert. All of these mutant inserts were similarly cloned into the EcoRI and BamHI sites of pEGFP-N1, upstream of and in-frame with the coding region for GFP.

Cell Culture and Expression Studies. COS-7 cells were obtained from the American Type Culture Collection (Manassas, VA). COS-7 cells were transfected at subconfluency on glass coverslips with a GRXCR1-GFP constructs or a control pEGFP-N1 vector, using the *Trans*IT-COS transfection kit (Mirus; Madison, WI). Cells were fixed 20 hours after transfection, permeabilized, and incubated with an antibody specific for GFP (Chemicon; Temecula, CA, USA), secondary anti-rabbit IgG antibodies conjugated to Alexa 488 (Molecular Probes; Eugene, OR, USA), and rhodamine-phalloidin (Molecular Probes; Eugene, OR, USA). Differentiated LLC-PK1-CL4 (CL4) epithelial cells were originally derived from pig kidney LLC–PK1 cells (Amsler, 1985). This cell line was helpfully provided by Dr. Mark S. Mooseker (Department of Molecular, Cellular, and Developmental Biology, Yale University, New Haven, CT) (Tyska, 2002). CL4 cells were transfected with a Grxcr1-GFP construct, fixed, permeabilized and incubated with Texas Red-phalloidin (Loomis, 2003). CL4 cells were analyzed with a Zeiss LSM 510 confocal microscope and COS7 cells were analyzed with a Leica TCS SP5 X confocal microscope.

Inner Ear Explant Studies. For explant studies, utricles were dissected from C57BL/6J mice at between postnatal day 4 (P4) and P8, cultured for 1 to 2 days in Dulbecco's modified Eagle's medium supplemented with 7% fetal bovine serum, transfected with a Helios gene gun (Biorad; Hercules, CA, USA) with the GFP fusion constructs coupled to 1.0 mm gold particles (Biorad), and processed for immunohistochemistry 24 hr later and analyzed with an Olympus FV-500 confocal microscope, as previously described (Belyantseva, 2003). The images from explant transfections are representative of GRXCR1-GFP expression data from three independent experiments (total number of expressing cell types: 6 vestibular hair cells and more than 14 nonsensory epithelial cells). Sensory cells and nonsensory cells were identified by the presence or absence, respectively, of stereocilia bundles, and by cell morphologies.

CHAPTER 4

A targeted mutation of *Grxcr2* results in hearing loss associated with defects in stereocilia development

Avenarius Contribution: Assembly of amino acid alignments (Figure 4.1 B,C and Figure 4.2 A), Targeting of *Grxcr2* locus (Figure 4.3 A), Genomic DNA genotyping PCR (Figure 4.3 B), *Grxcr2* and *Tfcr* RT-PCR (Figure 4.3 C), whole mount immunostaining (Figure 4.3 D) Assembly and statistics of ABR and DPOAE data (Figure 4.4 A,B,C) SEM dissection, preparation, and imaging (Figure 4.5 A-H) whole mount immunostaining (phalloidin and aceylated α-tubulin) qRT-PCR and GRXCR2 whole mount immunostaining (Figure 4.7 A-B) qRT-PCR (Figure 4.8 A) Assembly of ABR data and statistics and SEM dissction, preparation, and imaging (Figure 4.8 B-C)

INTRODUCTION

Congenital deafness is the most prevalent inherited sensory deficit, affecting nearly 1 in every 1,000 live births, of which approximately 50% are attributed to genetic aberrations (Kochhar, 2007). Pedigrees segregating autosomal dominant, autosomal recessive, X-linked, and mitochondrial deafness have been used to identify mutations in nearly 70 human deafness-associated genes to date (Van Laer, 2003). Allelic heterogeneity at some deafness loci accounts for patients presenting with hearing loss as the only clinical

manifestation and the pleiotropic effects observed in patients with syndromic hearing loss (McHugh, 2006).

Stereocilia are mechanosensory structures central to the perception of sound and vestibular stimuli and are located on the apical surface of sensory hair cells of the inner ear. As stereocilia bundles are deflected in response to auditory or vestibular stimuli, putative mechanosensory channel(s) in the membrane of the stereocilia tips open to depolarize the associated hair cell and alter neurotransmitter release at the base of the hair cell (Gillespie, 2009). Auditory or vestibular nerve fibers in turn conduct associated action potentials to the central nervous system that are ultimately perceived as sound or body position.

Stereocilia bundles are composed of 50 – 300 individual stereocilia that are arranged in a highly organized, graded staircase configuration (Lim, 1985). Analysis of mutant mouse models has begun to define a set of genes required for various aspects of the normal development of bundle morphology and function, including the final dimension of individual stereocilia, the organization of individual bundles, and the orientation of bundles with respect to the overall sensory organ (Petit, 2009; Belyantseva, 2003). Mutations in many of these genes have been implicated as the basis for hearing loss in humans, including nonsyndromic and syndromic forms, indicating the clinical relevance of the genes and the evolutionary conservation of pathways necessary for normal stereocilia development and sensory function (Van Laer, 2003; McHugh, 2006).

Grxcr1, a gene required for establishing normal stereocilia diameter during development, is mutated in the deaf, circling mouse mutant pirouette (Odeh, 2010). Similarly, mutations in human *GRXCR1* underlie early onset hearing loss in pedigrees segregating defects at the DFNB25 locus (Odeh, 2010; Schraders, 2010). *Grxcr1* encodes a cysteine-rich protein with sequence similarity in its central domain to the glutaredoxin family of proteins. The GRXCR1 protein localizes to stereocilia in the cochlea and in vestibular organs of the inner ear, where it is likely to influence actin filament architecture in the stereocilia core (Odeh, 2010).

Grxcr2, a paralogous vertebrate gene, encodes a protein with 30% sequence identity to *Grxcr1.* In the present study, we have evaluated the expression of *Grxcr2* and the effects on inner ear function of a targeted mutation at this locus. Similar to *Grxcr1*, *Grxcr2* is expressed in sensory hair cells in the cochlea and in vestibular organs and GRXCR2 protein is localized along the length of stereocilia. Mice homozygous for a *Grxcr2* mutation exhibit severe hearing loss associated with early postnatal defects in orientation and organization of stereocilia bundles in the cochlea. Unlike pirouette mice, *Grxcr2* mutants do not circle or show other overt behaviors typically associated with vestibular dysfunction. These differences in cochlear and vestibular phenotypes in *Grxcr1* and *Grxcr2* mutants indicate distinct roles in the inner ear for each gene and suggest GRXCR1 and GRXCR2 proteins, while similar in sequence and localization, carry out unique biological functions.

MATERIALS & METHODS

Grxcr2 conditional allele The PL451 (NCI Frederick) was used to insert LoxP recombination sites flanking exon 1 of *Grxcr2*. Exon 1 and flanking DNA sequences (490 bp 5' of exon 1 to 514 bp 3' of exon 1) were amplified from C57BL/6J genomic DNA using primers that included sequences for a proximal LoxP site and subsequently cloned into the PL451 vector. Contiguous genomic DNA extending 1,689 bp 5' of this exon 1 fragment was amplified and cloned into the PL451 vector as the 5' homology arm and the contiguous DNA in intron 1 extending 2,508 bp in the 3' direction of the exon 1 fragment was amplified and cloned into the PL451 vector as the 3' homology arm. The targeting vector was digested with Sac II and Cla I to liberate the 7,534 bp targeting construct. The targeting construct was electroporated into the BRUCE4G9 C57BL/6 ES cell line and Southern blotting was used to identify properly targeted clones. Three independent positive clones were microinjected into pseudopregnant females (B6 Cg-*Tyrc*^{2J}) to derive chimeric mice that were subsequently mated to generate germ line founders (wt/*Grxcr2*^{flox}). Founder mice were bred to mice homozygous for an Ella-CRE recombinase transgene. Mice that inherited the floxed allele and the Cre transgene were evaluated for exon 1 deletion by genomic PCR. Deletion carriers were mated to *C57BL/6J* mice and the resulting deletion heterozygotes were intercrossed to generate three genotypic classes (+/+, +/Δ, and Δ/Δ). *Grxcr2* homozygote mutants (Δ/Δ) were also mated to FVB strain mice and progeny were sib mated to evaluate the effect of the *Grxcr2* deletion on this genetic background.

Southern blotting Embryonic stem cell DNA was digested overnight with BbvcI and separated on a 0.8% agarose gel. The gel was incubated in 0.25 M HCL to depurinate the DNA and denatured in 0.4 M NaOH. DNA was transferred overnight in 10 x SSC buffer onto a positively charged Zetaprobe membrane (BioRad Hercules, CA) followed by UV cross-linking to the membrane. A probe, derived from genomic DNA flanking sequences in the targeting vector, was designed to recognize the endogenous and recombinant *Grxcr2* alleles was radiolabeled and hybridized. The membrane was washed several times and exposed to film for up to 2 days.

Genomic PCR genotyping A single reverse primer internal to the LoxP sites as well as a set of LOXP flanking primers were designed to recognize the intact or deleted *Grxcr2* allele. Using genomic DNA as a template these primers were used in a multiplex PCR genotyping reaction. The intact (wt) *Grxcr2* allele amplified a 532 bp product and the *Grxcr2* Δ allele amplified a 490 bp product.

RNA extraction and reverse transcriptase reaction Temporal bones were removed from mice ranging from P0 – adult time points and whole inner ear tissue was dissected in ice cold RNA Later (Ambion, Carlsbad, CA). Immediately prior to RNA extraction the RNA Later was removed and 1 mL of Trizol was added to each sample (Invitrogen Carlsbad, CA). The tissue was homogenized, and RNA was extracted using the Purelink RNA micro kit (Invitrogen Carlsbad, CA). 1 μg of RNA was used as the input to a Super Script III reverse transcription reaction (Invitrogen Carlsbad, CA) using oligo dT as a primer.

RT-PCR 1 μL of the RT product along with *Grxcr2* gene-specific primers designed to exons 1 and 3 were used in a standard RT-PCR reaction. A separate reaction, also using 1 μL of the RT product, was performed in parallel to amplify the endogenous Transferrin Receptor (*Tfrc*) house-keeping gene as an internal control.

Quantitative PCR (qPCR) Conditions for two sets of exonic primers, one designed to exon 1 and exon 2 of *Grxcr2* and the other designed to the ribosomal subunit 16S gene, were optimized for specific product amplification and minimal primer dimer production. The qPCR reaction consisted of Sybr green master mix, 1 μL of the RT-product derived from whole inner ear RNA, and primers designed to *Grxcr2* exon 1 and exon 2 or the ribosomal subunit 16S. Reaction cycling was performed on an ABI 7300 Real-Time PCR system (Applied Biosystems Foster City, CA) and gene expression was quantified (Arany, 2008).

Whole mount immunostaining Temporal bones were removed from mice at the appropriate age and placed in 4% paraformaldehyde. Genotype analysis was performed postmortem on tail biopsies. The sensory epithelium was microdissected and the tectorial membrane was removed. Tissue was washed in PBS and permeabilized in 0.3% Triton-X for 10 minutes. Tissue was washed in PBS and incubated in 5% goat serum for 1 hour. A 1:900 dilution of phalloidin 546 was applied to the tissue for 0.5 hour and then the tissue was incubated overnight in a 1:100 dilution of the rabbit-derived, anti-GRXCR2 primary antiserum. This antiserum had been affinity purified against recombinant, full-length GRXCR2 protein produced in bacteria, using published methods (Odeh,

2010). Tissue was washed in PBS several times and incubated in a 1:300 dilution of goat anti-rabbit 488 secondary antibody. The tissue was again washed in PBS, mounted, and imaged on a Leica SPX5 2-photon laser-scanning confocal microscope. Images were processed using either Photoshop or ImageJ.

Auditory brainstem response (ABR) Animals were anesthetized by using a xylazine/ketamine mixture, and ABRs were recorded as detailed previously (Halsey, 2005). In brief, stimuli were presented in 15 ms tone bursts at 4, 12, 24, and 48 kHz. Up to 1024 responses were obtained and were collectively averaged for each stimulus level. Tucker-Davis Technologies System II hardware and SigGen/Biosig software (TDT, Alachua, FL) were used to present tone bursts and record responses. Tones were delivered through a Beyer driver (Beyer Dynamics Inc., Farmingdale, NY; aluminum-shielded enclosure made in house).

Distortion Product Otoacoustic Emissions (DPOAE) Animals were anesthetized with a xylazine/ketamine mixture and DPOAE responses ($2f_1 – f_2$) to two tone stimuli (f_1= 8000 Hz and f_2= 9600) were recorded using a Tucker Davis Technologies system II and a custom-made MATLAB™ script as previously described (Halsey, 2005).

Scanning electron microscopy Temporal bones were removed from mice and placed in 2% glutaraldehyde + 0.2 M cacodylate buffer. Genotype analysis was performed postmortem on tail biopsies. The cochlea was microdissected to expose the sensory epithelium and incubated in 2%

glutaraldehyde + 0.2 M cacodylate buffer for a minimum of 2 days. Tissue was washed in water and processed using the OTOTO method, which alternates the application of osmium tetroxide and thiocarbohydrazide (Osborne, 1991). The samples were critical point dried using a Samdri-790 critical point dryer (Tousimis Research Corporation, Rockville, MD) and mounted on stubs using colloidal silver paste. The samples were analyzed using an Amray 1000B scanning electron microscope.

Quantifying bundle orientation The sensory epithelium from *Grxcr2* heterozygous and homozygous mutant mice was dissected and whole mount immunostained using phalloidin and acetylated-α-tubulin (Sigma Cat# T7451). Bundle orientation was determined by identifying the acetylated-α-tubulin kinocilium to mark the vertex (point A), the distal most aspect of the stereocilia bundle (Figure 4.6 A). The length between the vertex and the proximal most stereocilium (points B & C) was measured for both sides of the bundle. A horizontal line with respect to the pillar cells was drawn to connect the proxima most stereocilia (points B & C) on both sides of the bundle. The mid-point of that line was defined as the half the average of the two sides of the stereocilia bundle. A line, beginning at the stereocilia vertex, was constructed through the mid-point and bisected the pillar cells which served as an anatomical reference. To determine the degree of bundle orientation with respect to the polarity axis, the angle made by the bisecting line relative to the reference line was measured and subtracted from 90°. ImageJ was used to determine all lengths and angles measured.

RESULTS

Grxcr2 encodes a vertebrate specific cysteine-rich protein expressed in the inner ear

The *Grxcr2* gene encodes a predicted protein of 254 amino acids and is located on mouse chromosome 18 in a region paralogous with the *Grxcr1* locus (Figure 4.1 A). GRXCR2 exhibits approximately 30% amino acid identity with GRXCR1, with complete conservation of the arrangement of cysteines in the C-terminal region. (Figure 4.1 B). The central region of GRXCR1 exhibits similarity in primary sequence and predicted secondary structure to glutaredoxin proteins, a sub-member of thioredoxin family of proteins (Odeh, 2010). Thioredoxin-related proteins typically possess oxidoreductase activity and catalyze thiol exchange reactions (Pan, 2006). The central domains of GRXCR1 and GRXCR2 retain low level [19.6%] conservation with one another in this region of the proteins. Key residues in glutaredoxins, including putative active site cysteines, are absent in GRXCR2, indicating that GRXCR2 is very unlikely to possess oxidoreductase activity. Nonetheless, comparative sequence analysis suggests partial structural similarity of this central region of GRXCR2 with a catalytically inactive thioredoxin fold region (Figure 4.1 C, Odeh, 2010).

Grxcr2 orthologs are present in vertebrate species including human, opossum, chicken, frog, and fish with the most conserved residues at the –N and –C termini, including complete conservation of cysteine residues of the C-terminal domain ($CX_2CX_7CX_2CX_{20}CX_2CX_7C$) (Figure 4.2 A). The more divergent,

central region of GRXCR2 varies in relative size among orthologs and with GRXCR1.

In RNA prepared from the cochleae of wild type mice at 3 weeks of age, we observed a substantial level of *Grxcr2* transcripts containing the three coding exons of the gene (Figure 4.2 B). *Grxcr2* transcripts were undetectable in RNA from a variety of other tissues (Figure 4.2 B). All publicly available *Grxcr2* EST database sequences were also derived from inner ear cDNA libraries, consistent with relatively selective expression of the gene in the inner ear.

Targeting the *Grxcr2* locus to derive *Grxcr2* mutant mice

Based upon the conservation in sequence and expression pattern with *Grxcr1*, we hypothesized a similar requirement for *Grxcr2* in inner ear development. To directly test this, we generated a mutation of *Grxcr2* using homologous recombination in mouse ES cells and the targeting strategy summarized in Figure 4.3 A. Bioinformatic analysis of regions surrounding exon 1 was performed to identify positions for LoxP recombination sites that would be least likely to disrupt putative transcription factor binding sites or interfere with splicing. Southern blot analysis was used to identify ES cell clones with homologous integration of the floxed exon1 and downstream neomycin selection cassette into the endogenous *Grxcr2* locus (data not shown). Chimeric mice were generated from microinjection of correctly targeted ES clones into blastocysts and transferred to pseudopregnant females. These chimeras were mated with transgenic mice expressing Cre recombinase from an EIIa promoter-enhancer. Cre-mediated deletion of exon 1 early in embryogenesis produced

mice carrying the mutant *Grxcr2* allele. Intercross of these mice produced offspring at weaning age of the three expected genotypes at expected Mendelian ratios as determined by a Pearson $\chi^2(1,N = 46) = 0.02518$, $p = 0.05$, indicating that *Grxcr2* is not critical for general viability (Figure 4.3 B).

RT-PCR analysis of cochlear RNA indicated that heterozygote carriers of the deleted *Grxcr2* allele (wt/Δ) expressed full-length *Grxcr2* transcripts (Figure 4.3 C). Full-length transcripts were absent in mice homozygous for the *Grxcr2* mutant allele (Δ/Δ), consistent with deletion of exon 1 (Figure 4.3 C). Using antiserum generated against a GRXCR2 peptide encoded by exon 1, we detected immunoreactivity in the stereocilia of heterozygous animals (Figure 4.3 D). This reactivity was significantly diminished in tissue from homozygous mutants, consistent with loss of exon 1 and ablation of the GRXCR2 protein expression. Additional specificity controls for this antiserum, including incubation with cultured cells fixed after transfection with *Grxcr1* or *Grxcr2* expression constructs, supported GRXCR2 specificity (data not shown).

GRXCR2 mutants exhibit significant hearing loss

Grxcr2 homozygous mutants responded to loud sound with startle reflexes at two weeks of age, the onset of hearing in normal mice, indicating at least some auditory function in the mutants. For a more objective measure of hearing ability, we evaluated auditory brainstem responses (ABR), a measurement of synchronous auditory activity in response to sound, at a range of stimulus frequencies (4-48 kHZ) at 4 and 12 weeks of age. Wild type and *Grxcr2* heterozygote animals exhibited relatively low ABR thresholds in response to 4,

12, and 24 kHZ tones at 4 weeks of age (Figure 4.4 A). In contrast, hearing thresholds to these frequencies in *Grxcr2* mutants were elevated by approximately 30 to 60 dB above those of control mice (Figure 4.4 A). The requirement for two mutant alleles to manifest a phenotype indicated a recessive mode of inheritance of hearing loss. High thresholds in response to 48 kHZ tones were observed in both controls and homozygous mutant mice and likely reflects the effects of the *Ahl* locus segregating in the *C57BL/6* background, which predisposes many inbred strains to age-related hearing loss (ARHL) at high frequencies (Noben-Trauth, 2003). Similar ABR threshold shifts at 4, 12, and 24 kHZ were observed at 4 weeks of age in homozygous mutants from a second *Grxcr2* line that was derived from an independently targeted ES clone, verifying the role of the mutant *Grxcr2* locus in the abnormal phenotype (data not shown). We also observed similar threshold shifts in *Grxcr2* mutant homozygotes segregating an ARHL-resistant allele of *Ahl* derived from FVB mice (data not shown).

ABR measurements at 12 weeks of age indicated an average threshold shift in *Grxcr2* mutants of 40 to 70 dB at lower frequencies relative to littermate controls. The 10 dB progression in hearing loss between 4 and 12 weeks in *Grxcr2* mutant mice was statistically significant for 12, 24, and 48 kHz stimuli but not 4 kHz (Figure 4.4 A & B). The involvement of the *Grxcr2* mutation in progressive hearing loss at higher frequencies is likely complicated by the loss observed in the control strains due to the *Ahl* susceptibility locus and other potential genetic background effects.

We evaluated distortion product otoacoustic emissions (DPOAE) as a second objective measurement of hearing ability in the *Grxcr2* strain. DPOAE are responses of the cochlea that are evoked by delivery of 2 tones of similar frequency to the ear and are believed to be due principally to the amplification activity of outer hair cells (Kemp, 1978). At 4 weeks of age, littermate controls exhibited a stepwise increase in DPOAEs in response to a 12 kHz stimuli greater than 30 dB in intensity (Figure 4.4 C). In contrast, *Grxcr2* mutants exhibited significant DPOAEs only in response to stimuli at 70 and 80 dB SPL (Figure 4.4 C). These responses to very high intensity stimuli that likely represent distortion artifacts that are present even in euthanized animals (Mustapha, 2009). Similar reduced emissions in response to stimuli at 24 kHz were observed in *Grxcr2* mutants, supporting extensive loss of outer hair cell function at other locations along the cochlea (data not shown).

Hearing loss in *Grxcr2* mutants is associated with defects in stereocilia orientation and organization

In order to identify a potential developmental correlate of the hearing loss observed in *Grxcr2* mutant mice, we used scanning electron microscopy (SEM) to evaluate cochlear morphology at early postnatal time points. During the first postnatal week, *Grxcr2* heterozygotes exhibited a single row of inner hair cells and three rows of outer hair cells along the length of the cochleae (Figure 4.5 A, C). The apical surface of the sensory cells contained well organized, ‘V’ shaped stereocilia bundles with a single kinocilium at their vertices and orientated with axes perpendicular to the longitudinal axis of the cochlea (Figure 4.5 A,C).

Overall organization of inner and outer hair cells was normal in cochleae of *Grxcr2* mutant mice (Figure 4.5 B,D). At P0, however, many stereocilia bundles in *Grxcr2* mutants exhibited subtle deviations in their orientation (Figure 4.5 B). These defects were more obvious in bundles on outer hair cells. One week later (P7), progression of stereocilia defects were observed in *Grxcr2* mutants. Most bundles in the mutants exhibited orientation defects, with many showing more exaggerated deviation from the normal axis of polarity (Figure 4 E-H). In addition, most bundles were lacking the normal "V" shape found in control mice. Extreme disorganization was often observed, including examples of split, splayed, and even circular bundles (Figure 4.5 E-H).

We further characterized the early postnatal defects in stereocilia bundles by treating cochleae dissected at P3 from heterozygous controls and *Grxcr2* mutant mice with an antibody specific for acetylated-α-tubulin, which immunostains the microtubules present in the kinocilia of developing hair cells, and with phalloidin, which reacts specifically with actin filaments, including those in the core of stereocilia. All bundles in *Grxcr2* heterozygous cochleae exhibited alpha tubulin-positive kinocilia at their vertices and orientations of the bundles axes were tightly distributed around 90^0 with respect to the longitudinal axis of the cochlea, consistent with SEM analyses (Figure 4.6 B). In *Grxcr2* mutant cochleae, alpha tubulin-positive kinocilia were also observed at the vertices of bundles. However, the orientation of bundle axes exhibited significantly greater deviation from 90^0 and suggests a randomization of bundle polarity in the mutants (Figure 4.6 C).

Expression and localization of *Grxcr2* in the inner ear

Quantitative RT-PCR (qRT-PCR), using *Grxcr2* specific primers, was performed on RT-products generated from whole inner ear RNA from *C57BL/6J* mice during the first postnatal week and at 1 month of age after the cochlea is mature. The *Grxcr2* transcript levels attained were normalized to those present at birth in order to survey the transcript profile over time. *Grxcr2* expression shows an apparent peak at postnatal day three and declines through the first postnatal week and into maturity (Figure 4.7 A).

The sensory epithelium was dissected from *C57BL/6J* mice and immunostained using the GRXCR2 antibody. In the mid-cochlear region at birth, the primary site of GRXCR2 immunoreactivity was in stereocilia of inner and outer hair cells (Figure 4.7 B). Robust expression persisted in inner and outer hair cell stereocilia at postnatal day 3 and was substantially reduced at 1 week after birth (Figure 4.7 B). A similar time course of stereocilia expression was also observed at other locations along the length of the cochlea (data not shown). We have also observed similar lower relative levels of GRXCR2 in the stereocilia of vestibular organs (data not shown).

Progressive hearing loss in a *Grxcr2* hypomorphic mutant

Neomycin selection cassettes in targeted alleles have often been associated with decreased transcript levels of the targeted gene due to aberrant splicing from an endogenous exon into cryptic splice acceptor sites present in the neomycin cassette (Nagy, 1998). To test for this effect in the intact floxed *Grxcr2* allele, we used quantitative RT-PCR (qRT-PCR) to quantify *Grxcr2* transcripts in

the cochleae of mice heterozygous and homozygous for the floxed allele. A ~50% reduction in *Grxcr2* transcripts were observed in mice homozygous for the floxed allele relative to heterozygous controls when measured at 2 months of age (Figure 4.8 A).

To determine the effect of hypomorphic *Grxcr2* gene expression on auditory function we characterized mice carrying the *Grxcr2* floxed allele. ABR measurements at two months of age demonstrated that *Grxcr2* floxed homozygotes have auditory function equivalent to floxed heterozygous controls at 12 and 24 but with elevated thresholds at 4 kHz (Figure 4.8 B). By five months of age, mice homozygous for the *Grxcr2* floxed allele exhibited progression of hearing loss, with increases in thresholds relative to littermate controls at both 4 and 12 kHz (Figure 4.8 C). Evaluation of the apical surfaces of cochlear neuroepithelia of these mice by SEM indicated altered stereocilia bundles in a small number of outer hair cells from the *Grxcr2* floxed homozygotes at two months of age (Figure 4.8 B). Consistent with the increased thresholds at later ages, nearly all outer hair cells in seven month old *Grxcr2* floxed homozygotes exhibited severe bundle defects (Figure 4.8 C). These defects included flattened, split and misoriented bundles reminiscent of those observed in early postnatal mice carrying the *Grxcr2* null allele.

These results indicate that the hypomorphic level of *Grxcr2* expression in the floxed homozygote mutants is sufficient for relatively normal development of stereocilia bundles and hearing function at least in the more basal regions of the

cochlea. This level appears to be, however, unable to sustain normal cochlear function at later ages and is associated with severe bundle defects.

DISCUSSION

Evaluation of mouse deafness mutants has provided key insight into genes required for in inner ear development and function (Dror, 2009). Many of these genes function in the early development and maturation of stereocilia bundles, the specialized actin filament-rich extensions on the apical surface of sensory hair cells that are critical for mechanotransduction of auditory and vestibular stimuli (Petit, 2009). The present study demonstrates a critical role for *Grxcr2* in stereocilia bundle maturation and in normal auditory function. Based upon sequence analysis of *Grxcr2* and nearby genes, this region of mouse chromosome 18 is paralogous with a portion of central chromosome 5 containing *Grxcr1*, a gene previously implicated in sensory cell maturation based upon identification of mutations in the mouse deafness mutant pirouette (Odeh, 2010). *Grxcr2* is expressed at early postnatal time points and in adult mice and, like *Grxcr1*, expression is relatively restricted to the inner ear. These common expression characteristics of the paralogs suggest that both genes have retained common, cis-acting regulatory elements that control transcription in sensory cells. In addition, the GRXCR2 protein, like GRXCR1, is localized along the length of stereocilia of sensory cells in the cochlea and in vestibular organs, suggesting that both proteins are likely to rely on shared determinants that regulate cellular trafficking and/or localization. Consistent with this notion, we

have demonstrated that the N-termini of both proteins are necessary for subcellular localization to actin filament-rich structures (unpublished data).

In the current study, we generated a targeted deletion of the first exon of mouse *Grxcr2*, which encodes the N-terminal region of the GRXCR2 protein. Heterozygotes carrying this deletion allele exhibited ABR thresholds and DPOAE responses similar to those of wild type littermates, while responses in *Grxcr2* deletion homozygotes were significantly reduced, indicating a recessive mode of inheritance for hearing loss. The hearing loss in mutants is associated with alterations in stereocilia bundle maturation in the cochlea, which are observed during the first postnatal week and are most evident on outer hair cells. The extent of hearing loss in *Grxcr2* mutants is generally consistent with loss of the amplification function of outer hair cells (Dallos, 1973). Abnormal function would be predicted for the severe bundle organization defects found on outer hair cells in the mutants. Indeed, *Grxcr2* mutants exhibited significantly elevated DPOAE thresholds consistent with a decreased outer hair cell function. Hearing loss progresses somewhat in older *Grxcr2* mutants and suggests that inner hair cell function may also be compromised despite their relatively normal morphology at later ages.

At birth we observed misorientation of maturing bundles in the cochleae of *Grxcr2* mutants. Bundles on outer hair cells had significant deviations in both directions from the normal axis of symmetry. The precise orientation of stereocilia bundles in the cochlea depends in part upon components of planar cell polarity (PCP) pathways, an evolutionarily conserved set of pathways that play key roles

in coordinating the orientation of cells and structures in a two-dimensional plane in many tissues (Rida, 2009). Asymmetric localization of membrane-associated PCP proteins such as VANGL2 and FZ3 to the lateral or medial sides of developing neuroepithelial cells later in embryogenesis provide key polarity cues in the organ of Corti (Chacon-Heszele, 2009). Defects in these or other core PCP genes result in random orientation of bundles in the cochlea. These mutants often exhibit shortened cochleae, which may result from defects in convergent extension, a PCP-mediated process that directs orderly migration of epithelial cells in many tissues. Cochleae in *Grxcr2* mutants appear to be no different in length than those of control littermate mice (data not shown), suggesting that convergent extension processes are unaffected and that core PCP pathways are intact.

The microtubule-based kinocilium also plays a key role in the proper orientation of the bundles. Single kinocilium are located centrally on the apical surface of cochlear hair cells by approximately *E16* in the mouse and surrounded by short microvilli (Sobkowicz, 1995). As stereocilia develop by increases in the dimensions of these microvilli, the kinocilium moves toward the lateral side of hair cells and is positioned at the vertex of the developing bundle, adjacent to the longest rank of stereocilia. Several ciliary mutants that alter kinocilia formation also exhibit randomized bundle orientation, together with often flattened bundles, indicating the importance of this structure in the polarity process and in formation of the “V” shaped bundle (Ross, 2005;Park, 2006;Jones, 2008;Sipe, 2011). The kinocilia in the cochleae of early postnatal *Grxcr2* mutants were located at or

near the bundle vertex, suggesting that loss of *Grxcr2* function does not affect production of kinocilia or this early step in polarization of the bundle.

Stereocilia bundle organization and cohesion is dependent upon an intricate set of interstereocilia links that are first observed during early bundle development (Goodyear, 2005). The components of many of these links, as well as their associated proteins, have been identified as products of genes mutated in Ushers Syndrome, a sensory disorder that combines hearing loss with progressive retinal degeneration (Muller, 2008; Lefevre, 2008). Evaluation of several mouse models that carry mutations in these genes has demonstrated the critical requirement of Usher proteins for normal bundle maturation (Lefevre, 2008). These mutants exhibit a combination of phenotypes, including disorganization and fragmentation of bundles as well as bundle orientation defects that are associated with mislocalized kinocilia (Lefevre, 2008). These phenotypes indicate that interstereocilia links are required for cohesion of the developing bundles and also suggest that connecting links between the kinocilia and the tallest stereocilia are important for proper orientation of the bundle. *Rac1*, which encodes a small GTPase, although not implicated in Ushers Syndrome, also appears to similarly affect bundle maturation (Grimsley-Myers, 2009). Mice carrying a conditional *Rac1* mutation exhibit polarity defects and disorganization of stereocilia bundles associated with mispositioned kinocilia, suggesting that the *Rac1* pathway influences both PCP and kinocilia-stereocilia interactions.

The bundle polarity and organization defects in the mouse Usher mutants resemble but are clearly not identical to the phenotypes we observed in *Grxcr2*

mutants. Cochlear bundles in Usher mutants exhibit severe disorganization by late embryogenesis, including fragmented and flattened bundle morphologies. While similar disorganized bundles were observed in *Grxcr2* mutants, at early postnatal ages the bundles, although often misoriented, were relatively intact and associated with kinocilia, and then underwent a rapidly progressive disorganization. Although not investigated in detail, we do observe tip links in mutant bundles of the utricle (data not shown). This along with the appearance of relatively intact bundles in early postnatal *Grxcr2* mutants is consistent with normal initiation of the developmental linkages required for normal cohesion. In addition, the ability of outer hair cells in *Grxcr2* mutants to generate relatively normal transduction currents suggests normal assembly of the apparatus necessary for mechanotransduction, including tip links. The timing of orientation and disorganization phenotypes in *Grxcr2* mutants is more similar to that observed in the *Rac1* mutants, although progression of disorganization has not been fully investigated due to the perinatal lethality of this *Rac1* mutation. *Grxcr2* mutants, however, do not exhibit the early kinocilia mispositioning found in *Rac1* mutants.

The transcriptional profile of *Grxcr2* across developmental and adult time points identified an apparent peak in expression early during the first postnatal week of life and diminished thereafter. Coincidentally, whole mount immunostaining demonstrated a similar pattern for GRXCR2 localization to the stereocilia. Consistent with a predicted role for this gene in development, these studies demonstrate the presence of GRXCR2 in the bundle during a time in

which hair bundles are still establishing their orientation and organization (Nayak, 2007). Despite GRXCR2 localization to stereocilia of sensory hair cells of the cochlear and vestibular organs, the primary effect of the *Grxcr2* mutation is most prominent in developing stereocilia of outer hair cells with little or no effects observed in stereocilia of other sensory hair cell types cells. Perhaps it is the case that another protein, with the likeliest candidate being GRXCR1, is playing a partially redundant function in the stereocilia of cells types other than outer hair cells. This hypothesis would account for an outer hair cell specific phenotype and could be directly tested by crossing a null mutant allele of *Grxcr1* onto a homozygous *Grxcr2* mutant background. Analysis of inner hair cell and vestibular hair cell stereocilia on a background with 50% less GRXCR1 may uncover a phenotype consistent with a partially redundant function.

Evaluation of mice that carried the neo cassette (floxed allele) used in generation of the *Grxcr2* deletion allele indicated a potential role of the gene in maintaining bundle structure and function in the mature cochlea. By quantitative RT-PCR (qRT-PCR) we demonstrate that the steady state level of full-length *Grxcr2* transcripts in cochleae from mice homozygous for the floxed allele were reduced by approximately 25% compared to floxed heterozygote controls. At two months of age, the homozygous floxed mice exhibited ABR thresholds similar to those of littermate controls (wild type and floxed heterozygotes), suggesting that reduced levels of *Grxcr2* transcripts are sufficient for development of normal function of the cochlea. The reduced level of transcripts in the homozygous floxed mice, however, was associated with progressive increases in threshold

responses at later ages, along with misoriented and disorganized stereocilia bundles. We also observed a milder disorganization phenotype at two months of age, indicating that function of outer hair cells may be only minimally affected by such bundle defects. This situation is similar to the normal ABR thresholds observed in mice carrying mutations in the *Alms1* gene, which appears to affect basal body/kinocilia function in cochlear hair cells and results in mild bundle polarization defects in young mice (Jagger, 2011). Although we cannot rule out secondary effects due to solely a developmental defect as the basis for this loss of function in the hypomorphic mutants, the observed progressive functional loss associated with more severe bundle defects suggests that higher levels of *Grxcr2* are required for continued cohesion and normal polarity of the bundle in the mature cochlea. The molecular control of bundle maintenance is not well understood. The association of progressive hearing loss in humans with mutations in either Myo7a (Liu, 1997) or Actg1 (Van Wijk, 2003;Zhu, 2003) suggests that other genes required for stereocilia development (Gibson, 1995; Belyantseva, 2009) may be similarly required to maintain cochlear function in the adult. Evaluation of hearing in conditional mutant mice that undergo deletion of the floxed exon 1 after auditory development and maturation should more directly clarify the role of *Grxcr2* in the mature inner ear.

The current study of *Grxcr2* mutant mice, together with analysis of pirouette mice that carry null mutations in *Grxcr1* (Erven, 2002;Odeh, 2010; Beyer, 2000;Odeh, 2004), indicate that both genes are required for normal development of auditory function. While both loss of function mutations result in

significant hearing loss at early ages, notable differences in cochlear pathology are associated with each mutation. Hearing loss in *Grxcr1* mutants is associated with relatively thin stereocilia of both inner and outer hair cells by postnatal day 1, these thin stereocilia fail to increase significantly in diameter beyond this age (Erven, 2002). Bundles in *Grxcr1* mutants exhibit relatively normal polarity and organization/cohesion at birth, although bundles become progressively disorganized during the first 2 weeks of age. Notably, the disorganization in pirouette is quite different in appearance from that observed in *Grxcr2* mutants. Stereocilia dimensions in *Grxcr2* mutants do not appear qualitatively different than those in control littermates, suggesting that GRXCR1 and GRXCR2 have distinct biological functions despite their similarities in primary sequence and localization.

Interestingly, *Grxcr2* mutants do not exhibit the behavioral defects typical of vestibular dysfunction present in many mouse deafness mutants, including mice that carry mutations in *Grxcr1*. Although GRXCR2 is normally expressed in sensory cells of vestibular organs and localized to stereocilia, in *Grxcr2* mutant mice we observed well-organized stereocilia bundles with no apparent defects in bundle orientation. While GRXCR1 and GRXCR2 appear to have distinct roles during the maturation of sensory cells in the cochlea, we cannot rule out potential overlap in the roles of these proteins in the vestibular system. GRXCR1 could partially compensate for loss of GRXCR2 function in vestibular stereocilia, similar to the apparent compensation of the actin binding protein ezrin in the vestibular organs of mice carrying null mutations in radixin (Kitajiri, 2004).

The early sensory cell defects in *Grxcr2* mutants indicate a critical role in mediating maturation of stereocilia bundles in the cochlea. The mechanism underlying this role is unclear at present. The localization of GRXCR2 protein throughout the stereocilia suggests that it plays a local, intrinsic role in bundle development that influences normal orientation, organization and cohesion of the bundles. GRXCR2 is unlikely to possess the putative redox activity suggested for GRXCR1 (Odeh, 2010), as the central domain of GRXCR2, while retaining some secondary structural characteristics of a thioredoxin fold, does not contain the cysteine motifs found in the active sites of oxidoreductase proteins. Thioredoxin fold domains have been implicated in other roles that are independent of redox activity, including serving as interaction sites for other cellular proteins, as predicted for the thioredoxin domain in the PICOT/GRX3 protein (Jeong, 2008) and as either intrinsic (Kern, 2003;McGee, 2006) or accessory chaperones (McCormack, 2009). Although we have evidence that the conserved C-terminal Cys-rich domain is required for putative homo-multimer formation of GRXCR2 (unpublished data), similar Cys-rich regions have been implicated in heteromeric protein interactions, such as the interaction of the zinc-finger motif of yeast YY1 with its co-factor ATF/CRE binding protein (ATF/CREB) (Zhou, 1995). Interactions of GRXCR2 with other stereocilia components such as the Usher protein network may be required for appropriate integration of PCP and bundle cohesion/organization pathways for normal maturation of a functional bundle.

In addition to the role of GRXCR1 in regulating stereocilia dimension and our current demonstration of a requirement for GRXCR2 in bundle orientation

and organization, a homolog of this gene family has also been implicated in actin filament-related processes. Mutations in Thrumin1, an *Arabidopsis thaliana* homolog of GRXCR1 and GRXCR2, result in loss of the light-mediated chloroplast movement response (Whippo, 2011). Movement enhances light absorption for photosynthesic reactions in chloroplast and appears to occur through actin filament reorganization at the plasma membrane (Kadota, 2009;Suetsugu, 2011). The actin filament binding and bundling activity that has been demonstrated for Thrumin1 is likely to directly regulate filament reorganization. Given the likely importance of actin filament elongation or bundling in the determination of stereocilia dimension, the role of GRXCR1 in this process may also involve a more direct effect on actin filament dynamics. Consistent with this notion, Thrumin1 exhibits higher overall sequence similarity to GRXCR1 than to GRXCR2, particularly in the central region of the proteins. General similarities in the molecular pathways that regulate mechanosensory cell development across extant species are consistent with the notion that evolution of mechanosensation has been driven at least in part by derivation from a common ancestral cell (Fritzsch, 2006). The apparent absence of *Grxcr2* orthologs in extant non-vertebrate species and the critical requirement of *Grxcr2* for precise bundle orientation and organization, a prominent feature of sensory cells in the inner ear of vertebrates, are consistent with a key role of *Grxcr2* in the evolution of the inner ear in this subphylum.

Numerous genes have been implicated in the proper development of the stereocilia (petite, C 2009). The current genes are not all encompassing and the

functional roles of many known genes are not elucidated. Here we develop a mouse model of *Grxcr2* and demonstrate a requirement for it in normal cochlear function and define a role for this gene in proper stereocilia development. This mouse models provides a resource to further characterize the functional role *Grxcr2* in stereocilia development. The hearing phenotype identified in *Grxcr2* mutant mice suggests that mutations in *GRXCR2* may similarly underlie inherited hearing loss in humans. Through collaborative screening, we have evaluated genomic DNA from over 500 individuals with recessive, congenital, severe to profound hearing loss for variants in *GRXCR2* but have not identified any likely causative mutations (unpublished data). Additional phenotypic analysis of the *Grxcr2* mouse model, including the residual hearing, absence of overt vestibular phenotypes and distinct organization and orientation stereocilia defects suggest that human *GRXCR2* mutations may instead underlie a class of Ushers Syndrome patients with moderate or variable hearing and vestibular clinical manifestations.

CHAPTER 5

Structure-function approach to identifying biochemical properties of GRXCR1 and GRXCR2

Avenarius contribution: All work and figures presented in this chapter was original work complete by Avenarius, M.

INTRODUCTION

The glutaredoxin-like cysteine-rich family of genes is required for auditory function in mammalian species (Odeh, 2010; Schraders, 2010; Avenarius M, 2011). Mutations in *Grxcr1* and *Grxcr2* are associated with distinct defects in early stereocilia development. *Grxcr1* mutants fail to achieve proper stereocilia dimensions and *Grxcr2* mutants exhibit defects in hair bundle orientation and organization (Odeh, 2010; Schraders, 2010; Avenarius M, 2011). Vertebrate species commonly encode the two novel glutaredoxin-like cysteine-rich proteins GRXCR1 and GRXCR2, while invertebrates and plants encode proteins that appear to be orthologous to GRXCR1. Genetic and biochemical studies in *Arabidopsis thaliana* identified *Thrumin-1*, a plant homolog of *Grxcr1*, and demonstrated a functional role for THRUMIN1 in chloroplast transport

(Whippo, 2011). THRUMIN1 directly binds and bundles actin filaments at or near the plasma membrane in response to light stimuli to facilitate the transport of chloroplasts (Whippo, 2011). Regulation of the actin filament cytoskeleton is a common mechanism in plants to localize chloroplasts to proper subcellular compartments (Maly, 2001; Sun, 2010).

Overexpression of *Grxcr1* in heterologous cell types induces a qualitative lengthening of actin filament-rich structures, consistent with a role for GRXCR1 in regulating actin filament architecture (Odeh, 2010; Avenarius M, 2011). *tasmanian devil*, a mouse strain carrying a null mutation in *Grxcr1*, is associated with quantitatively thin stereocilia, a developmental defect correlated with a decrease in actin filament content (Erven, 2002). These studies and those conducted in plants demonstrate effects on actin dynamics in response to loss of *Grxcr1* function and suggests an evolutionarily conserved role for GRXCR1 in the dynamic regulation of actin biology. The similar co-localization of GRXCR2 to the stereocilia suggests that it too may impact actin filament processes involved in bundle organization and orientation.

Sequence analysis of GRXCR1 and GRXCR2 paralogs suggests three discrete domains in these proteins: an N-terminal domain, a central/glutaredoxin-like domain, and a C-terminal cysteine-rich domain (Figure 5.1 A,B). The N-terminal domains of GRXCR1 and GRXCR2 do not show sequence similarity to any other known proteins (Figure 5.1 A). The C-terminus encodes a series of cysteine residues ($Cx_2Cx_7Cx_2Cx_{20}Cx_2Cx_7C$) configured in a putative zinc finger motif that are conserved between the two paralogs and throughout all known

GRXCR1 and GRXCR2 homologs (Figure 5.1 A). Lastly, the central, and most divergent, domain encodes a thioredoxin-like fold that in GRXCR1 shows similarity to the glutaredoxin-like family of proteins (Figure 5.1 A).

A structure-function approach was used in the current study to identify functional domains of the glutaredoxin-like cysteine-rich family of proteins. This approach attempts to correlate a discrete set of amino acid residues with a specific property of the protein. Like the studies presented in Chapter 3 detailing the role of the N-terminus of GRXCR1 in localization to actin filament-rich structures, I have demonstrated a similar role in localization of GRXCR2 to actin-rich structures for its N-terminal domain. Using two different interactions assays, I have also obtained evidence of the importance of conserved cysteines in the C-terminal region of both proteins for homo- and heteromeric interactions of the two paralogs. Finally, I present data relating to initial attempts to purify recombinant GRXCR2 protein. Although these studies were incomplete due to difficulties in obtaining soluble protein, analysis of purified protein will likely be critical for understanding possible activities of these proteins. For example, based on similar domains in functionally characterized proteins (Pan, 2006), the central glutaredoxin-like domain of GRXCR1 may possess intrinsic redox activity or alternatively, may act as a molecular chaperone. Similarly, the conserved cysteine residues configured in a putative zinc finger motif at the C-terminal regions of both GRXCR1 and GRXCR2 suggests that this domain may bind zinc or other divalent cations. Collectively, structure-function analyses and investigation of the *in vitro* properties of purified proteins should provide

important insight into the mechanisms of action of GRXCR1 and GRXCR2 in the context of stereocilia development.

METHODS

Constructs (Yeast-two-hybrid). The open reading frame of mouse *Grxcr1* was amplified and cloned downstream of the coding sequences of the GAL4 binding domain (p-GBKT7) and the GAL4 activation domain (p-GADT7) (Clontech, Mountain View, CA).

Yeast-two-hybrid. Yeast (Y187 or AH109) was transformed with the following constructs: p-GBKT7 (empty 'bait' vector), p-GADT7 (empty 'prey' vector), *Grxcr1*-pGBKT7, *Grxcr1*-pGADT7, *Grxcr2*-pGBKT7, *Grxcr2*-pGADT7, and a series of *Grxcr1* and *Grxcr2* mutants (Cys→Ala of zinc finger motif) in the pGBKT7 vector (Zymo Research, CA). Matings were performed by combining a single colony from a pGADT7 containing strain (AH109) with a pGBKT7 strain (Y187) in YPAD and incubating for 20 hours at 30 degrees. The mated cells were plated on single drop-out plates (-Leu or -Trp) to assay transformation efficiency and double drop-out plates (-Leu, -Trp) to assay mating efficiency. A single colony from the DDO plate was picked and resuspended in 200 μL of H_2O, vortexed and a loop full was streaked out in a patch on DDO, TDO (-Leu, -Trp, -His), QDO (-Leu, -Trp, -His, -Ade), and in some cases QDO plates containing X-gal to assay activation of interaction reporter genes. Plates were incubated up to 6 days and scored for growth.

Constructs (Native gel). The open reading frames of mouse *Grxcr1* and *Grxcr2* were amplified with a C-terminal MYC tag and cloned into peGFP-N1 (BD

Biosciences, Palo Alto). A stop codon was inserted after the C-terminal MYC tag so that the downstream green fluorescent protein (GFP) was not translated. Overlap PCR was used to generate a series of deletion constructs.

Native gel electrophoresis. Cos-7 cells were transfected using the Mirus reagent (Madison, WI) with the following constructs: GRXCR1::myc, GRXCR1::flag, GRXCR1(5' cysteines mutated)::myc, GRXCR1(3' cysteines mutated)::myc, GRXCR1(5' + 3' cysteines mutated)::myc. Lysates were harvested, quantified, and 35 µg of total protein was resolved on a 12% polyacrylamide gel under native conditions (25 mM Tris-Cl, pH 8.4 and 192 mM glycine with 0.2% sodium deoxycholate) for 1.5 hours at 100 volts. The gel was transferred to a polyvinylidene difluoride (PVDF) membrane and incubated with 1:1500 mouse α-myc (Invitrogen-Carlsbad, CA) after blocking of non-specific protein binding with 5% nonfat dried milk. Immobilized antigens were detected by the ECL Plus Western blotting reagent (GE Healthcare - Piscataway, NJ).

Constructs (protein purification). The open reading frame of mouse *Grxcr1* and *Grxcr2* was amplified with a C-terminal MYC tag and cloned into the pET-15b vector (Novagen) to generate a minimal His tagged version of the MYC-GRXCR2 fusion protein and the pMAL-4a5 vector (NEB) to generate a Maltose Bind Protein (MBP) tagged version of the MYC-GRXCR2 fusion protein.

GRXCR1 and GRXCR2 protein purification. Constructs were transformed into the BL21 STAR *E. coli* strain. A single colony was used to inoculate a 5 mL starter culture and the next day was used to inoculate a large culture at 1:100. The culture was grown to on OD_{600}= 0.5 and was induced with

0.25 mM IPTG for 4 hours at 37°C or overnight at 15°C. After induction the cells were centrifuged at 4,000 x g for 15 mins (4° C) and resuspended in lysis buffer (0.2 M NaCL, 20 mM Tris-HCl, 1 mM EDTA, 3 mM Sodium Azide, and 1 mM DTT, 0.2 M PMSF and a Roche protease inhibitor tablet). Samples were sonicated (5 rounds of 15 second bursts) and centrifuged at 14,000 rpm for 20 mins (4°C) to separate the soluble from insoluble fraction. The soluble fraction was combined and incubated with amylose resin for 1 hour to affinity capture the GRXCR2-pMAL hybrid protein. After incubation the resin + GRXCR2-pMAL mixture was washed by centrifuging at 2,000 x g for 7 mins, the supernatant was decanted and replaced with lysis buffer; this wash was repeated a total of 5 times. After the final wash 1 mL of 20 mM Maltose resuspended in lysis buffer was added to the affinity mixture and incubated for 10 minutes to competitively eliminate GRXCR2-pMAL protein interactions with the amylose resin. A final centrifugation step was performed and the supernatant was removed. Mass spectrometry and Western blotting were used to assess the levels and purity of GRXCR2 hybrid protein in the supernatant.

RESULTS

Transfection of a construct expressing wild type GRXCR2 into CL4 cells indicated primary localization of the protein in apical microvilli (Figure 5.2 A). Mutant proteins that lacked the central domain or the C-terminal Cys-rich domain of GRXCR2 were also capable of microvilli localization, albeit at slightly reduced efficiencies relative to wild type protein (Figure 5.2 B,C). Mutant protein lacking the N-terminus of GRXCR2, however, failed to localize to the apical surface and

was present mainly in the cytoplasm and nucleus of transfected cells (Figure 5.2 D) similar to GFP alone (Figure 5.2 F). A mutant protein containing only this N-terminal domain (Figure 5.2 E) localized to microvilli much like the wild type protein, indicating that this domain is both necessary and sufficient for microvilli localization in CL4 cells.

TESTING FOR AUTOACTIVATION OF Y2H CONSTRUCTS. AH109 or Y187 derived strains carrying the constructs *Grxcr1*-pGBKT7, *Grxcr1*-pGADT7, *Grxcr2*-pGBKT7, and *Grxcr2*-pGADT7 were initially tested for autoactivation of the yeast reporter genes by mating to the appropriate control strains carrying empty pGADT7 or pGBKT7 vectors. In each case reciprocal mating of the experimental strains to the empty vector control strains produced colonies on DDO media, petite 'satellite' colonies on TDO, and no colonies on QDO. These results confirm that strains carrying full-length Grxcr1 or Grxcr2 hybrid constructs do not autoactivate the yeast reporter genes (Figure 5.3 & 5.4).

GRXCR1 HOMODIMERIZATION - Y2H EVIDENCE. To test the hypothesis that GRXCR1 interacts with itself, yeast strains separately carrying GRXCR1-pGADT7 and GRXCR1-pGBKT7 were mated. Colonies were observed on DDO media confirming successful mating of the two strains (Figure 5.5). The presence of colonies on TDO, QDO, QDO + X-gal media is consistent with a positive GRXCR1 self-interaction (Figure 5.5).

We next sought to identify the structural domain(s) required for putative GRXCR1 homodimer formation through testing a series of constructs with deletions of each of the three GRXCR1 domains (Δ N-terminus, Δ glutaredoxin-

like, Δ cysteine-rich). The only construct that produced a stable hybrid-protein, Δ cysteine-rich domain, was mated to full length GRXCR1. Successful mating was observed by the presence of colonies on DDO media but the absence of colonies on TDO, QDO, and QDO + X-gal media implicated the cysteine-rich domain in the homodimerization of GRXCR1 (Figure 5.5).

Site directed mutations were made within the cysteine-rich C-terminal domain to test the necessity of the conserved cysteine residues for GRXCR1 homodimer formation (Figure 5.1 A,B). Successful mating of strains carrying GRXCR1(5' Cys→Ala), GRXCR1(3' Cys→Ala), and GRXCR1(5' + 3' Cys→Ala) to full length GRXCR1 was evident by the presence of diploid colonies on DDO media. Diploid colonies were unable to grow on TDO, QDO, or QDO + X-gal media, indicating lack of interactions and consistent with the Cys residues of the C-terminal domain as the structural element underlying homodimerization of GRXCR1 (Figure 5.5). Note that constructs containing Cys→Ala alterations expressed stable mutant protein (data not shown).

GRXCR1 HOMODIMERIZATION - NATIVE GEL ELECTROPHORESIS EVIDENCE. To further validate the necessity of the Cys residues in GRXCR1 homodimer formation a second, native gel electrophoresis approach was taken. GRXCR1 protein in whole cell lysates migrated as two distinct species, one at approximately 30 kD and the other at 75 kD (Figure 5.6). The two products are consistent with the sizes expected for GRXCR1 monomeric and dimeric species, respectively. A similar pattern is observed when the C-terminal group of cysteine residues (3' Cys→Ala) is mutated to alanines, indicating that these four cysteines

are dispensable for GRXCR1 homodimer formation (Figure 5.6). Only a single monomeric product for the GRXCR1 protein containing mutations in the N-terminal most group of cysteines (5' Cys→Ala) was observed (Figure 5.6). As expected, a single monomeric species was also observed from lysates generated by the construct containing mutations in both N- and C-terminal groups of cysteines (Figure 5.6). Consistent with the Y2H interaction studies, these results demonstrate the requirement for the cysteine residues of the C-terminal domain in the formation of GRXCR1 homodimers.

GRXCR2 SELF INTERACTIONS - Y2H EVIDENCE. Given the interaction results observed for GRXCR1 and the similarity of its primary amino acid sequence with GRXCR2, the ability of GRXCR2 to interact with itself was tested. To do this a GRXCR2-pGADT7 containing strain was mated to a GRXCR2-pGBKT7 containing strain. Colonies were observed on DDO confirming successful mating of the two strains (Figure 5.7). The presence of colonies on TDO, QDO, QDO media is consistent with a positive GRXCR2 self-interaction (Figure 5.7). To evaluate a dependence of these interactions on the conserved cysteine-rich C-terminal domain of GRXCR2, yeast strains carrying Cys→Ala mutants were generated. Successful mating of GRXCR2(5' Cys→Ala), GRXCR2(3' Cys→Ala), and GRXCR2(5' + 3' Cys→Ala) to wild type GRXCR2 was evident by the presence of diploid colonies on DDO media. Diploid yeast carrying wild type GRXCR2 along with either the N-terminal cysteine mutants or the C-terminal cysteine mutants were able to grow on selective TDO media, while double mutants were not (Figure 5.7). On selective QDO media, none of

the cysteine mutants exhibited evidence of interaction with wild type GRXCR2 (Figure 5.7). The inability to activate reporter genes required for growth on TDO and QDO by single or double mutants is consistent with a requirement of the conserved cysteine residues of GRXCR2 for self-interactions.

GRXCR2 - NATIVE GEL ELECTROPHORESIS. Similar to the results with GRXCR1, Y2H studies suggest the ability of GRXCR2 to interact with itself. To test this hypothesis with an independent approach, we again used PAGE under native conditions. Protein lysates derived from bacteria expressing a MYC-tagged GRXCR2-MBP construct were separated under native conditions. Oligomeric complexes migrating well above the expected ~75 kD size of MYC tagged GRXCR2-MBP were identified when immunoblotted with an anti-myc antibody (data not shown). Similar high molecular weight complexes were also observed using a GRXCR2-specific antibody, although minor products consistent with the expect ~75 kD size were present also. Lysates generated from GRXCR2 constructs with mutations in the cysteine-rich domain yielded similar, high molecular weight complexes. The inability to consistently observe species migrating at the predicted molecular weights of monomeric and multimeric GRXCR2 suggests the resolution capacity of the native gel approach may be inadequate to reliably identify such multimers and any dependence upon the cysteine-rich domain. Alternatively, this result may reflect aggregation of the GRXCR2 protein.

GRXCR1/GRXCR2 HETERODIMERIZATION. Given the evidence of apparent self interactions of GRXCR1 and GRXCR2 and their similar localization

to stereocilia *in vivo* (Odeh, 2010; Avenarius M, 2011), we tested for potential heteromeric interactions of the two proteins. Mating of yeast individually carrying GRXCR1-GAD and GRXCR2-pGBK produced diploids that were able to grow on TDO but not on QDO selective media (Figure 5.8). In the reciprocal experiment, in which the GRXCR1-pGBK containing strain was mated to the GRXCR2-GAD strain, colonies were not observed on TDO, QDO, or QDO + X-gal media (Figure 5.8). This inconsistency may reflect a tag specific effect on either GRXCR1 or GRXCR2 that causes interference of a putative heteromeric interaction. Overall, these results suggest any potential GRXCR1-GRXCR2 interactions are relatively weak and in fact may be in direct competition with the respective homotypic interactions.

GRXCR1 AND GRXCR2 PROTEIN PURIFICATION. Testing the hypothesized properties of GRXCR1 and GRXCR2 including chaperone activity, glutaredoxin enzymatic activity, and binding of Zinc ions relies on successful purification of GRXCR1 and/or GRXCR2. A collaboration with Dr. Ursula Jakob (University of Michigan, Department of Molecular, Cellular, and Developmental Biology) was established to assist in the purification of GRXCR1 and GRXCR2. I generated several constructs to produce various tagged hybrid versions of each protein in bacteria for affinity purification approaches (GRXCR1-HIS, GRXCR1-pMAL, GRXCR2-HIS, GRXCR2-pMAL). Induced expression of each of the constructs produced hybrid proteins of the expected sizes, but only GRXCR2-pMAL remained in the soluble fraction. Purification using a standard affinity capture approach, however, failed to yield soluble GRXCR2 despite alterations of

several variables in the protocols, including growth, lysis, and buffer conditions (Figure 5.9).

DISCUSSION

The structure-function analyses presented in the current study indicate the critical role for the conserved N-terminal and C-terminal domains of GRXCR1 and GRXCR2. Similar to GRXCR1 experiments presented in Chapter 3, transfection studies of GRXCR2-GFP fusion constructs in CL4 epithelial cells demonstrated that the N-terminal domain of GRXCR2 is necessary and sufficient for subcellular localization to actin filament-rich microvilli. Although we have not investigated the determinants of GRXCR2 required for its *in vivo* localization to stereocilia in hair cells, based on related studies with GRXCR1, the N-terminus is likely to be critical for localization in this context also. Similar structure-function studies with THRUMIN 1 also indicates that the N-terminus of this plant protein is necessary for localization to actin filament structures in association with chloroplasts (Whippo, 2011). Although GRXCR1 and GRXCR2 exhibit considerable sequence similarity in this N-terminal domain, the N-terminus of THRUMIN1, as in other plant and invertebrate homologs, is quite divergent. Together these results suggest an evolutionarily conserved role for the N-termini of GRXCR homologs in localization to actin filament structures. Higher resolution structure-function studies using more discrete deletions or amino acid substitution mutations, as well as analysis of chimeric mutant proteins derived from individual homologs, will be required to identify N-terminal residues that are important for precise subcellular localization.

As with GRXCR1, no apparent actin binding motifs were identified in GRXCR2. This suggests that the mechanism of localization may not involve direct interactions with actin filaments and implies an accessory protein(s) in the proper localization of these proteins to actin filament-rich structures. In the context of the stereocilia, one example of localization that does not require a direct interaction with actin is the dependency of whirlin on full length Myo15a for localization to the tips of the stereocilia (Belyantseva, 2005). This suggests that Myo15a or other myosin motor proteins may be important for localization of GRXCR1 and GRXCR2 to the stereocilia and that the N-terminus is a potential site of interaction with such a motor protein.

The conserved arrangement of cysteines in the C termini of GRXCR1, GRXCR2 and all other homologs suggests a critical role for this region. The roles of zinc finger motifs have broadly been implicated in the binding of nucleic acids (Laity, 2001). Many transcription factors encode zinc finger motifs to facilitate binding to DNA in a Zn^{2+} dependant manner (Laity, 2001). Zinc fingers also act at the RNA level to bind and subsequently inhibit translation by directly binding to mRNA to inhibit the binding of translation initiation factors (Laity, 2001). GRXCR1 and GRXCR2 do not localize to either the nucleus or ribosomes suggesting that the zinc-finger motif encoded by these proteins does not function to bind nucleic acids.

Alternative roles for putative zinc-finger motifs in mediation of protein interactions have also been described. For instance, Qingjun and colleagues demonstrate that the zinc-finger domain encoded by the *Yy1* transcription factor

is necessary and sufficient for interaction with its co-factor ATF/CRE binding protein (ATF/CREB) (Zhou, 1995). This example and others support the hypothesis that the zinc-finger encoded by the C-terminal domain of GRXCR1 and GRXCR2 may be involved in protein-protein interactions. Consistent with such a property, Y2H and native gel electrophoresis experiments in the current study support a critical requirement of conserved cysteine residues in the C-terminus of both proteins in the formation of homotypic interactions.

The biological relevance of these interactions remains unknown. Perhaps it is the case that GRXCR1 and/or GRXCR2 homodimerize or heterodimerize with one another to carry out their normal function. The yeast-two-hybrid and native gel approaches taken to identify the homo/heterodimerization of GRXCR1 and GRXCR2 do not of course prove such interactions occur *in vivo* in stereocilia. Approaches such as BiFC using fluorescent GRXCR1 and GRXCR2 hybrid proteins could be performed in cultured epithelial cells to further test for self- interactions in a more relevant context. The requirement of this and other conserved domains of GRXCR1 and GRXCR2 in the context of stereocilia bundle maturation could be directly addressed by expressing a mutated transgene version of either of these proteins in the cysteine-rich domain (wild type = $Cx_2Cx_7Cx_2Cx_{20}Cx_2Cx_7C$ mutant = $Ax_2Ax_7Ax_2Ax_{20}Ax_2Ax_7A$) in the appropriate mutant background and assessing the ability to rescue the dimension (GRXCR1) or disorganization/orientation (GRXCR2) phenotype. Finally, the self-interactions identified here could be an artifact due to the overexpression of

GRXCR1 and GRXCR2 proteins rather than self-interactions, and instead the C-terminal domain could be a motif for interaction with other sensory cell proteins.

The central domain of GRXCR1 and GRXCR2 exhibit sequence and/or predicted structural similarity to the thioredoxin-like family of proteins. Thioredoxin folds present in many proteins consist of a single domain containing five β-sheets and four α-helices arranged in a βαβαβαββα configuration (Holmgren, 1975). This family of proteins typically has enzymatic activity associated with the putative active site C-X-X-C, which functions to enzymatically reduce glutathionylated proteins in response to cellular stress. Divergence within the active site has given rise to a group of noncanonical glutaredoxins that alternatively function as protein chaperones and in iron-sulfur cluster biosynthesis (Hoffmann, 2011; Berndt, 2008).

Direct evaluation of oxidoreductase activity of GRXCR1 and other potential properties of GRXCR1 or GRXCR2 were hampered by the difficulty in purifying these soluble recombinant proteins. With respect to oxidoreductase activity, however, consideration of evolutionary conservation across thioredoxin-like proteins is informative. Some thioredoxin-like proteins function as redox proteins and possess the conserved dithiol (C-X-X-C) or 5' monothiol (C-X-X-X) catalytic active site. A 3' monothiol active site (X-X-X-C) is conserved in one but not both glutaredoxin-like cysteine-rich proteins and 3' monothiol active sites are not implicated in traditional redox activity (Berndt, 2008). Structure-function studies indicated that a mutant version of plant THRUMIN1, which lacks the putative monothiol active site, was still able to rescue the chloroplast transport

defects in a mutant background (Whippo, 2011). These data are consistent with an alternative, non-redox role for GRXCR1 and GRXCR2. One example of an alternative role for a thioredoxin-like protein is PLP2, a yeast protein that also lacks any recognizable active site, binds the chaperone TCP-1 and functions to facilitate the folding of cytosolic actins (McCormack, 2009; Lou, 2009). Such an actin related function may be relevant to GRXCR homologs in the context of the actin-rich stereocilia.

CHAPTER 6

Discussion

Mutations in the gene encoding GRXCR1 are associated with profound deafness and vestibular dysfunction in the pirouette mouse. *Grxcr1* is located on mouse chromosome 5 and homologous genes are found throughout all sequenced vertebrate, invertebrate, and plant species. *Grxcr1* shows significant, full-length similarity to only one other gene in mouse, in a paralogous region located on chromosome 18. This gene, originally identified as *gm851*, encodes a protein that exhibits ~30% amino acid identity to GRXCR1. On the basis of amino acid similarity, *gm851* represents the second glutaredoxin-like cysteine-rich family member and therefore was given the gene name *Grxcr2*. Vertebrate genomes contain genes with sequence similarity to *Grxcr1* and *Grxcr2* whereas invertebrate genomes and plants contain genes with greater similarity to *Grxcr1*.

The presence of the two glutaredoxin-like cysteine-rich genes in vertebrate genomes raises the question of the mechanism by which these two genes arose. Several hypotheses have been put forth to explain the presence of vertebrate gene families. One proposed mechanism is two independent rounds of whole genome duplications early in vertebrate evolution. Such large-scale duplications are supported by the presence of a single Hox cluster in

invertebrates whereas four Hox clusters are found in vertebrates, an observation summarized as the 4:1 rule. Detailed comparison between vertebrate and invertebrate genomes demonstrates that only 5% of homologous genes actually follow this 4:1 rule (Meyer, 1999). The widespread distribution of conserved syntenic clusters of paralogous genes, each at four locations in the genomes of extant vertebrates, however, supports a large-scale 2-fold duplication model followed by gene loss and rearrangements within many of the clusters (Dehal, 2005). Alternatively, paralogous genes can be derived from smaller segmental duplications and dispersion to different chromosomes through translocation events (Levasseur 2011).

The presence of *Grxcr1* and *Grxcr2* orthologs in extant vertebrates but only a single related gene in most non-vertebrate species indicates the ancestral duplication event that gave rise to these two genes occurred early in vertebrate evolution. Two additional paralogous gene pairs, *Kctd8*/*Kiaa1317* and *Yip1b*/*Yip1a* are part of a conserved syntenic cluster of genes within 1 Mb of *Grxcr1* and *Grxcr2* on mouse chromosomes 5 and 18, respectively, and are clearly part of this ancestral duplication. Further analyses of the corresponding syntenic regions on human chromosomes 4 and 5 indicates a much larger set of genes (120) are likely to be part of these paralogous clusters, which extends across nearly the entire length of chromosome 4 and a substantial portion of chromosome 5 (Catchen, 2009). Although no other *Grxcr1*- or *Grxcr2*-related genes appear to be present in vertebrate genomes, a number of genes in these clusters appear to have additional related paralogous clusters at other genomic

locations, suggesting that the clusters may have derived originally from the predicted early 2-fold, large-scale duplication events. If so, additional duplicates of the original *Grxcr1/2* ancestral gene were likely lost early in vertebrate evolution due to accumulation of deleterious mutations (Nei, 1973).

Grxcr1 and *Grxcr2* are expressed in cochlear and vestibular sensory hair cells in development and at maturity and their encoded proteins localize to the stereocilia. Mutations in *Grxcr1* and *Grxcr2* are associated with inner ear dysfunction together with abnormal maturation of sensory cells. Our detailed characterization of these loss of function mouse models, together with structure-function studies of both genes, suggest related yet distinct biological roles for these genes.

Auditory function in GRXCR mutants

Measurement of the auditory brainstem response (ABR) objectively assays the function of the peripheral and central auditory pathways. Evaluation of compound action potentials (CAPs) provides a similar quantitative measure of cochlear function. In general, ABR and CAP response studies indicate that loss of function mutations in *Grxcr1* result in more severe hearing loss than similar mutations in *Grxcr2*. Threshold measurements demonstrate that the original pirouette (*pi*) allele (Beyer, 2000), as well as the pi^{tde} (Erven, 2002) and pi^{tg370} (Odeh, 2004) alleles, typically exhibit shifts of at least 60 dB at multiple frequencies consistent with hearing loss due to inner and outer hair cell dysfunction. Somewhat better hearing (approximately 50 dB threshold shifts) was demonstrated in 6 week old mutants homozygous for the pi^{4J} allele

(Avenarius M, 2011). All of these alleles lack expression of full-length *Grxcr1* transcripts and thus, believed to be null, exhibit qualitatively similar morphological defects in stereocilia (Odeh, 2010; Odeh, 2004; Avenarius M, 2011), differences in the severity of hearing loss that are likely attributable to genetic background differences, a common feature of inherited hearing loss in mice (Johnson, 2006). Most of the *pi* alleles are on *C57BL/6J* backgrounds, with the exception of the pi^{4J} allele, which is on a *NZB/NZW* mixed background. The *C57BL/6J* strain carries a number of variant loci that contribute to an early onset hearing loss (Noben-Trauth, 2009) and may thus contribute to loss of function in many of the *pi* alleles.

An approximate 50 dB SPL shift in ABR thresholds is observed in *Grxcr2* homozygote mutants indicating a less severe hearing loss relative to most *Grxcr1* mutants. This level of functional loss was observed in *Grxcr2* mutants on the *C57BL/6J* (age related hearing loss locus 1 sensitive) and FVB (age related hearing loss locus 1 resistant) backgrounds (Noben-Trauth, 2003). The degree of hearing loss exhibited by *Grxcr2* mutants is generally consistent with complete loss of the amplification provided by the outer hair cells and is apparently independent of ahl1 (Dallos, P 1973). Outer hair cell function was directly assayed by determining the level of Distortion Product Otoacoustic Emissions (DPOAE) from *Grxcr2* mutants and heterozygous littermate controls. *Grxcr2* mutants exhibit a significant reduction in DPOAEs in comparison to controls indicating loss of outer hair cell function.

In the *C57BL/6J* background, *Grxcr2* mutants also exhibited a slight progression of progressive hearing loss relative to littermate control mice by three months of age. The progression of hearing loss supersedes the amplification provided by outer hair cells reflecting a possible gradual deterioration of inner hair cell function over time in this mutant background. Additional evaluation of inner hair cell function, such as measurement of summating potentials using an electrode at the round window of the cochlea, will be required to more precisely determine the relative contributions of inner and outer hair cell defects in the *Grxcr2* mutants.

ABR and CAP analyses provide assays of response to external sound after the cochlea is functionally mature, which occurs at approximately two to three weeks of age in the mouse. To determine the effects of *Grxcr1* and *Grxcr2* mutations on sensory function at early postnatal ages, we measured mechanotransduction currents in response to deflections of the stereocilia bundles of individual hair cells through collaborative studies. The status of mechanotransduction in *Grxcr1* and *Grxcr2* mutant mice sensory hair bundles of the utricle were mechanically stimulated at early postnatal ages, prior to a bundle phenotype. An additional set of measurements was collected from *Grxcr2* mutant outer hair cell bundles prior to any morphological phenotype. In all cases transduction currents of *Grxcr1* and *Grxcr2* mutants were comparable to those of littermate controls, suggesting that these genes do not significantly impact the initial formation and activity of the transduction complex or the associated

molecules involved in activities such as trafficking the complex to the tips of stereocilia at early postnatal ages.

Stereocilia bundle defects in GRXCR mutants

Evidence from physiological testing demonstrated a significant degree of hearing loss, this coupled with the localization of GRXCR1 and GRXCR2 to the stereocilia suggested that analysis of mutant and littermate controls should be performed to determine the morphological status of the stereocilia. Mutations in *Grxcr1* result in an inability to achieve proper stereocilia dimensions observed in inner and outer hair cells where as mutations in *Grxcr2* clearly affects the organization and orientation of stereocilia bundles mainly on outer hair cells (Erven, 2002; Avenarius M, 2011). The effects of mutations in *Grxcr1* and *Grxcr2* on the morphology of stereocilia are similar to those of other stereocilia development genes discussed. Like the dimensional defects observed in some mouse models such as deaf jerker, with mutations in *Espn*, *Grxcr1* mutant mice exhibit similarly thin stereocilia (Sekerkova, 2011;Zheng, 2000). Deaf jerker mice also have apparent defects in achieving proper stereocilia height like other mice such as shaker2 and whirler (Probst, 1998; Mburu, 2003). The primary stereocilia pathology in *Grxcr1* mutant mice does not include lengthening defects suggesting some but not complete phenotypic overlap with other dimensional genes.

The organization and orientation defects observed in *Grxcr2* null mice are consistent with those observed in mouse models of Usher syndrome and with planar cell polarity (PCP) defects. Quantitative measurements determined a

significant portion of outer hair cells exhibited improper orientation, a characteristic shared with many PCP mutants. Combined defects in organization and orientation are seen in mouse models of Usher syndrome, a phenotype that resembles that of *Grxcr2* mutant mice. One difference between *Grxcr2* mutants and those observed in PCP and Usher mutants is the phenotypic onset. PCP and Usher mutants exhibit phenotypes prior to birth whereas *Grxcr2* mutant phenotypes are observed at postnatal time points. These observations are consistent with an interaction between *Grxcr2* and/or PCP and Usher genes but considering the temporal delay in phenotype perhaps this putative interaction does not occur initially. Considering the distinct stereocilia pathology associated with mutations in *Grxcr1* and *Grxcr2* it is apparent that each gene plays distinct roles in stereocilia development.

Vestibular function in GRXCR mutants

Unlike the common effects of both *Grxcr1* and *Grxcr2* mutations on auditory function, the vestibular phenotypes of these two mutants are distinct. The *pi* strains all exhibit circling and head bobbing behaviors that indicate overt vestibular dysfunction and implicate an essential role for GRXCR1 in the vestibular system. In contrast, *Grxcr2* mutants do not exhibit circling or head bobbing behaviors, suggesting relatively intact vestibular responses. *Grxcr2* mutants do, however, have subtly altered electrophysiological responses to vestibular stimuli suggesting that GRXCR2 is necessary at some level for normal function at least with respect to detection of linear acceleration at later ages (data not shown). Utricular and saccular organs in the vestibular system are thought to

be responsible for detection of linear acceleration. The normal morphology of stereocilia bundles on utricular cells in *Grxcr2* mutants at 7 days of age is consistent with the lack of a behavioral phenotype. We have not, however, evaluated morphology in older mutants to determine if the altered electrophysiological responses might be correlated with structural defects in stereocilia bundles. Identification of a progressive defect in vestibular morphology would provide additional evidence of a role for GRXCR2 in maintenance of stereocilia. In addition, further electrophysiological studies using rotational stimuli would be helpful to more fully evaluate GRXCR2 in semicircular canal function.

Despite the morphological differences observed in the stereocilia of auditory hair cells and the vestibular phenotypes in *Grxcr1* and *Grxcr2* mutants, we cannot rule out the possibility of at least some functional redundancy between the two genes, especially considering the homology between GRXCR1 and GRXCR2 as well as their overlapping localization in stereocilia. Studies characterizing the human and mouse deafness gene *Rdx* (radixin) revealed that upon knockout of mouse *Rdx,* the related actin cross linking protein Ezrin was upregulated in vestibular stereocilia (Kitajiri, 2004). Ezrin appeared to compensate for the absence of *Rdx* during stereocilia development in the cochlea, but not at adult ages as these mutants exhibited a progressive hearing loss associated with degeneration of stereocilia bundles (Kitajiri, 2004). The knockout mutants lacked behavioral defects, suggesting that ezrin was sufficient for normal bundle function in the vestibular organs during development and in the

adult and setting a precedent for functional compensation in the stereocilia (Kitajiri, 2004; Khan, 2007).

Functional redundancy of the two genes could be directly tested by crossing the *Grxcr2* mutation onto a *Grxcr1* mutant background and comparing the phenotypes among progeny carrying various combinations of the two mutations. For instance, perhaps in the context of *Grxcr2* null mice with half the gene dosage of *Grxcr1* (*Grxcr1*+/-; *Grxcr2*-/-) an inner hair cell or vestibular hair cell phenotype would be observed consistent with at least partial redundancy of function in those cell types. Ideally the effect of the *Grxcr2* mutation on a *Grxcr1* null background could be examined however the early stereocilia phenotype observed in each of the single mutants would likely make the analysis and interpretation of results difficult. Further evidence for redundancy between these two genes is discussed later in the context of possible protein-protein interaction mediated by their cysteine-rich domains. In the context of the stereocilia perhaps it is the case that in the absence of one GRXCR protein the other could compensate and bind a subset of its proteins to carry out some partial function.

The glutaredoxin-like cysteine-rich family of genes in the maintenance of stereocilia

The continued expression into adulthood of many genes involved in stereocilia development, together with identification of genetic variants in a subset of these genes that are associated with progressive or age-related hearing loss suggests an ongoing requirement for these genes in the mature inner ear. For example, characterization of the age related hearing loss locus

(*Ahl1*) in mouse demonstrated that a hypomorphic mutation of *Cdh23*, an Usher syndrome gene involved in bundle cohesion and also a constituent of tip links, is associated with hearing loss in aged mice (Noben-Trauth, 2003). The association of progressive hearing loss in humans with mutations in either *MYO7A* (Liu, 1997) or *ACTG1* (Van Wijk, 2003;Zhu, 2003) also suggests that other genes required for stereocilia development may be similarly required to maintain cochlear function in the adult.

Two month old mice homozygous for the “intact” floxed allele (*Grxcr2* floxed exon 1, FRT flanked neomycin cassette in intron 1) exhibited hearing equivalent to heterozygous littermate controls while at five months, the homozygotes exhibited significant threshold shifts that were associated with severe bundle defects. Reductions in transcript levels have been identified in other transgenic mouse lines generated with neo cassettes, presumably by splicing from an endogenous exon into cryptic splice acceptor sites present in the selection cassette (Nagy, 1998). We demonstrated a 50% reduction of *Grxcr2* transcripts in the floxed homozygotes relative to heterozygote controls, suggesting that the amount of *Grxcr2* expressed by the hypomorphic allele is sufficient to support normal development of hearing but insufficient to maintain normal stereocilia bundle morphology and auditory function later in life.

The later onset phenotype in these hypomorphic mutants could result from one or more alternative processes. The lower levels of *Grxcr2* could result in an abnormal developmental state that, despite normal hearing function in early life, predisposes stereocilia bundles to a progressive degeneration and loss of hair

cell function. The mild bundle defects at two months of age in the hypomorphs suggests this might be the case. Alternatively, progressive deterioration of stereocilia bundles may indeed reflect a requirement of *Grxcr2* expression above some threshold level in the mature cochlea to maintain normal orientation and organization of the bundle. This requirement may be due to continuous remodeling of the bundle itself. Although the kinetics are not well understood, experimental evidence from the chick cochlea demonstrated dynamic turnover of proteins in the stereocilia (Pickles, 1996). Furthermore, the actin filament core of stereocilia, at least in early postnatal rodents, undergoes continuous turnover of actin monomers in a process known as 'treadmilling' (Schneider, 2002).

Although the phenotype of the *Grxcr2* hypomorphic mutant suggests a potential role in stereocilia maintenance, a more rigorous test would make use of the floxed allele after deletion of the neo cassette by Flp recombinase. We expect this allele to express wild type levels of *Grxcr2*. A temporally conditional knockout of *Grxcr2* could be generated by breeding these *Grxcr2* floxed mice to mice carrying an Atoh1::CRE-ER transgene, which drives expression of a tamoxifen-responsive Cre recombinase in sensory hair cells (Machold, 2005; Chow, 2006). Administration of tamoxifen at adult ages, after the maturation of stereocilia, should catalyze deletion of exon 1 and permit us to characterize the effects of a *Grxcr2* conditionally null allele on stereocilia bundle morphology and auditory function.

Evidence for *Grxcr2* in stereocilia maintenance may implicate similar roles for *Grxcr1* or other stereocilia developmental genes. Like the tamoxifen-induced

ablation of *Grxcr2* described above, investigating other developmental genes relies on the availability of conditional alleles to ablate gene expression after maturation of the bundles (P14). Further study of the genes that play a role in maintenance of stereocilia may provide insight into genetic mechanisms that underlie age-related and noise-induced hearing loss.

Structure-function analysis

GRXCR1 and GRXCR2 are novel proteins that exhibit sequence similarity in selected regions to other known proteins. I have used structure-function analysis to correlate discrete regions and residues of GRXCR1 and GRXCR2 with their intrinsic properties. While the N-terminal domain of each protein lacks similarity to other known proteins, I demonstrated this domain as necessary and sufficient for localization of GRXCR1 and GRXCR2 to actin-rich structures. The central domains of GRXCR1 and GRXCR2 exhibit the most divergence from one another but exhibit primary sequence and/or structural similarity to the thioredoxin-like family of proteins. More specifically the central domain of GRXCR1, but not GRXCR2, resembles the glutaredoxin family of proteins as determined by the putative, monothiol, active site encoded within this domain. Lastly, the C-terminal domains contain a conserved arrangement of cysteines that resembles a zinc finger motif. I demonstrated that this domain functions in mediating protein-protein interactions.

The role of the N-terminal domain of GRXCR1 and GRXCR2 in localization to actin filament-rich structures

Despite the amino acid divergence between GRXCR1 and GRXCR2, localization to actin filament-rich structures is a common feature of these proteins. Expression of GFP hybrid proteins in cultured epithelial cells demonstrated a role for the N-terminal domain of both proteins in this localization property. A collaboration was initiated with Dr. James Bartles (Northwestern University) to purify GRXCR1 and test for actin interactions in order to determine if the localization was due to a direct association with actin filaments. Although purification of soluble, full-length GRXCR1 has been unsuccessful to date (see below), purification of the N-terminal of GRXCR1 yielded soluble protein and was found to lack any significant actin filament binding or bundling activities (data not shown). This was consistent with the lack of any known actin binding motifs in the N-terminal domain of GRXCR1. Although we cannot rule out that direct actin binding may be dependent upon other regions of GRXCR1, these data suggest that GRXCR1 and GRXCR2 are likely dependent upon interactions with other proteins for localization to actin filament-rich structures.

THRUMIN1, a plant homolog of GRXCR1, was found to localize to actin filament-rich structures much like that of mouse GRXCR1 and GRXCR2 (Whippo, 2011). Whippo and colleagues took a structure-function approach to demonstrate a role for the N-terminal domain in localizing THRUMIN1 to actin filaments associated with the plasma membrane. Additional data showed that THRUMIN1 directly interacted with actin and that full length THRUMIN1 was able

to bundle actin filaments suggesting that the proper localization of this protein, at least in part, was achieved by directly binding actin.

Further investigation of the N-terminal domain in the localization of GRXCR1 and GRXCR2 is warranted in actin filament-rich stereocilia of sensory cells. Attempts to transfect GFP hybrid constructs into sensory cells, the site of endogenous *Grxcr1* and *Grxcr2* expression, were successful using a biolistic gene gun but were difficult to interpret due to false positive localization of control GFP protein to the stereocilia. Given the necessity of the N-terminal domain of both proteins for localization to actin filament-rich structures in other cell types, this domain is likely to be involved in localization to stereocilia of sensory cells too. Directly testing this will require alternative approaches to express these hybrid constructs in sensory cell types. Several serotypes of adeno-associated virus vectors have been shown to be capable of sensory cell infectivity and the expression of recombinant proteins (Stone, 2005; Ballana, 2008) and represent an alternative strategy for expressing GRXCR1 and GRXCR2 hybrid constructs in sensory cells.

The C-terminal cysteine-rich domain is required for homodimeric and heterodimeric interactions of GRXCR1 and GRXCR2

The role in protein-protein interactions determined for other cysteine-rich domains is consistent with the homodimerization of GRXCR1 and GRXCR2 demonstrated in Chapter 5 (Zhou, 1995). These interactions are dependent upon the conserved cysteine residues located in the C-terminal cysteine-rich domain. This finding indicates the functional role of GRXCR1 and GRXCR2 may

be dependent upon multimerization of these proteins to carry out their functions during stereocilia maturation in the inner ear. Expressing versions of GRXCR1 and GRXCR2 with mutations in conserved cysteine residues in hair cells and comparing with wild type proteins for rescue of the stereocilia bundle phenotype in the respective null sensory cells would formally test the requirement of dimer formation.

The evidence for a heterodimeric interaction of GRXCR1 and GRXCR2 is less solid. This interaction was only defined in yeast two hybrid studies and could not be demonstrated under full selection of all interaction reporter genes. This 'directed' Y2H assay only presented two proteins, GRXCR1 and GRXCR2, both of which happen to have an identical configuration of cysteine residues in the cysteine-rich domain and may therefore represent a false interaction. The cysteine-rich domain of either protein could bind other cellular proteins, which of course are not evaluated in this assay.

Many examples of protein interactions have been demonstrated among stereocilia-localized proteins, including the Usher network of proteins. This example along with others suggests that protein interactions may be needed to achieve proper subcellular localization within the stereocilia or for the assembly of protein complexes necessary to perform their biochemical function. Recent advances have utilized the stereocilia bundle twist off method combined with a mass spectroscopy approach to more completely detail the stereocilia proteome (Shin, 2009). One possible method to identify other stereocilia proteins that may interact with GRXCR1 and/or GRXCR2 would be to harvest bundles at an early

postnatal time point from *Grxcr1* and *Grxcr2* mouse mutants and compare the proteins identified by mass spectroscopy with corresponding litter mate controls. Proteins either absent or significantly reduced in abundance in the mutants would be considered as candidate proteins that may interact with the glutaredoxin-like cysteine-rich family of proteins. Although reduction of specific protein levels in the mutants could be a secondary effect due to loss of GRXCR1 or GRXCR2, such candidates could be further validated by coimmunoprecipitation and other related approaches including BiMolecular Fluorescence Complimentation (BIFC) or FRET to test in an *in vivo* context.

The relationship of the central domains of GRXCR1 and GRXCR2 to the thioredoxin-like family of proteins

The central domain of GRXCR1 and GRXCR2 demonstrate structural similarity to the thioredoxin-like family of proteins. More specifically GRXCR1 shows homology to the glutaredoxin-like family of proteins as determined by the presence of the monothiol active site X-X-X-C within this domain. Mutations of this C-terminal cysteine within the active site of traditional glutaredoxins, however, seem to retain enzymatic activity suggesting that this position is not likely important for function (Meyer, 2009). This, and the ability of a C-terminal cysteine mutation in the comparable motif of THRUMIN1 to rescue the chloroplast movement defect *in vivo* (Whippo, 2011) implies that GRXCR1 is not likely to function as a glutaredoxin. The precedent for monothiol glutaredoxins with a conserved C-terminal cysteine and other thioredoxin fold containing proteins in the literature is primarily in protein-protein interaction and as

molecular chaperones (Berndt, 2008; Lillig, 2008). The inability to obtain soluble GRXCR1 or GRXCR2 has prevented a direct test of any oxidoreductase or other activity and therefore has left the biochemical function of the central domain unresolved.

Hypothesized mechanisms of GRXCR1 and GRXCR2 function in stereocilia development and maintenance

With the current understanding of proteins involved in stereocilia development it is somewhat challenging to conceptualize a functional role for a small family of genes with similarity to thioredoxin-like proteins. An initial hypothesis as to the roles the glutaredoxin-like cysteine-rich family of genes plays in the stereocilia stems from sequence similarity to other known proteins, findings obtained through structure-function analysis and characterization of mouse models of *Grxcr1* and *Grxcr2*.

Grxcr1 and *Grxcr2* mutant mice show stereocilia specific defects during inner ear development indicating that their gene products play a necessary role in establishing this structure. This observation was supported by the identification of GRXCR1 and GRXCR2 in the stereocilia of sensory hair cells and indicates an intrinsic, local role in bundle development. I also demonstrated a likely role for the N-terminus of GRXCR1 and GRXCR2 in stereocilia localization and provided suggestive evidence that GRXCR1 and GRXCR2 may interact in a homotypic fashion through interaction with their C-terminal cysteine-rich domains (Figure 6.1). This interaction between GRXCR1 and GRXCR2 may be required to carry out their normal function and the protein-protein interaction

mediated by their cysteine-rich domains may imply interactions with other stereocilia proteins. It is hypothesized, based on the similarity to the thioredoxin-like family of proteins, that GRXCR1 and GRXCR2 could perform biochemical role(s) consistent with those of the noncanonical glutaredoxin family of proteins (Figure 6.1).

The failure of *Grxcr1* mutants to achieve normal stereocilia diameters suggests a more direct impact of GRXCR1 on actin filament architecture or dynamics. Our demonstration of an ability of GRXCR1 to induce dimensional changes of microvilli, principally elongation (Odeh, 2010), suggests that it may act to enhance actin polymerization in stereocilia during development. Polymerization of new actin filaments and their incorporation into the existing filament core is necessary for increases in diameter during maturation of stereocilia (Tilney, 1986;Tilney, 1986). Through protein-protein interactions, GRXCR1 may influence actin polymerization machinery required for these diameter increases. If GRXCR1 functions as a molecular chaperone like other thioredoxin-like proteins, it may assist in the proper folding or stability of interacting proteins. To test for this biochemical activity an *in vitro* chaperone assay would be performed with purified GRXCR1 to identify if it had the ability to stabilize/fold various substrates (Buchner, 1998). Candidate interactions extend from known actin polymerization proteins to candidates identified in the mass spectrometry approach proposed above.

The similarity of orientation and disorganization defects in *Grxcr2* and Usher mouse mutants suggests a possible relationship of GRXCR2 with Usher

protein pathways. The Usher proteins form a small interaction network that establishes and maintains the links between stereocilia ultimately acting to hold and shape stereocilia bundles. Like the function of other thioredoxin-like proteins in protein-protein interaction (Jeong, 2008), GRXCR2 may interact with the Usher family of proteins to stabilize stereocilia links. Alternatively, like that described for GRXCR1 may alternatively act to chaperone Usher proteins. Direct interaction with the Usher proteins could be address through coimmunoprecipitation or yeast-two-hybrid methodologies as well as *in vivo* BIFC approaches. Some insight into the interaction of GRXCR2 with the Usher proteins may be gained from whole mount immunostaining *Grxcr2* mutant inner ear tissue with antibodies to the Usher proteins and looking for aberrant stereocilia localization.

Generating soluble GRXCR1 and GRXCR2 would provide a valuable resource to carry out *in vitro* assays to specifically test putative thioredoxin-fold activities such as glutaredoxin or chaperone activity as well as the ability to bind zinc ions. Given the general problems of insolubility and protein aggregation, it may be advantageous to attempt a similar bacterial purification strategy with other single domains of GRXCR1 and GRXCR2 or attempt purification of GRXCR1 and GRXCR2 in a different system such as baculovirus or insect cells.

Grxcr1 and *Grxcr2* in hearing and deafness

Over the past ~15 years many genes have been implicated in aspects of stereocilia development (Petite, 2009). The current genes are not all encompassing and the functional roles of many known genes are not elucidated. Here I engineer a mouse model of *Grxcr2* and analyze an allele of the

spontaneously arising deaf mutant pirouette to understand the role of these genes in normal cochlear function. The experiments presented here identify a novel role for *Grxcr2* and supporting evidence for *Grxcr1* in the proper development of the stereocilia bundles specifically in establishing the dimension, orientation and organization of stereocilia bundles.

In the context of human disease, mutations in *GRXCR1* have been associated with patients segregating nonsyndromic deafness at the DFNB25 locus (Schraders 2010, Odeh 2010). For the first time, characterization of the *Grxcr2* mutant mouse suggests that mutations in *GRXCR2* may similarly underlie inherited hearing loss in humans. Through collaborative screening, we have evaluated genomic DNA from over 500 individuals with recessive, congenital, severe to profound hearing loss for variants in *GRXCR2* but have not identified any likely causative mutations (unpublished data). It is formally possible that variants do exist in this patient population and additional screening is required to identify *GRXCR2* as a nonsyndromic deafness-causing gene in humans.

Perhaps it is the case that other deafness populations including those diagnosed with Usher syndrome, a form of syndromic hearing loss in which patients also present with retinitis pigmentosa, should be considered. Furthermore observations noted in *Grxcr2* mutant mice including the presence of residual hearing, absence of overt vestibular phenotypes and distinct organization and orientation stereocilia defects supports the possibility that mutations in human *GRXCR2* may underlie a clinical subtype of Usher syndrome. With this notion in mind I did a retrospective analysis of *Grxcr2*

transcripts in the eye (data not shown). I found that *Grxcr2* transcripts were present in whole eye cDNA at early postnatal time points indicating that *Grxcr2* may also be required for aspects of eye development. This result along with the similarities in bundle phenotypes between *Grxcr2* mutants and Usher mutants provides compelling evidence for screening human *GRXCR2* in a subset of patients affected with Usher syndrome type II or III.

In addition to identifying a novel gene involved in stereocilia development I also performed various assays to understand the biochemical role of GRXCR2 in the developing stereocilia. This type of analysis is critical to understand how stereocilia proteins function in normal development and later maintain of stereocilia. Once the details of these molecular processes are elucidated the pathogenic mechanism of hearing loss including aging effects, noise exposure, and toxic effects of pharmacologic agents may be more fully understood. Ultimately, understanding the molecules and molecular pathways involved in establishing and maintaining the stereocilia could assist in designing therapeutics.

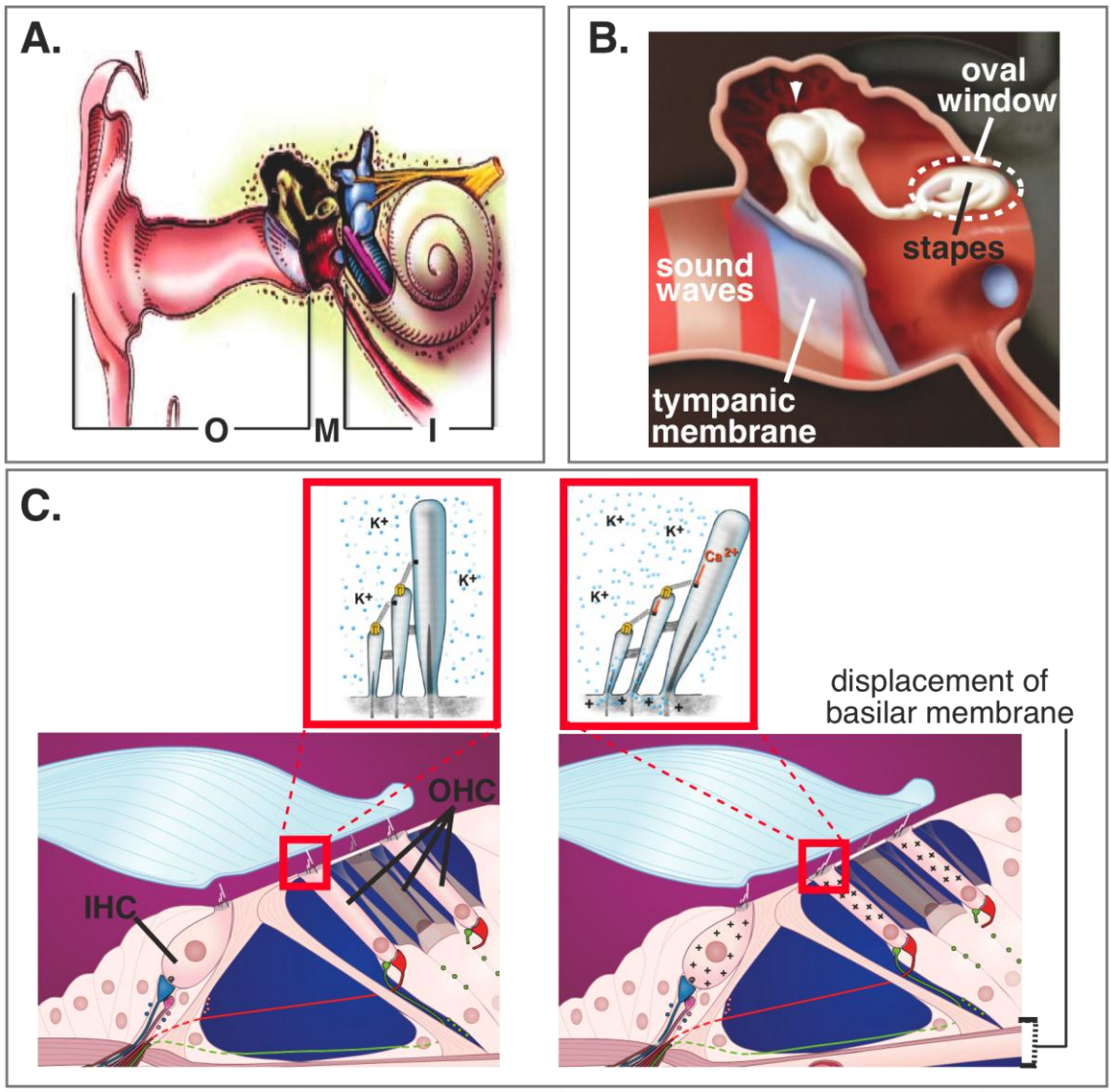

Figure 1.1 Anatomy of the peripheral auditory system and structural basis of hearing. A.) The ear is divided into three principal components: The outer ear (O), the middle ear (M) and the inner ear (I) B.) Sound waves traveling through the ear canal vibrate the tympanic membrane causing the inner ear bones to pivot (triangle demarcates pivot point) allowing the sound waves to be transduced into the cochlea. C.) The inner ear is comprised of two sensory cells types, a single row of inner hair cells and three rows of outer hair cells, each with apical stereocilia. Transduced sound waves displace the basilar membrane in a frequency specific manner causing deflection of the stereocilia and opening of associated channels at the tips of stereocilia. This mechano-transduction mechanism allows the influx of Ca2+ ions causing the hair cell to depolarize. A-C.) Images were reproduced/adapted from "Journey into the world of hearing" http://www.cochlea.org with permission from Remy Pujol et al.

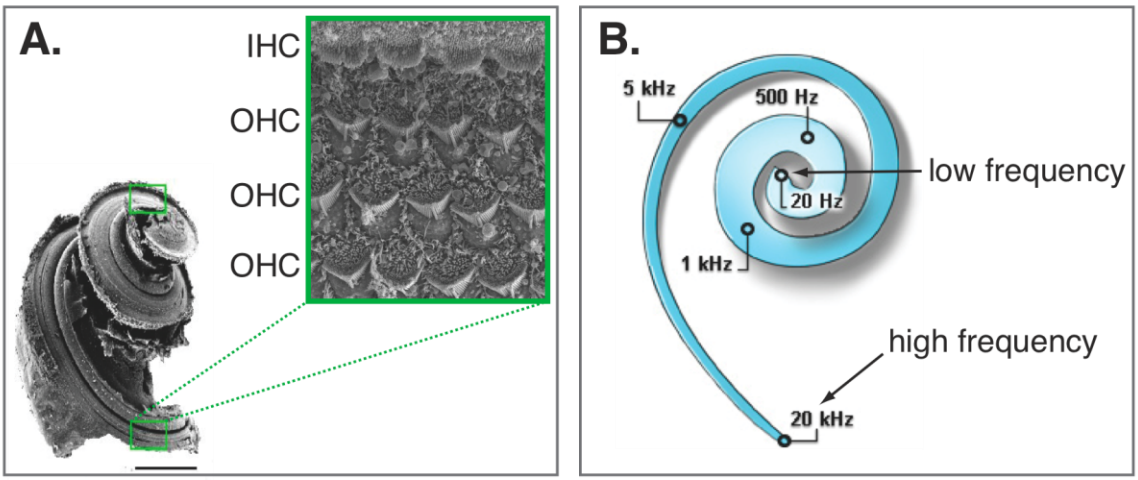

Figure 1.2 Structural arrangement of hair cells for detection of sound frequencies. A.) The organ of Corti, which includes both sensory hair cells and nonsensory supporting cells, is distributed in a spiral pattern along the length of the cochlea. The green inset shows a magnified scanning electron micrograph of the surface that demonstrates "V" shaped stereocilia of the inner and outer hair cells. B.) Tonotopic frequency map of the human cochlea with higher frequencies detected at the base and lower frequencies detected at the apex. A-B.) Images were reproduced/adapted from "Journey into the world of hearing" http://www.cochlea.org with permission from Remy Pujol et al.

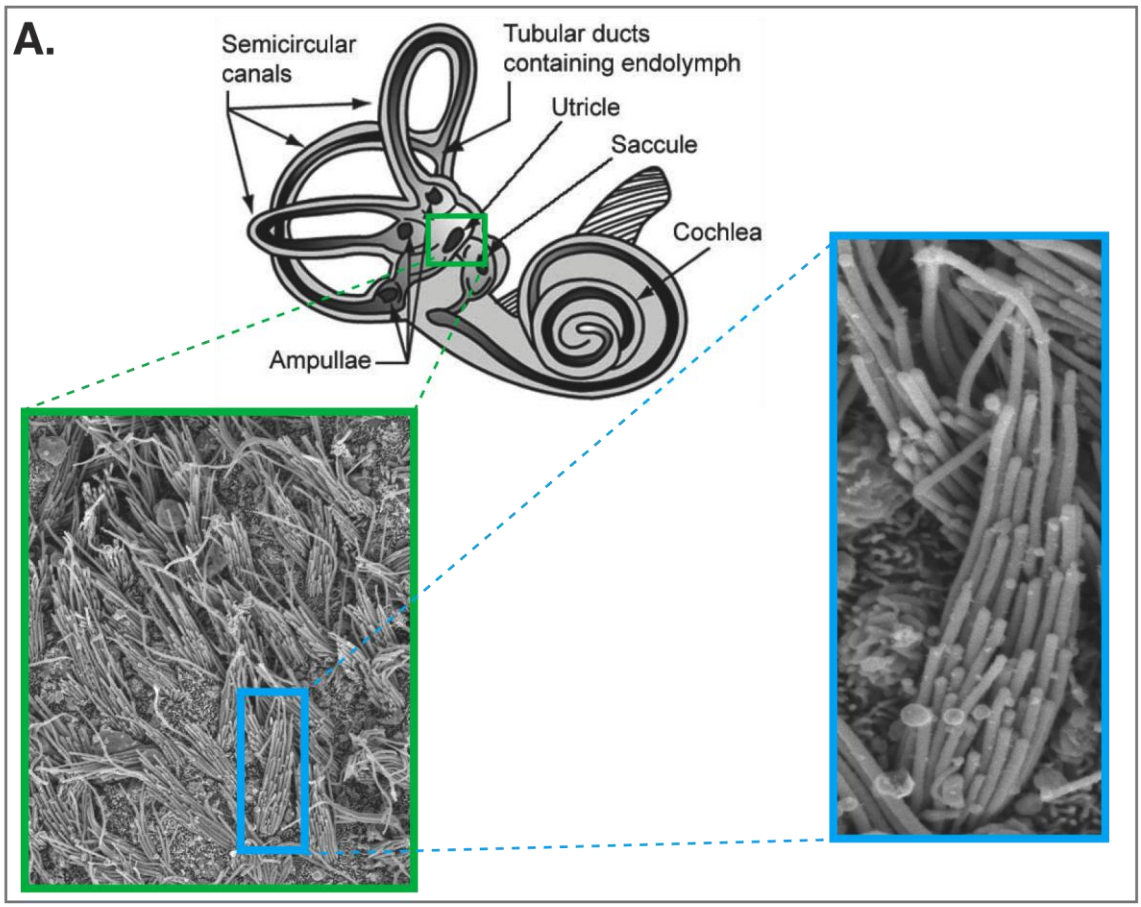

Figure 1.3 The anatomy of the peripheral vestibular system.
A.) The vestibule in the inner ear is comprised of a utricle, saccule, and three semicircular canals with their associated ampullae. Unlike cochlear hair cells, the sensory cells of the vestibular system are clustered in patches and the stereocilia are organized in large non-"V" shaped bundles. Although stereocilia morphology differs between the two systems, the basic process of mechano-transduction is the same. Vestibular system images were adapted from NASA educational material: EB-2002-09-011-KSC authored by Coulter GR and Vogt GL.

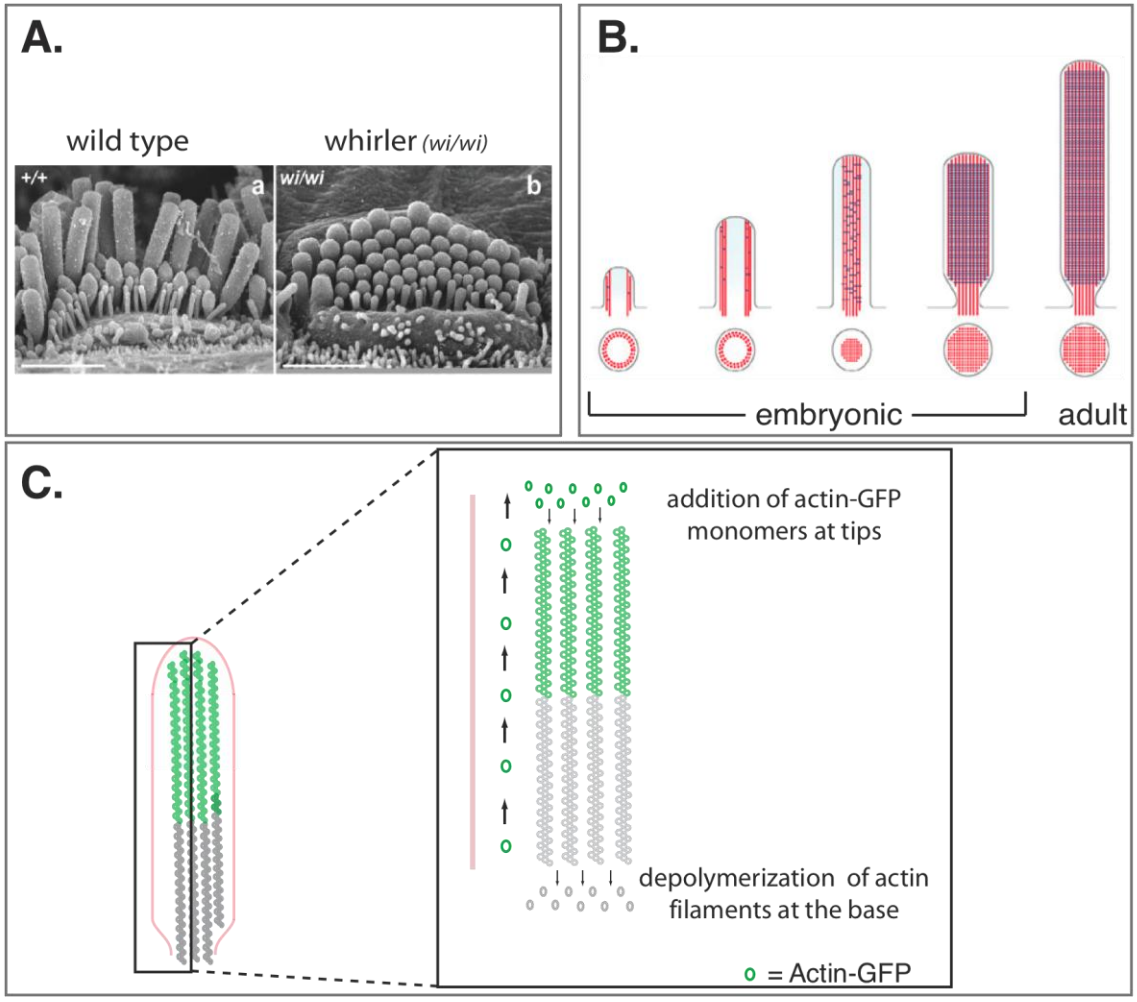

Figure 1.4 Establishment and maintenance of stereocilia dimensions. A.) whirler mice have a mutation in the gene *whirlin* and exhibit profound deafness and overt vestibular dysfunction. Scanning electron micrographs of surface preparations taken from wild type and whirler mutants demonstrate defects in stereocilia length (Mogensen MM et al, 2007). B.) Model highlighting the dimensional aspects of stereocilia development. Actin filaments first migrate to the center to generate a denser filament core. Additional filaments are then incorporated into the core to increase the stereocilia diameter. Finally, filaments are elongated to achieve the appropriate height. (Frolenkov, G et all 2004) C.) Model of actin filament elongation and maintenance of stereocilia length. Actin monomers are added to the barbed ends of actin filaments at the tips of stereocilia to increase stereocilia length. When the appropriate length is achieved, the dissociation of actin monomers at the base is in equilibrium with the addition of actin monomers at the tips, creating a steady state 'treadmilling' effect (Lin HW et al, 2005). A-C). Images were adapted from Mogensen MM et al (2007), Frolenkov, G et all (2004), Lin HW et al, (2005), respectively, with permission from John Wiley and Sons.

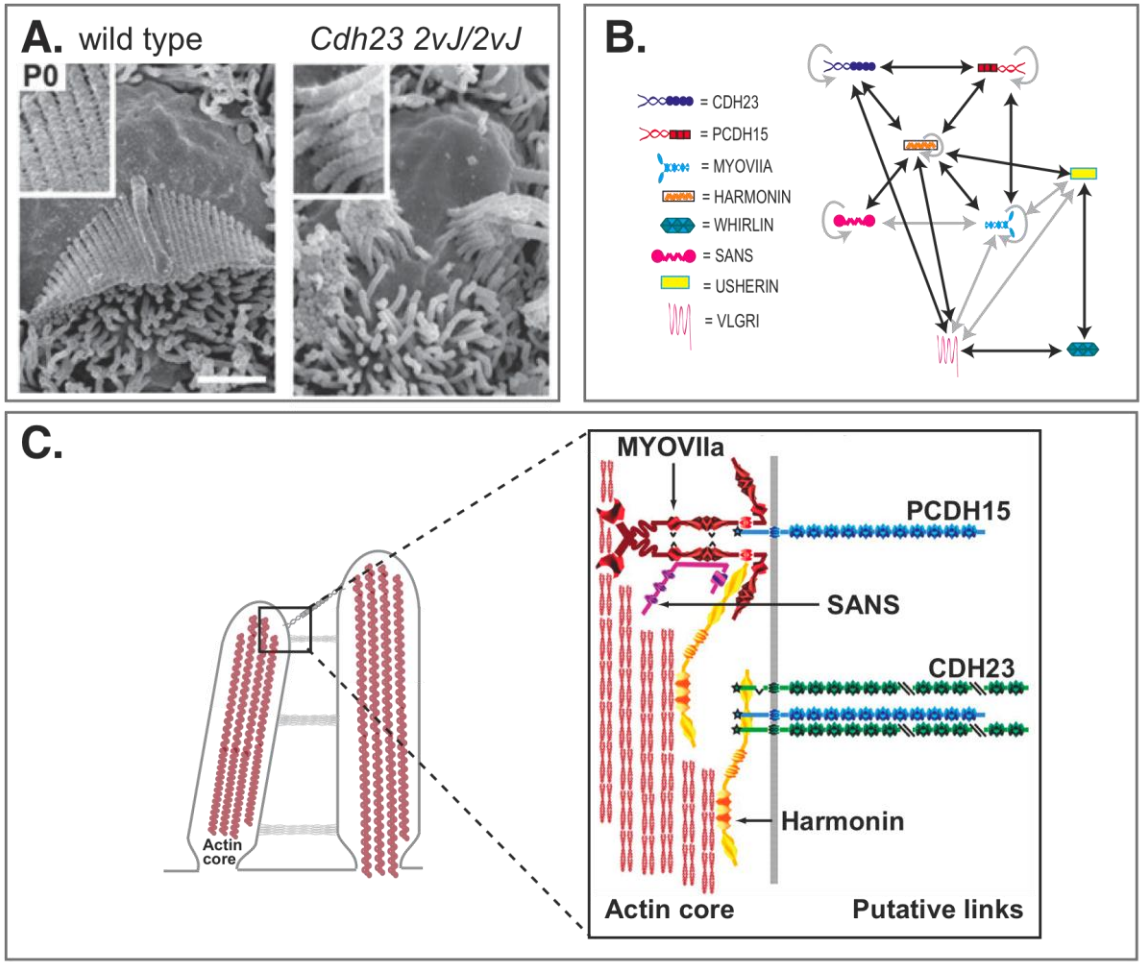

Figure 1.5. Molecules involved in stereocilia organization. A.) waltzer mutants have mutations in the *Cdh23* gene and exhibit profound deafness and overt vestibular dysfunction. Scanning electron micrographs of surfaces preparations taken from mutants and controls demonstrate defects in stereocilia organization (Lefevre, G et al 2008). B.) Stereocilia proteins associated with Usher syndrome have been shown experimentally to interact with one another to form an interactome. This diagram summarizes pairwise interactions. C.) Schematic incorporating the interactions described in figure 1.5 B The resulting network anchors components of the stereocilia links (PCDH15 and CDH23) to the dense actin filament core (Lefevre, G et al 2008). A & C). Images were adapted from Lefevre, G et al. (2008) with permission from Development.

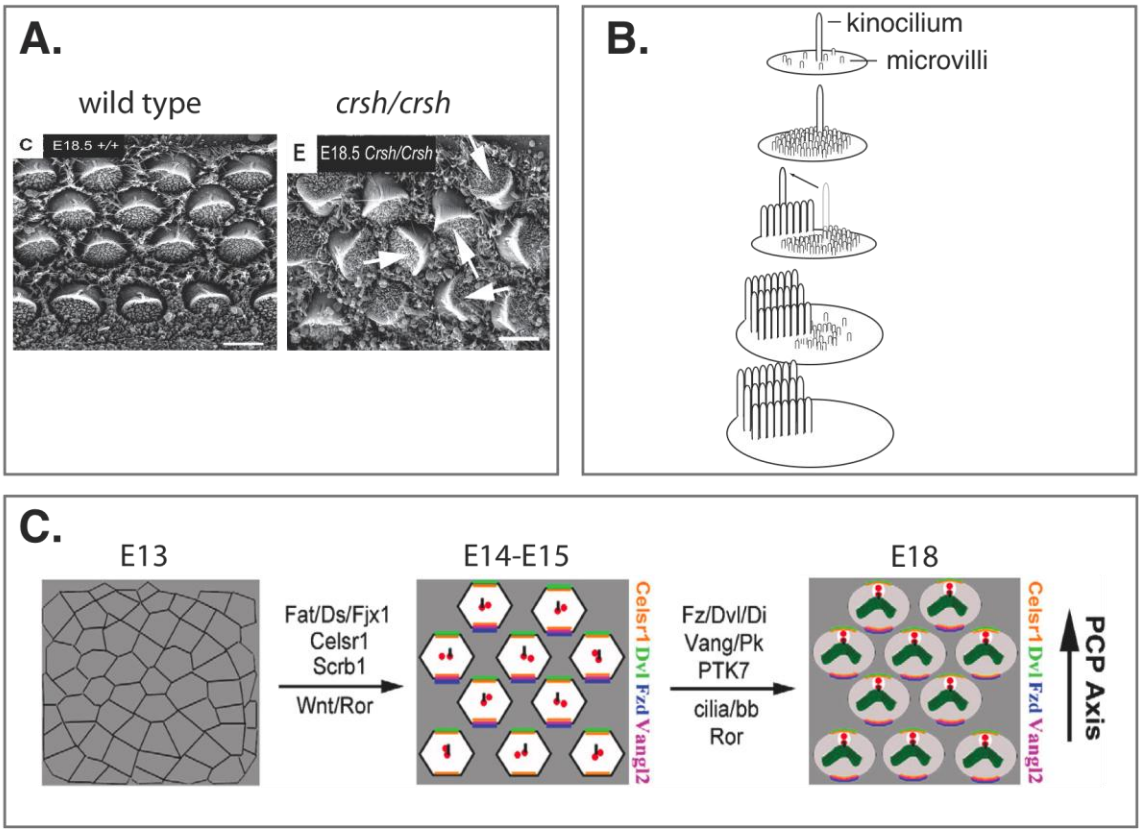

Figure 1.6. Molecules involved in stereocilia orientation. A.) crash mice have a mutation in the planar cell polarity gene *Celsr1* and exhibit defects in orientation of stereocilia bundles. Homozygotes also have neural tube defects. Scanning electron micrographs of surface preparations from E18.5 crash mutants and controls indicate defects (arrows) in bundle orientation (Curtain, J. et al 2003). B.) Early in development, a single microtubule-based kinocilium protrudes from the apical surface of cochlear hair cells. The kinocilium, on the apical surface of sensory hair cells, exhibits gradual migration lateralward. Maturing stereocilia co-migrate with the kinocilium and elongate, forming the mature, staircase-shaped bundle. Kinocilia are transient structures in the cochlea and are resorbed postnatally C.) Schematic depicting the apical surface of sensory and nonsensory cells at embryonic day 13 in the mouse. During the next two days (E14-E15) these cells organize into defined rows, under the control of genes implicated in regulation of planar cell polarity (PCP) processes. Vangl2 and Frizzled display asymmetric localization on the surface of the hair cells, which may be facilitated by Scrb1 and Celsr1, and other cytoplasmic mediators are recruited to the cell surface. PCP cues direct kinocilia movement and orient stereocilia bundles (Chacon-Heszele, M.F. et al 2009). Images were adapted from Curtain, J. et al (2003), Chacon-Heszele, M.F. et al (2009), respectively with permission from John Wiley and Sons.

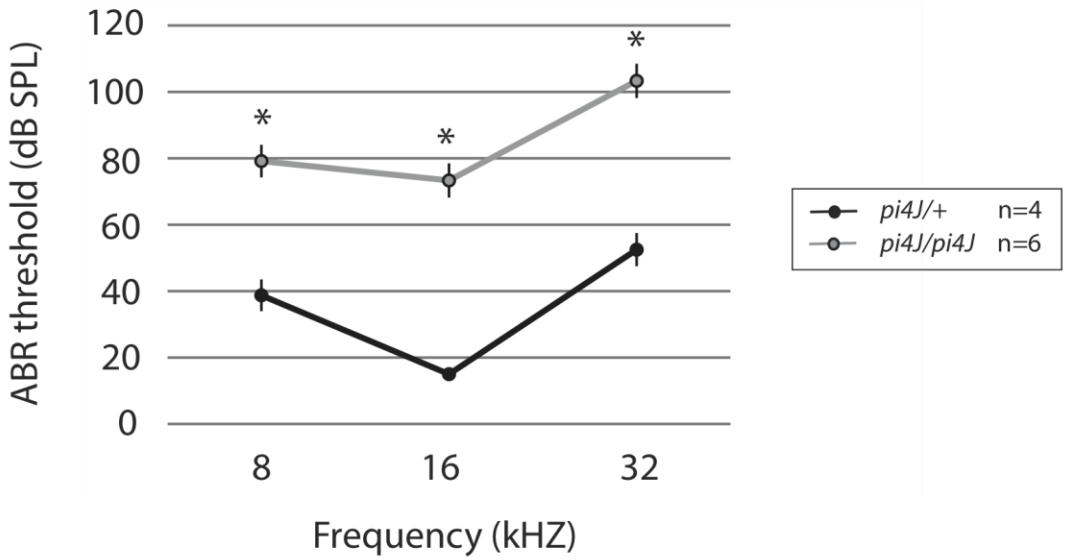

Figure 2.1 *pi4J* mice exhibit significant hearing threshold shifts. Auditory brainstem responses (ABR) of 5 week old mice to pure-tone stimuli. *pi4J/+* (black line) demonstrate relatively low hearing thresholds, whereas *pi4J/pi4J* (gray line) demonstrate ~50 dB SPL elevated thresholds, demonstrating severe hearing loss. Asterisks indicate significance of threshold differences (nonparametric t-test, $p < 0.05$). db, decibel; SPL, sound pressure level; kHz, kilohertz.

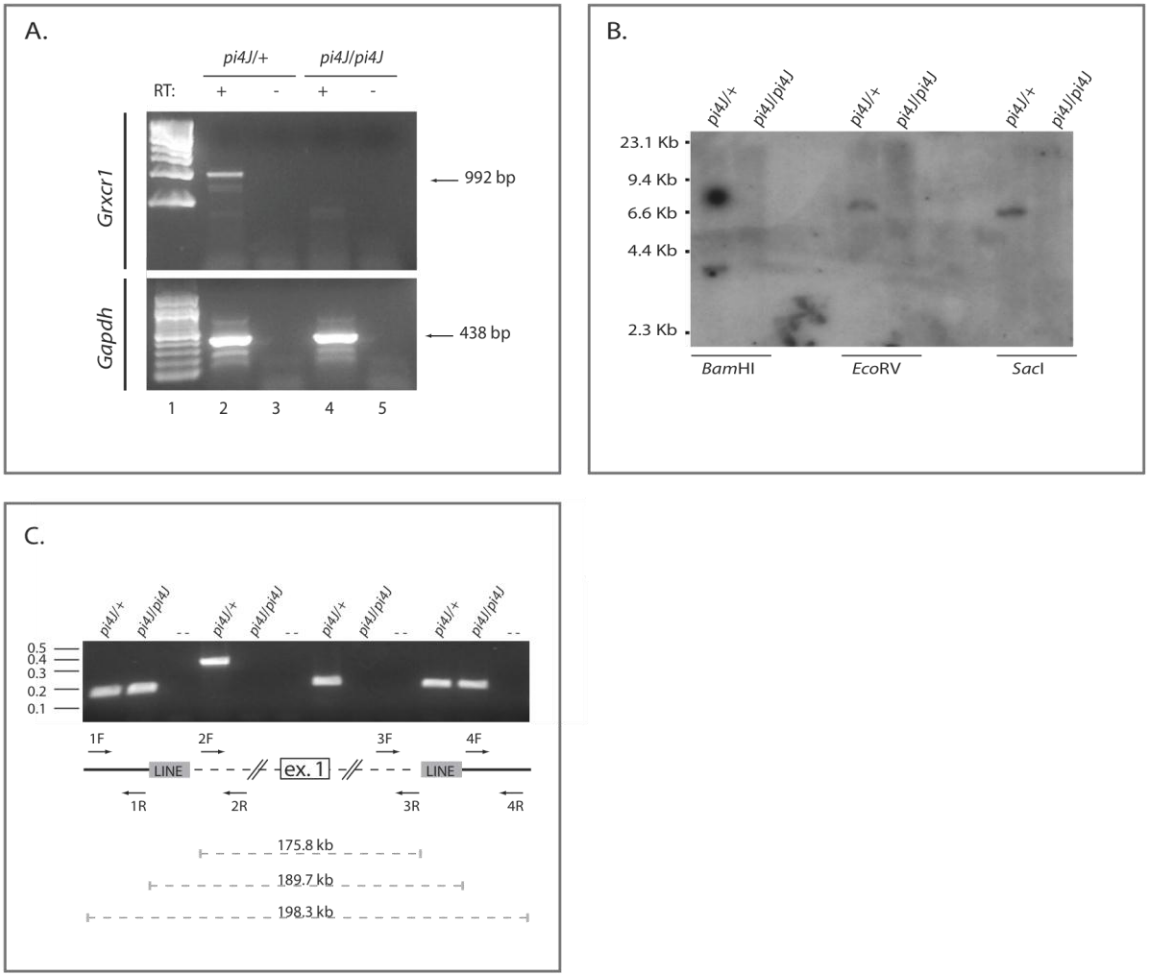

Figure 2.2 Large chromosomal deletion in *pi4J* mice results in loss of full-length *Grxcr1* transcripts. A.) A 992 bp RT-PCR product containing exons 1 through 4 of *Grxcr1* was amplified from *pi4J/+* cochlear cDNA (lane 2) but not from *pi4J/pi4J* cDNA (lane 4). *Gapdh* products were amplified from cDNA of both genotypes (lanes 2 and 4) B.) A radiolabeled DNA probe encompassing the first 490 bp of *Grxcr1* exon 1 of *Grxcr1* hybridized to 3.8 kb (*Bam*HI), 7.1 kb (*Eco*RV) and 6.8 kb (*Sac*I) genomic fragments of *pi4J/+* mice but failed to hybridize with *pi4J/pi4J* DNA, consistent with a deletion of this region of the gene. C.) Primer pairs derived from genomic sequences approximately 120 kB upstream of exon 1 (primer pair 1F/1R), immediately flanking exon1 (primer pairs 2F/2R and 3F/3R) and near exon 2 (primer pair 4F/4R) were used to amplify genomic DNA of *pi4J/+* and *pi4J/pi4J* mice. Expected products were amplified from *pi4J/pi4J* DNA with the 1F/1R and 4F/4R primer pairs but not with the 2F/2R or 3F/3R primers, indicating the relative positions of the centromeric and telomeric break points of the deletion (hashed line). RT, reverse transcriptase.

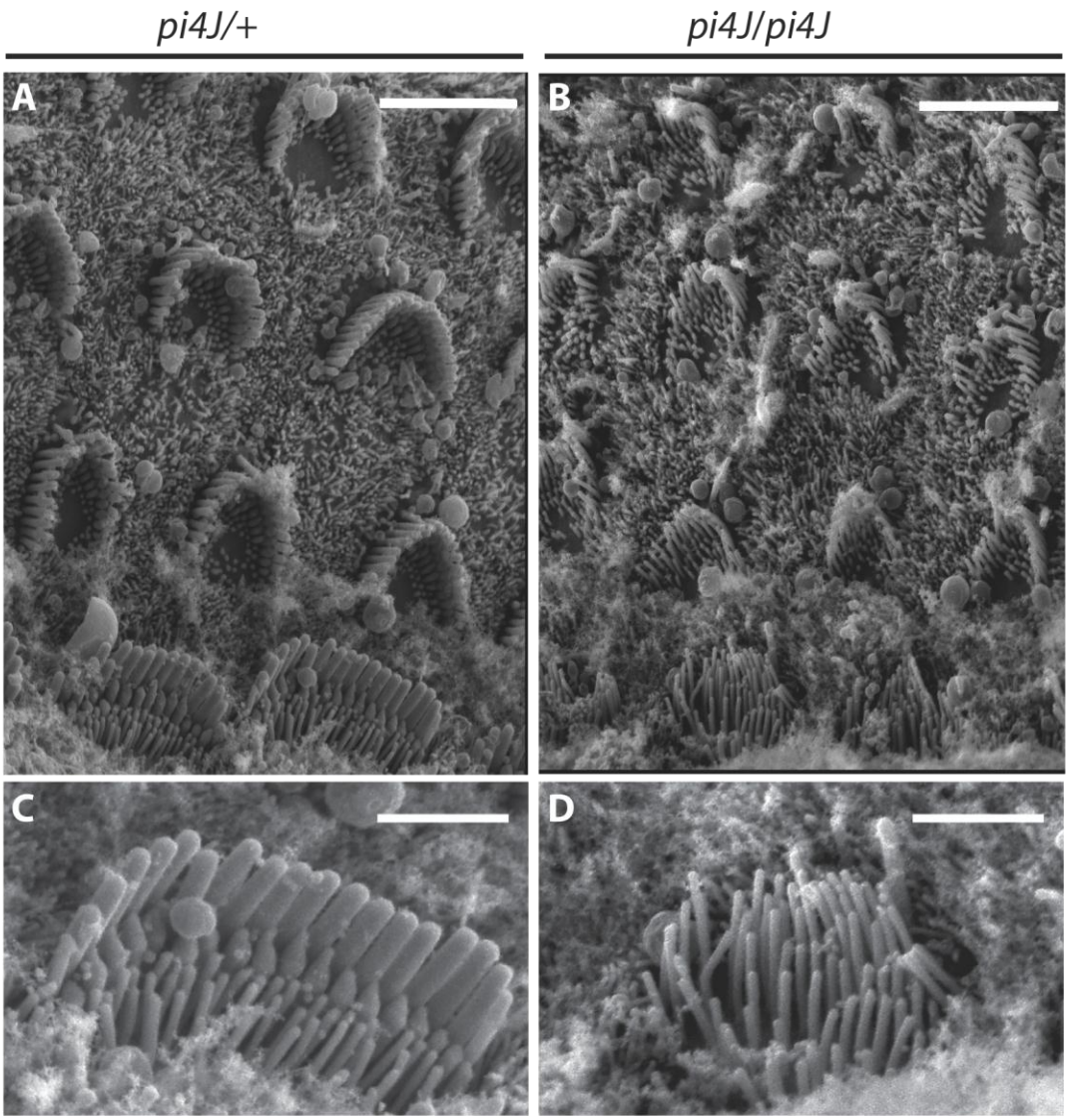

Figure 2.3 *pi4J* mutants exhibit thin stereocilia on cochlear hair cells. Inner ear tissue from postnatal day 7 mice was dissected and processed for scanning electron microscopy (SEM) analysis. A & C) Heterozygote control mice (*pi4J/+*) with normal-stereocilia morphology on inner and outer hair cells. B & D) *pi4J* homozygotes with thin stereocilia on inner and outer hair cells. Scale bar represents 5 microns in A-B, 2 microns in C-D. SEM, scanning electron microscopy

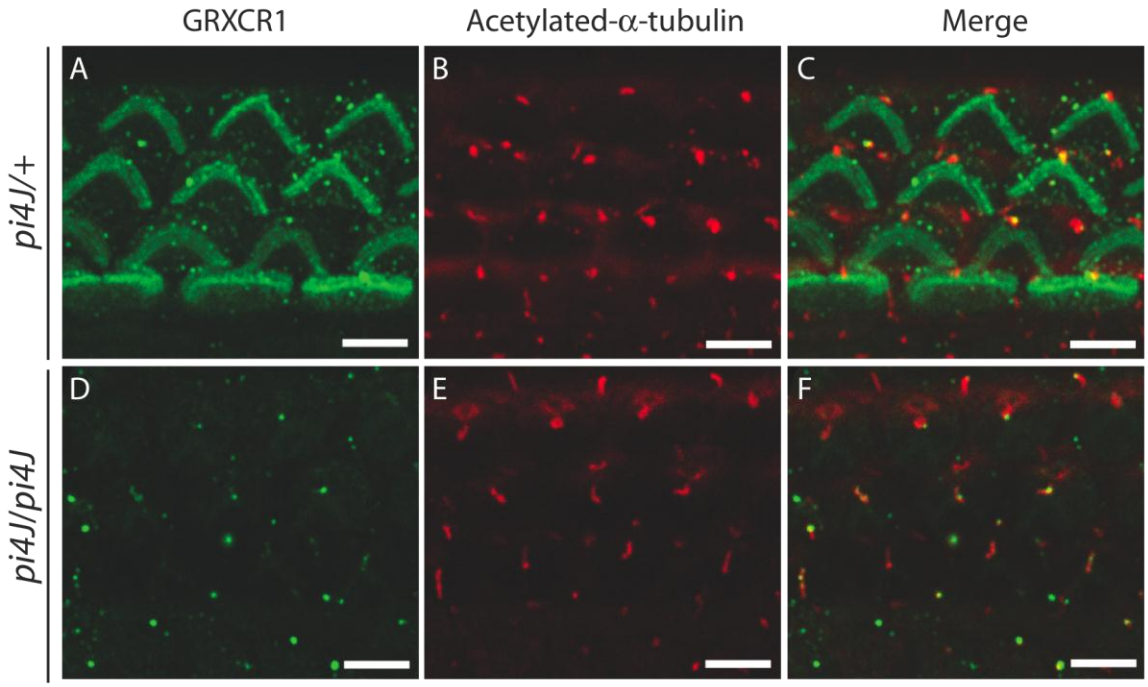

Figure 2.4 GRXCR1 does not localize to the kinocilia of inner and outer hair cells. Wholemount preparations of cochleae from *pi4J/+* and *pi4J/pi4J* mice were dissected at postnatal day 3 and immunostained with antibodies reactive with GRXCR1 and acetylated α-tubulin. A & D) *pi4J/+* mice exhibit GRXCR1 immunoreactivity in the stereocilia bundles of inner and outer hair cells while no reactivity is detected in the bundles of *pi4J/pi4J* mice. B & E) *pi4J/+* and *pi4J/pi4J* mice demonstrate immunoreactivity to acetylated α-tubulin which demonstrates the presence of the kinocilia. C & F) Merged images demonstrate a lack of general colocalization of GRXCR1 and acetylated α-tubulin in either *pi4J/+* or *pi4J/pi4J* mice. A-F) White scale bar = 5 microns.

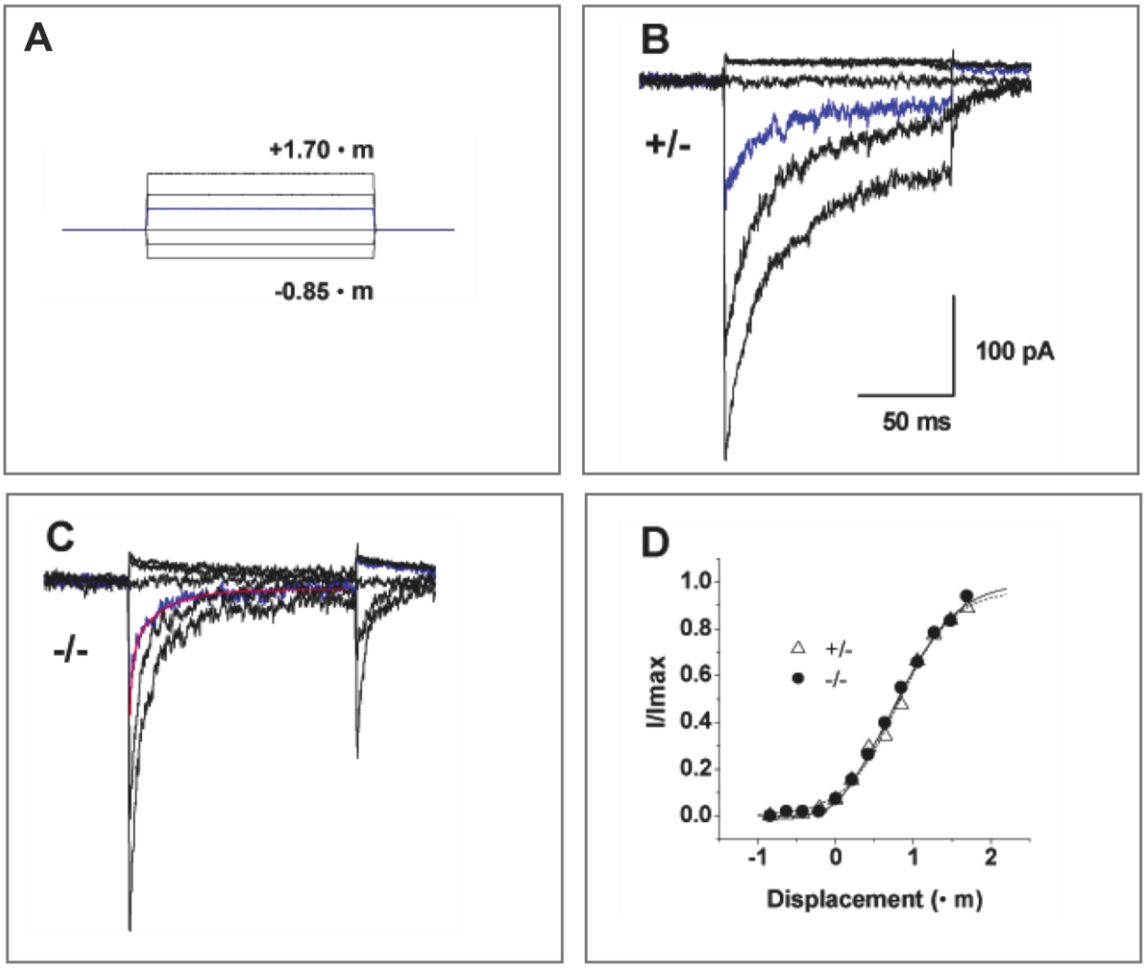

Figure 2.5 ***pi*** **mice exhibit normal mechanotransduction currents.** Transduction currents induced by square step bundle displacements (A) in outer hair cells of heterozygote (+/-) (B) and homozygote (-/-)(C) pirouette mice at postnatal day 4. Fast and slow adaptation is observed in the homozygote mutant mouse. Blue traces illustrate currents induced by 0.6 micrometer bundle displacements. Homozygote recordings are best fit by a double exponential (red trace) with time constants $\tau 1 =$ 3.1 ms and $\tau 2 =$ 31.9 ms. Single exponential best fit heterozygote recordings: $\tau =$ 39.5 ms. Extent of adaptation reaches 92% for the homozygote and 79% for the heterozygote. (D) Normalized current-displacement relationships obtained from analysis of the peak current recorded in B and C. Second order Boltzmann fit (Solid: -/-; dash: +/-) reveals a 10-90% operating range of 1.6 micrometer for both sets of recordings. Percentage of current activated at rest is 5.9% (Imax = 182pA) for the homozygote and 10.3% (Imax=232 pA) for the heterozygote.

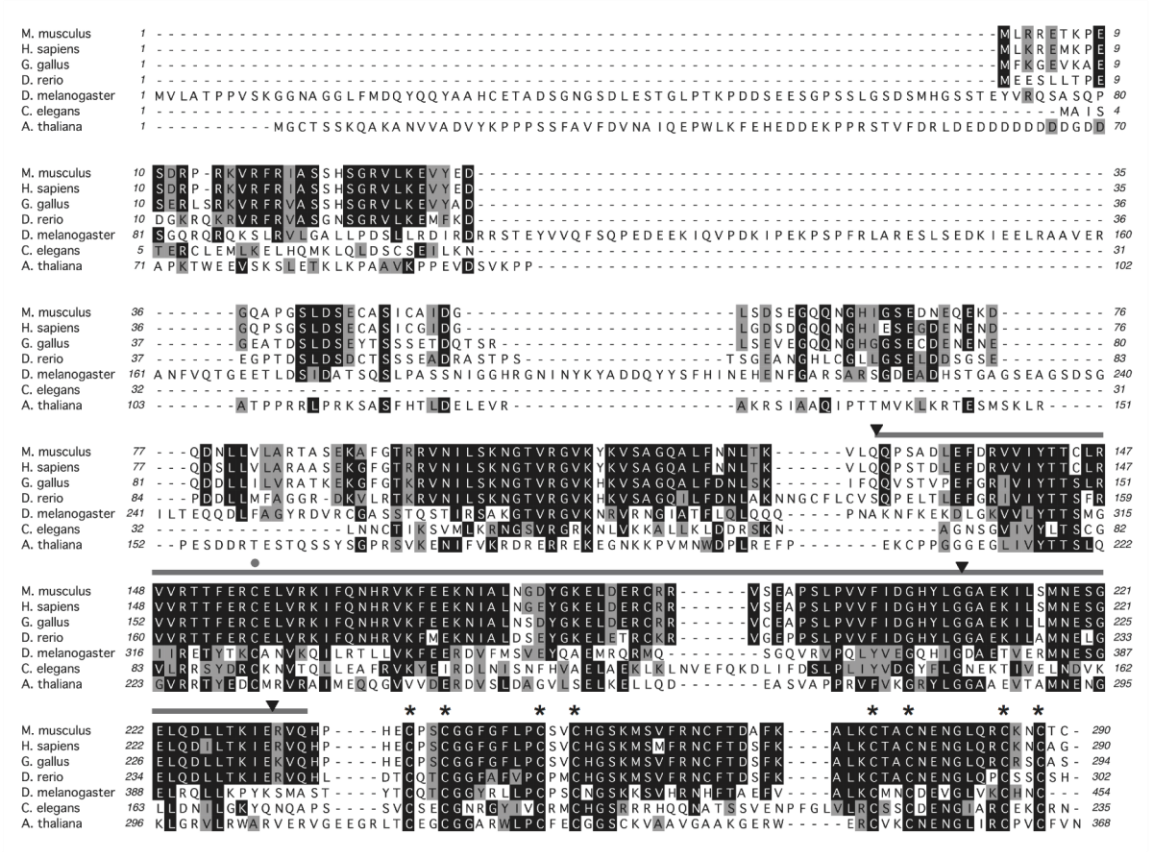

Figure 3.1. GRXCR1 exhibits deep evolutionary conservation. A. Amino acid alignment of mouse GRXCR1 with homologous proteins from a range of metazoan species. The region of similarity of GRXCR1 with glutaredoxin (Grx) proteins is indicated with a gray bar, the putative Grx active site cysteine is indicated with a gray dot, and conserved cysteines in the C-terminus are marked with asterisks. Inverted triangles indicate the positions of the three exon boundaries in the corresponding four-exon mouse *Grxcr1* gene. Amino acids shaded in black are identical in at least four of the sequences; those shaded in gray are biochemically similar in at least four of the sequences. Accession numbers: mouse – M. musculus (AAU84851); human – H. sapiens (NP_001073945); chicken – G. gallus (ENSGALT00000037467); zebrafish – D. rerio (XP_002664501); fly – D. melanogaster (AAF51916); worm – C. elegans (NP_497453); plant – A. thaliana THRUMIN1 (AAF19670).

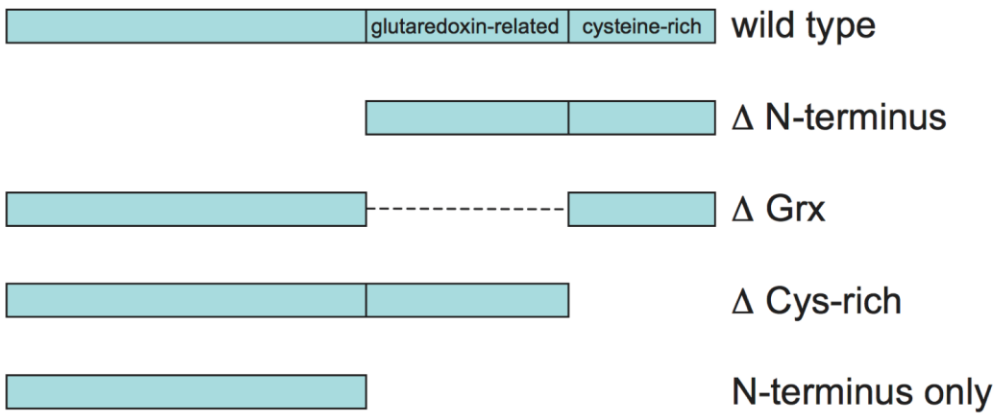

Figure 3.2. GRXCR1 expression constructs. Diagram of wild type and mutant versions of GRXCR1 that were analyzed in the current study. Deletion boundaries in the mutants correspond to the exon 1-2 and/or the exon 3-4 boundaries as noted in Figure 3.1.

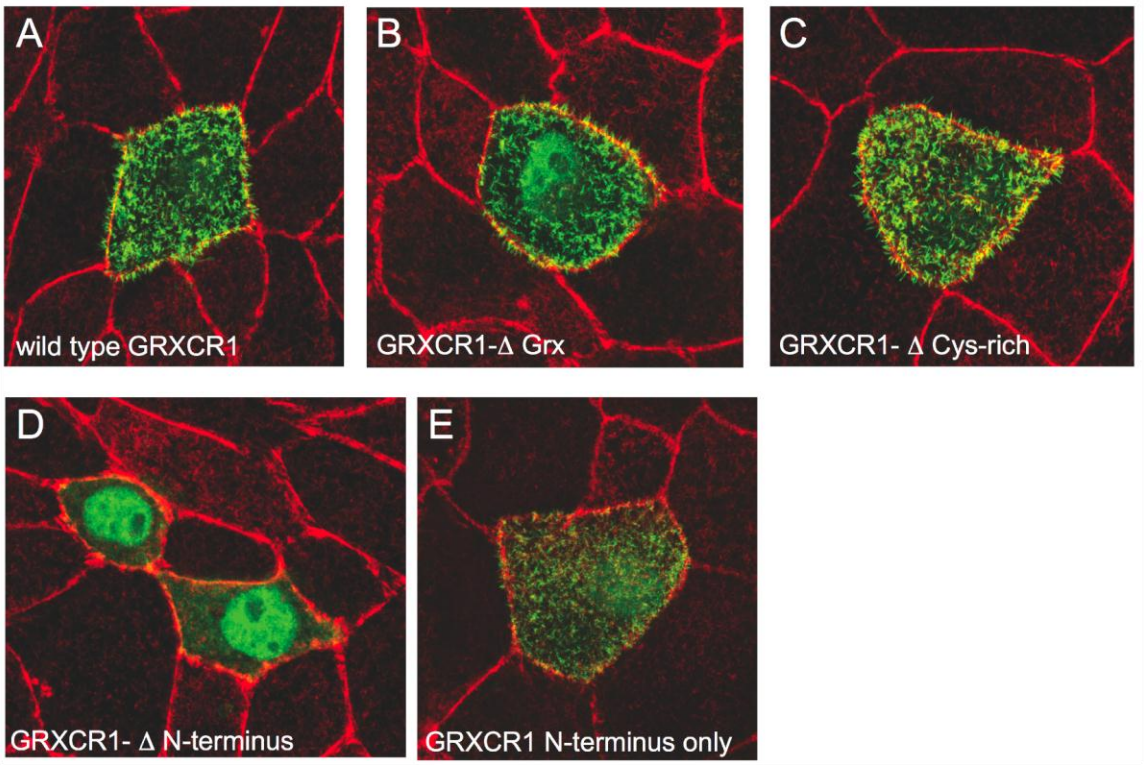

Figure 3.3. The N-terminal domain of GRXCR1 is necessary and sufficient for localization to apical microvilli. Wild type GRXCR1-GFP (green) co-localizes with actin filaments (red) in the apical microvilli of transfected CL4 epithelial cells (A). Similar localization in microvilli was observed with mutant versions lacking the Grx-like domain (B) and the C-terminal Cys-rich domain (C). A fusion protein lacking the N-terminus of GRXCR1 (D) localized mainly in the cytoplasm and nucleus, while the N-terminal domain was sufficient to drive localization to microvilli (E). Images are representative of at least three independent transfections with each construct.

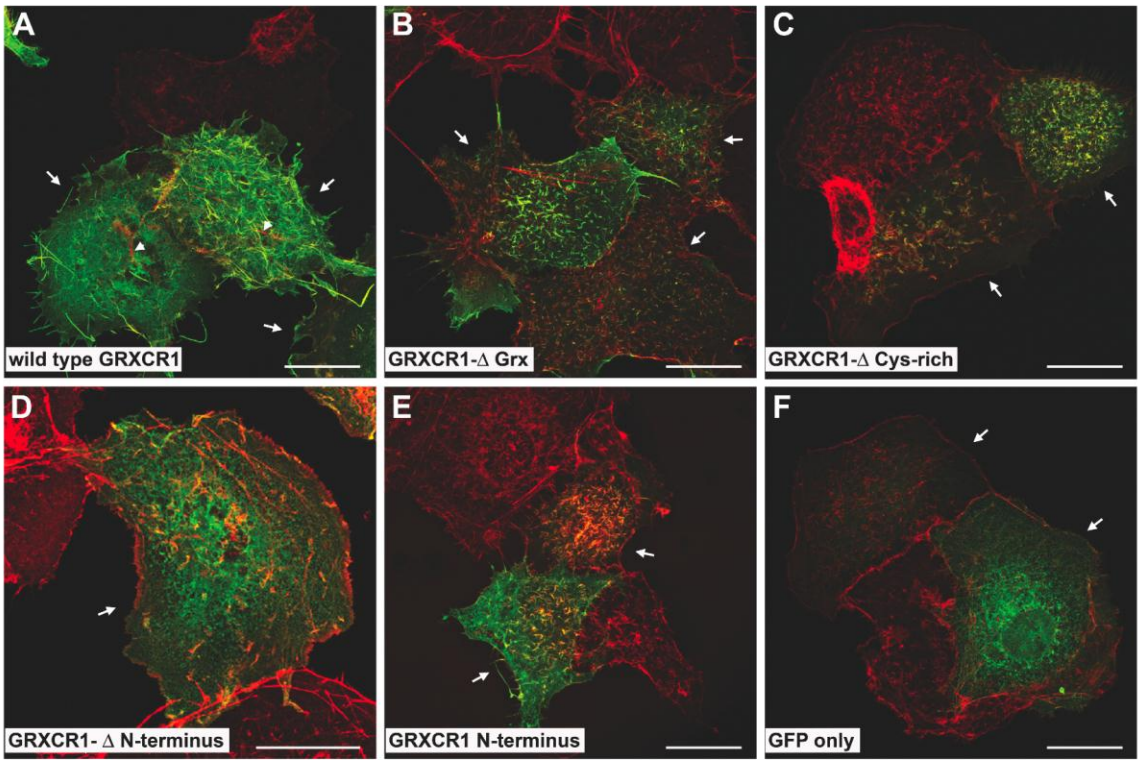

Figure 3.4. The N-terminal domain of GRXCR1 is necessary and sufficient for localization to dorsal filopodia. Wild type GRXCR1-GFP (green) co-localizes with actin filaments (red) in the dorsal filopodia of transfected COS-7 fibroblasts cells (A). Note the lack of co-localization of GRXCR1 with stress fibers in the cytoplasm of the two expressing cells in A (arrowheads). Similar localization in dorsal filopodia was observed with mutant versions lacking the Grx-like domain (B) and the C-terminal Cys-rich domain (C). A mutant protein lacking the N-terminus of GRXCR1 (D) localized mainly in the cytoplasm, while the N-terminal domain-only mutant exhibited localization to dorsal filopodia (E). GFP alone exhibited cytoplasmic and nuclear localization (F). Arrows indicate individual cells expressing varying levels of the GFP fusion proteins. Images are representative of at least three independent transfections with each construct. Scale bars represent 25 μm.

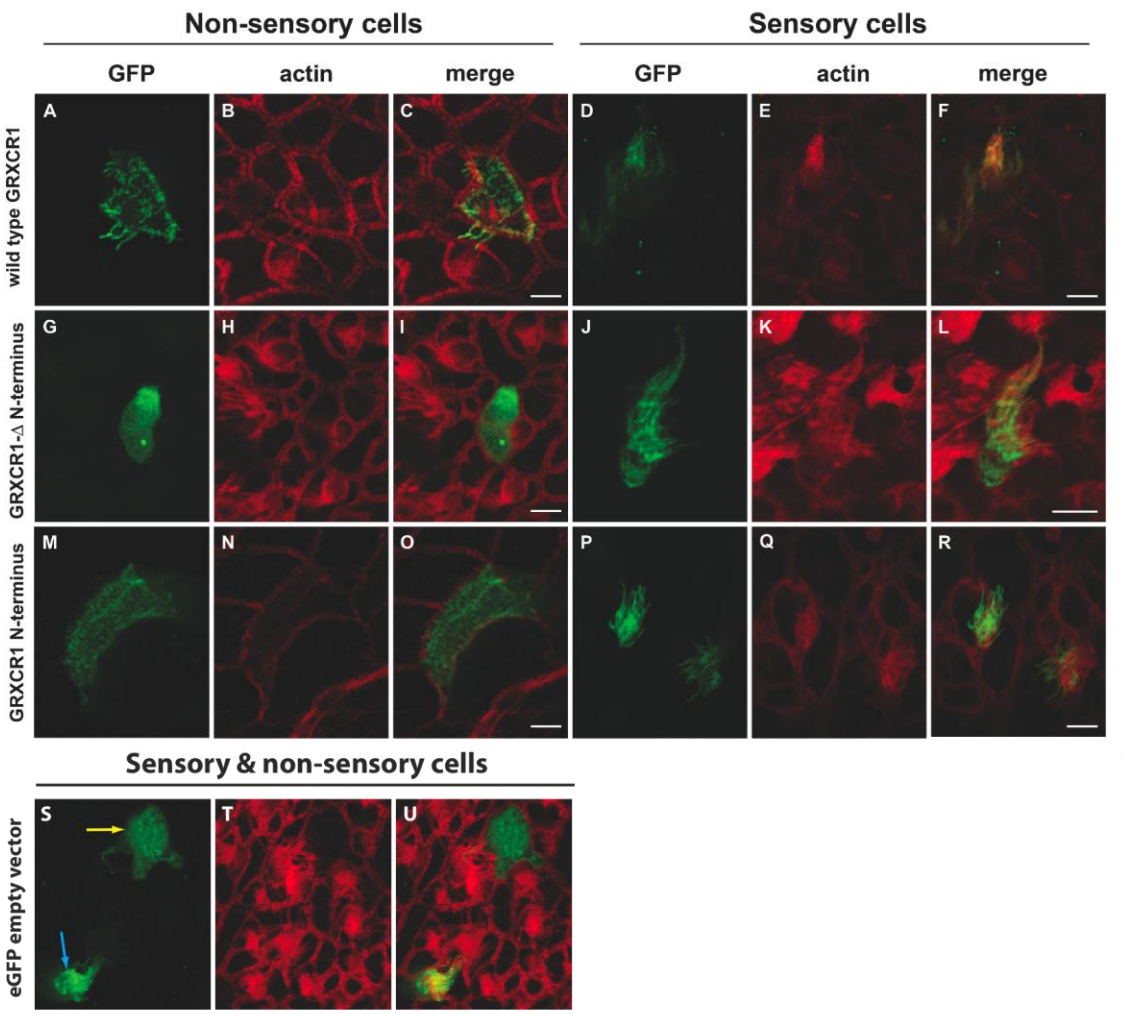

Figure 3.5. The N-terminal domain of GRXCR1 is sufficient for localization to apical actin filament-rich structures in inner ear cells. Wild type and mutant GFP expression constructs were transfected into utricle explants and analyzed for expression in nonsensory cells (A-C; G-I; M-O) and sensory cells (D-F; J-L; P-R). Wild type GRXCR1 localized to the apical microvilli of nonsensory cells and lengthened these structures (A-C). Wild type GRXCR1 localized to stereocilia of sensory cells (D-F). GRXCR1 lacking the N-terminal domain localized to the cytoplasm in nonsensory cells (G-I) but retained the ability to localize to stereocilia of sensory cells (J-L). The N-terminal domain alone was sufficient to localize the fusion protein to the apical microvilli of nonsensory cells, although microvilli did not exhibit elongation (M-O). The N-terminal domain deletion mutant was also localized to the stereocilia of sensory cells (P-R). The control GFP protein localizes to the stereocilia bundles of sensory cells (blue arrow) while it shows diffuse cytoplasmic localization in non-sensory cells (yellow). Scale bars represent 5 μm (A-L; P-R) and 21 μm (M-O).

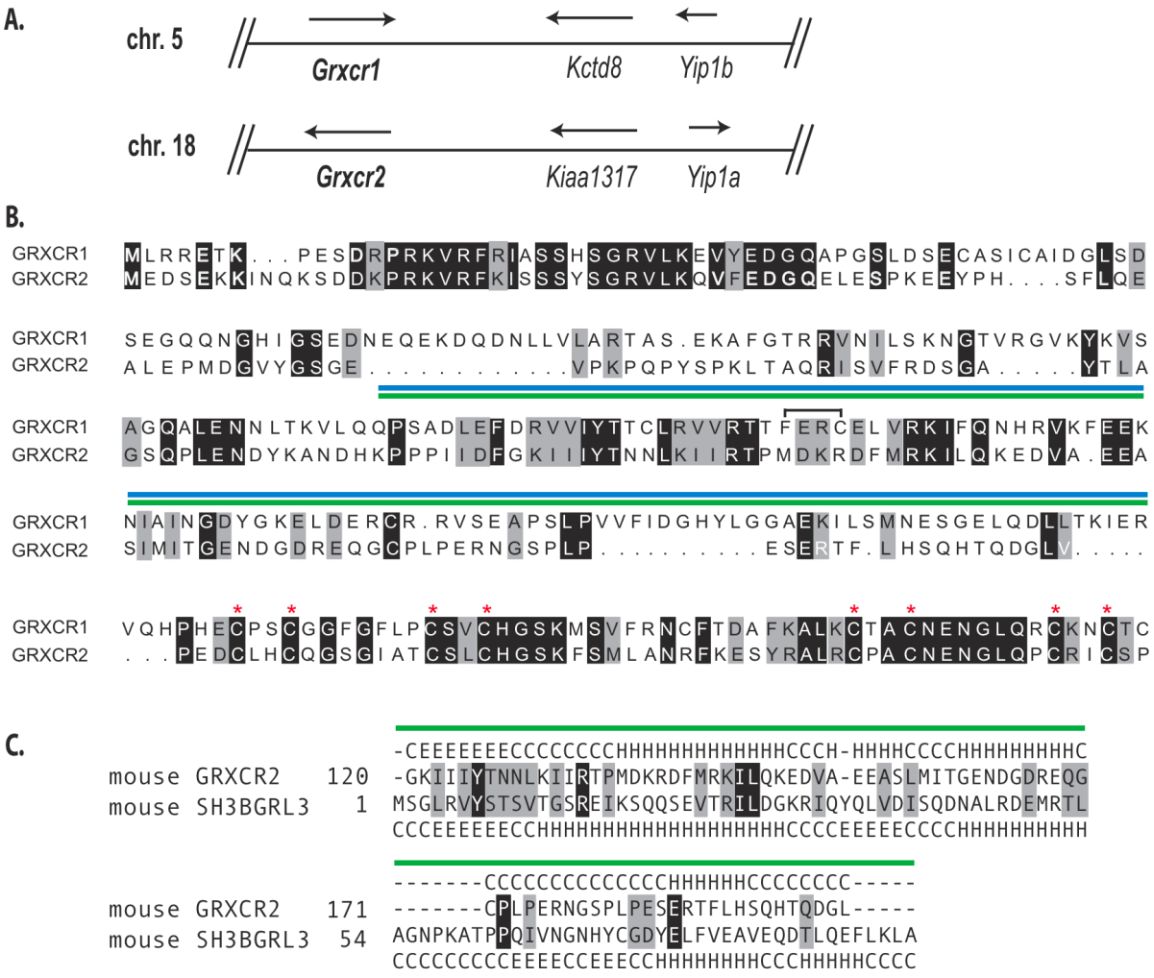

Figure 4.1 *Grxcr2* is paralogous to the previously identified deafness-causing gene *Grxcr1*. A.) Regions of mouse chromosomes 5 and 18 that contain the *Grxcr1* and *Grxcr2* loci, respectively. These regions contain conserved gene pairs (*Grxcr1,Grxcr2; Kctd8, Kiaa1317;* and *Yip1b, Yip1a*) indicative of an ancestral duplication. B.) Amino acid sequence comparison of mouse GRXCR1 and GRXCR2. Highest conservation is observed at the N- and C- termini, while the central domains are more divergent. Blue bar, glutaredoxin-like domain of GRXCR1; green bar, thioredoxin-like domain of GRXCR2; bracket, putative GRXCR1 active site; black boxes, identical residues; gray boxes, biochemically similar residues; and red asterisks, conserved bipartite arrangement of cysteine residues. C.) Secondary structure similarity between the thioredoxin-like fold containing protein SH3BGRL3 and GRXCR2 was recognized by the PHYRE protein fold recognition server. Green bar, thioredoxin-like domain of GRXCR2, C, random coil; E, beta sheet; and H, alpha helix.

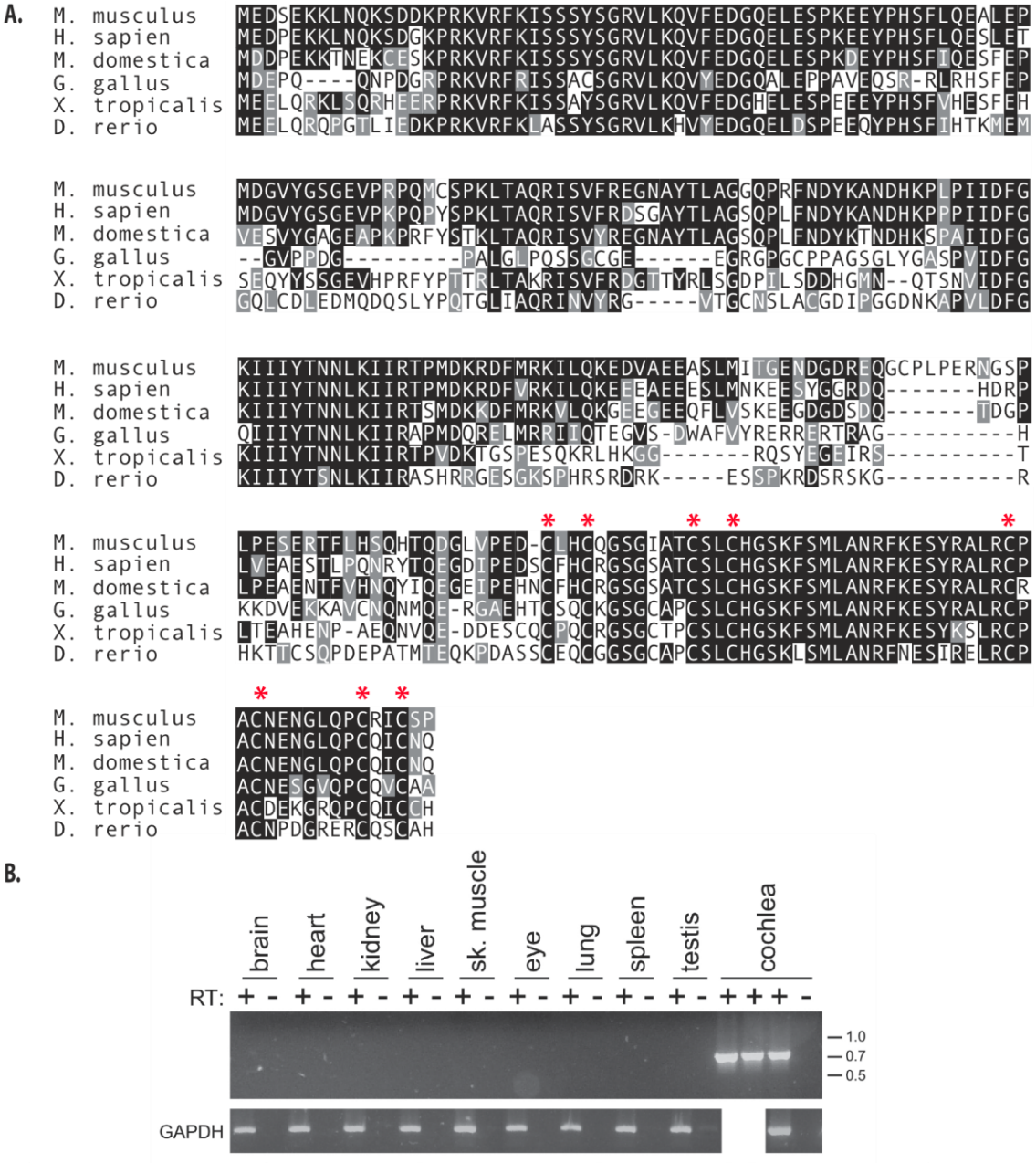

Figure 4.2 GRXCR2 is conserved among vertebrates and demonstrates inner ear specific expression. A.) GRXCR2 orthologs are found among vertebrate species and exhibit a high degree of conservation to mouse GRXCR2. Black boxes, identical residues; gray boxes, biochemically similar residues; and red asterisks, conserved bipartite arrangement of cysteine residues. B.) RT-PCR products corresponding to full-length *Grxcr2* transcripts that were amplified from cochlear RNA but not from RNA derived from a variety of other tissues.

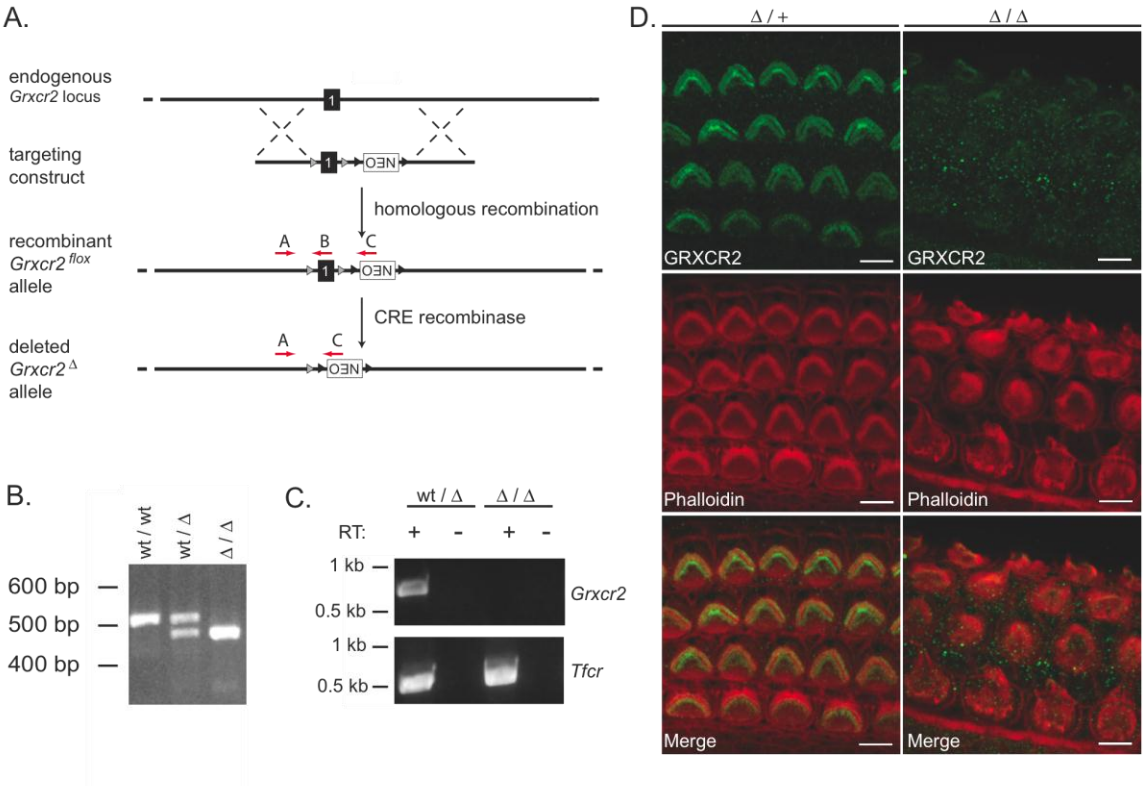

Figure 4.3 Mutational targeting of exon 1 of *Grxcr2*. A.) The wild type *Grxcr2* locus, the recombinant allele after homologous integration of the targeting construct, and the deleted allele (*Grxcr2* Δ) after CRE recombination are shown. Red arrows indicate the positions of genotyping primers to detect the endogenous (primer pair A& B) and deleted (primer pair A & C) alleles of *Grxcr2*. B.) Triplex PCR of genomice DNA using primers A,B, and C generateda 532 bp product from wild type mice (wt/wt), a 490 bp product from homozygous mutants (Δ/Δ), both products from heterozygotes (wt/Δ). C.) RT-PCR of cochlear RNA from heterozygous wt/Δ mice generated a 719 bp product, indicating expression of normal *Grxcr2* transcripts. The absence of this product from Δ/Δ mutants demonstrated loss of normal *Grxcr2* expression. Amplification of *Tfrc* transcripts from cochlear RNA of both genotypes demonstrated similar RNA quantity and quality. D.) GRXCR2 immunoreactivity was demonstrated in stereocilia bundles in the cochlea of *Grxcr2* heterozygotes at postnatal day 3 but was absent from Δ/Δ mutants. Phalloidin reactivity indicates actin filament content in the stereocilia of mice of both genotypes. *Tfrc*, transferrin receptor; RT, reverse transcriptase

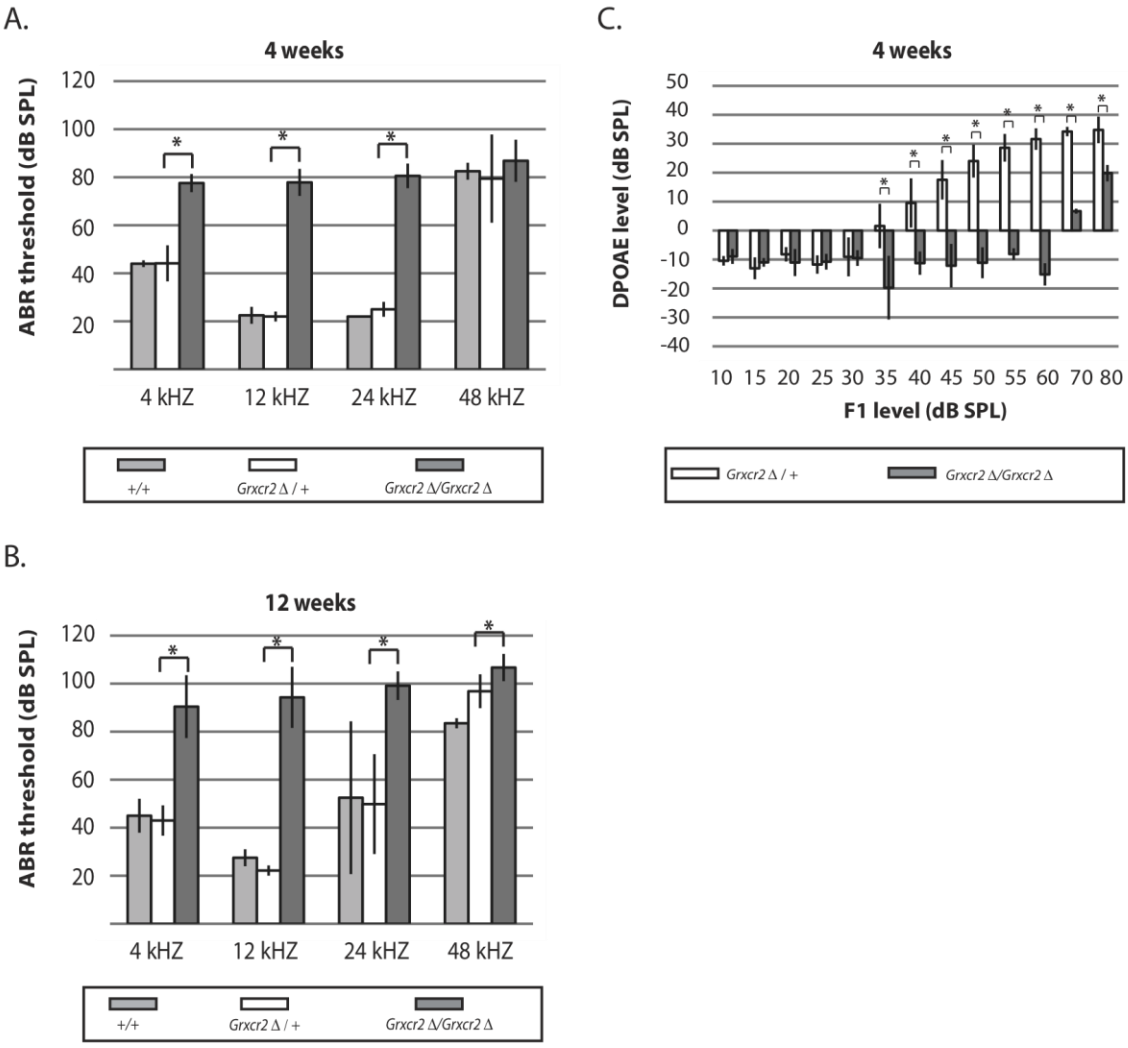

Figure 4.4 *Grxcr2* mutants exhibit auditory defects including outer hair cell dysfunction. A.) At 4 weeks of age, *Grxcr2* homozygous mutants exhibited increased ABR thresholds in response to pure tones at 4, 12, and 24 kHz relative to wild type and heterozygous littermate controls (non-parametic t-test p-value < 0.05). B.) Similar ABR threshold increases were demonstrated in *Grxcr2* homozygous mutants at 12 weeks of age (p-value < 0.05). C.) At 4 weeks of age, *Grxcr2* homozygous mutants exhibited significantly reduced DPOAE in response to 12 kHz stimuli, relative to DPOAE of wild type and heterozygous littermate controls (non-parametic t-test p-value < 0.05)

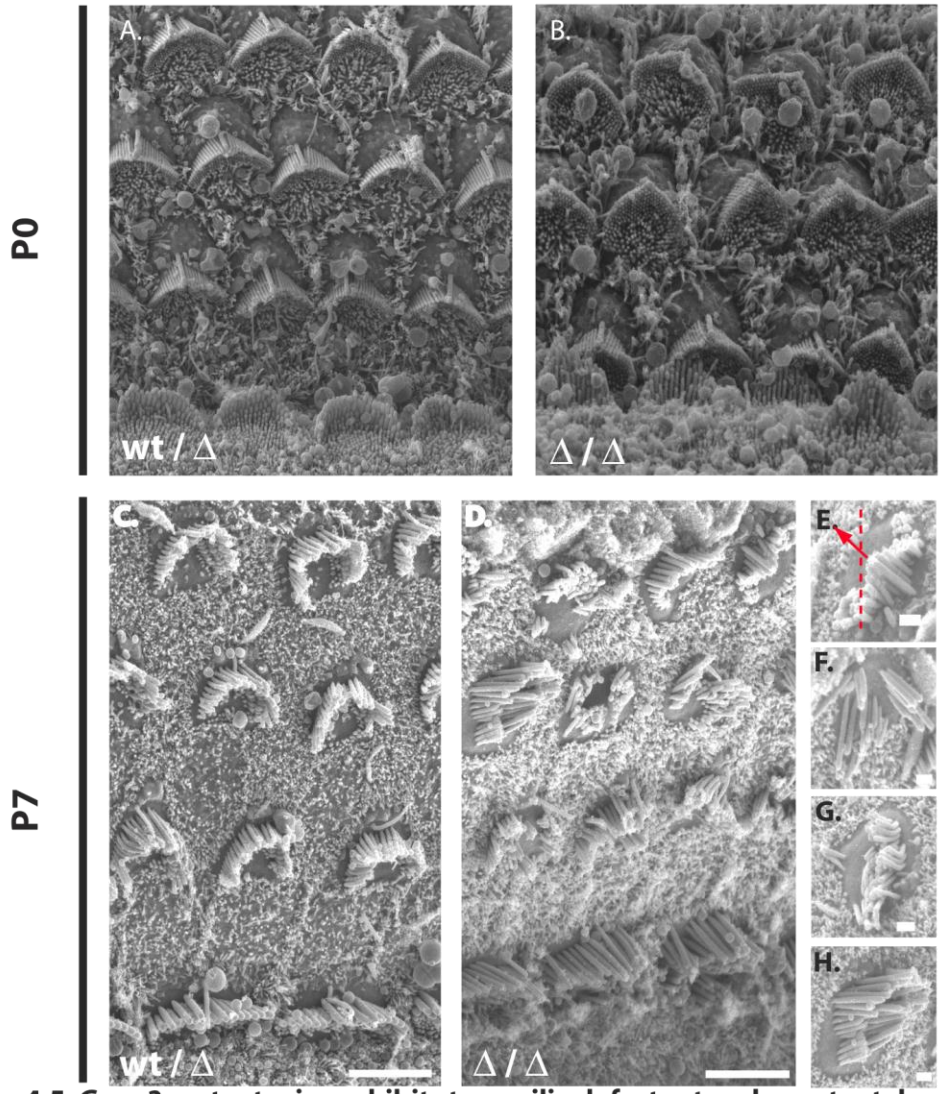

Figure 4.5 *Grxcr2* mutant mice exhibit stereocilia defects at early postnatal ages. A & C) Scanning electron micrographs of the cochlear sensory epithelium from *Grxcr2* heterozygotes demonstrated an organized mosaic of inner and outer hair cells and normal stereocilia bundle morphology at P0 and P7. B.) The cochlear sensory epithelium from *Grxcr2* mutant homozygotes exhibited normal organization of sensory cells. Bundle morphology was also relatively normal, but bundles on outer hair cells exhibited slight deviations in bundle orientation P0. D.) At P7, outer hair cell bundles exhibited more severe orientation defects and were severely disorganized. E.) Example of a misoriented bundle from a P7 *Grxcr2* homozygote. Red dashed line indicates the expected orientation axis of normal bundle; the red line with arrow indicates the orientation of this mutant bundle. F-H). Examples of splayed, flattened and circular bundles from a P7 *Grxcr2* homozygote. Scale bars indicate 5 microns (A-D) or 1 micron (E-H).

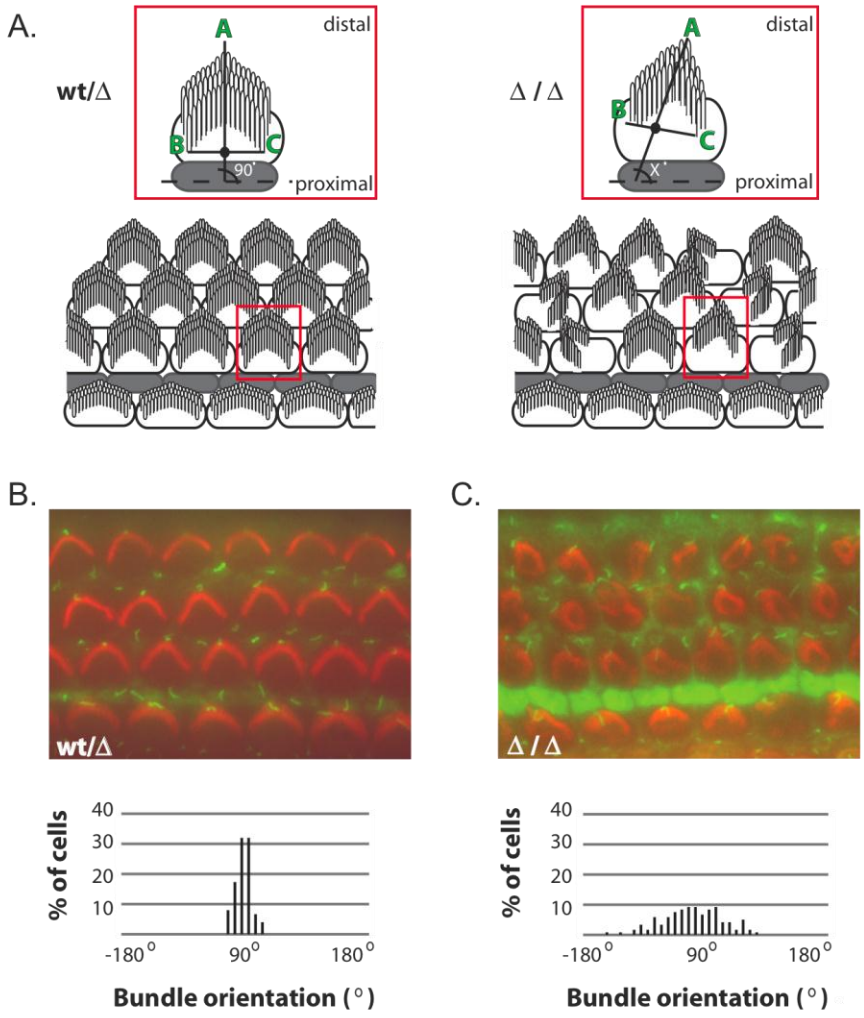

Figure 4.6 Loss of *Grxcr2* function results in stereocilia orientation defects. A.) Schematic representation of the orientation of stereocilia bundles in *Grxcr2* heterozygotes and homozygous mutants. Bundle orientation was calculated by identifying the kinocilium at the vertex of the bundle and the mid-point (solid black dot). The angle between a line was extended through these two landmarks and a longitudinal reference line through pillar cells was measured. B.) Cochlea from a *Grxcr2* heterozygote was stained with phalloidin (red) to mark the stereocilia and acetylated-α-tubulin (green) to mark the kinocilium. The bundles appeared morphologically normal with a kinocilium at the vertex of each bundle. The angles measured show a tight distribution around 90 degrees with respect to the longitudinal axis of the cochlea. C.) Kinocilia were present at the vertex of bundles from the cochlea of a *Grxcr2* homozygote, but bundles were misoriented with significant deviation from 90 degrees.

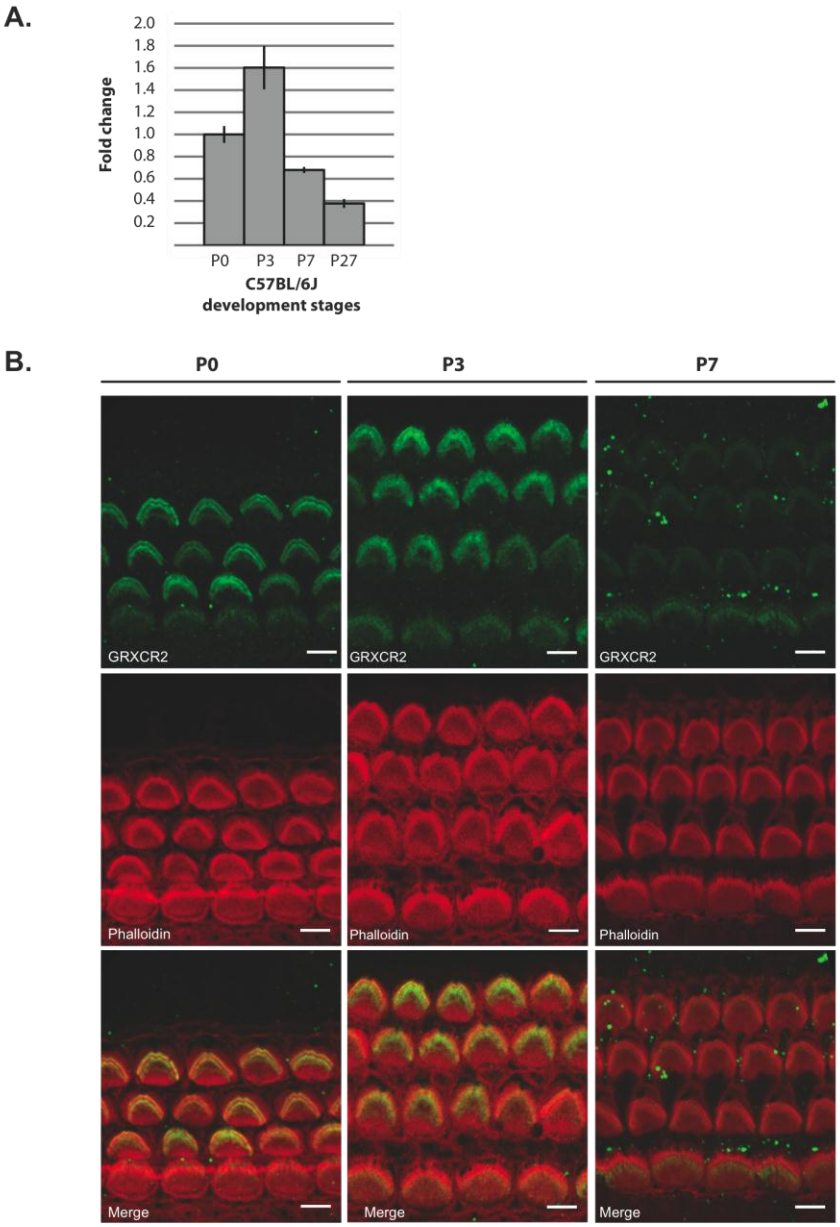

Figure 4.7 *Grxcr2* transcript and protein exhibit peak levels in the cochlea at early postnatal time points. A.) *Grxcr2* transcript levels in the cochleae of C57BL/6J mice at early postnatal time points and in adults were determined by quantitative PCR (qPCR) and normalized to those present at birth (P0). *Grxcr2* expression peaked at P3 and declined through the first postnatal week and young adulthood (P27). B.) The sensory epithelium from the cochleae of C57BL/6J mice was immunostained using an anti-GRXCR2 antibody and phalloidin to mark the stereocilia bundles. Bundles of mice at P0 and P3 exhibited robust GRXCR2 reactivity while bundles from P7 and adult (data not shown) mice exhibited lower reactivity.

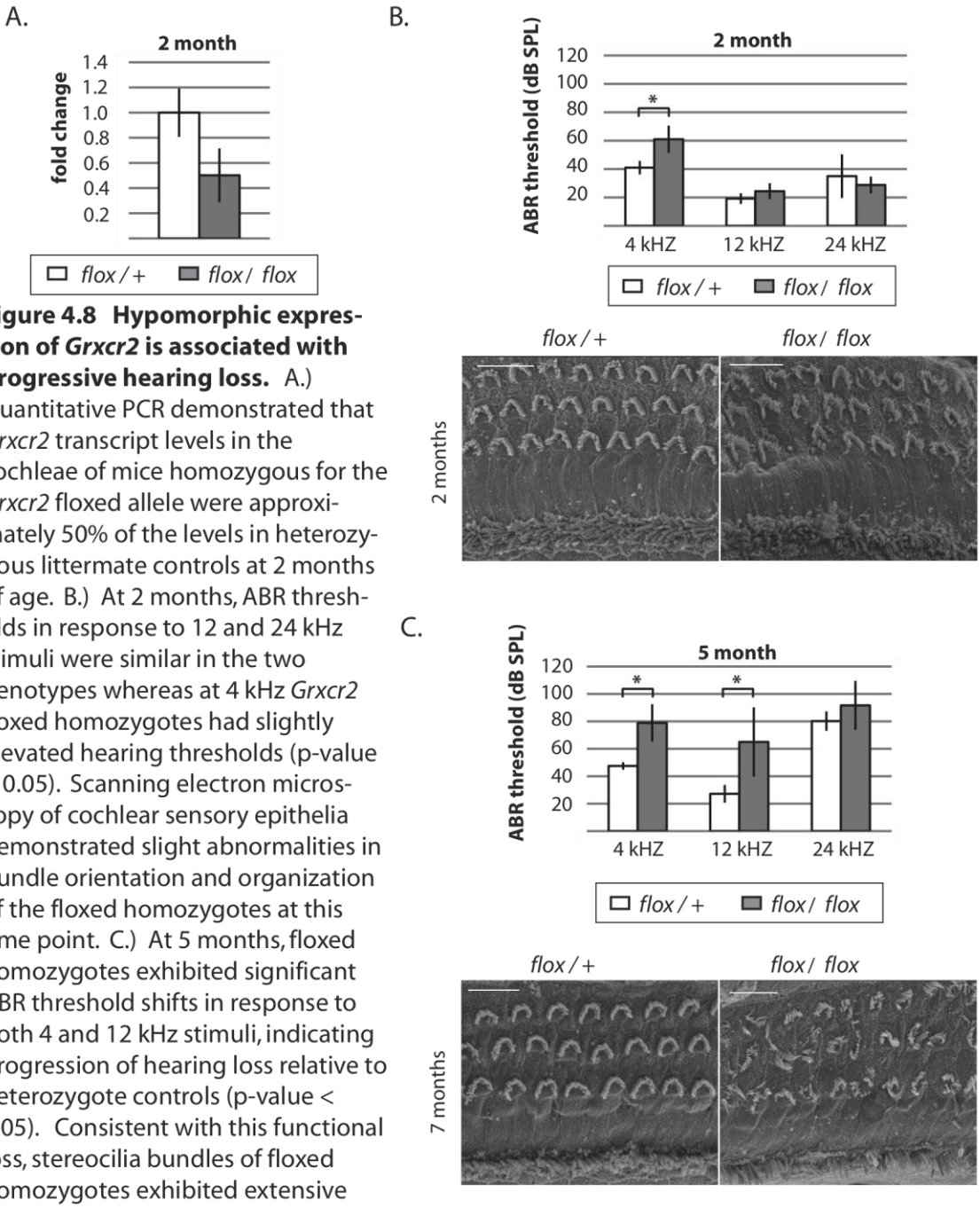

Figure 4.8 Hypomorphic expression of *Grxcr2* is associated with progressive hearing loss. A.) Quantitative PCR demonstrated that *Grxcr2* transcript levels in the cochleae of mice homozygous for the *Grxcr2* floxed allele were approximately 50% of the levels in heterozygous littermate controls at 2 months of age. B.) At 2 months, ABR thresholds in response to 12 and 24 kHz stimuli were similar in the two genotypes whereas at 4 kHz *Grxcr2* floxed homozygotes had slightly elevated hearing thresholds (p-value < 0.05). Scanning electron microscopy of cochlear sensory epithelia demonstrated slight abnormalities in bundle orientation and organization of the floxed homozygotes at this time point. C.) At 5 months, floxed homozygotes exhibited significant ABR threshold shifts in response to both 4 and 12 kHz stimuli, indicating progression of hearing loss relative to heterozygote controls (p-value < 0.05). Consistent with this functional loss, stereocilia bundles of floxed homozygotes exhibited extensive defects in orientation and organization.

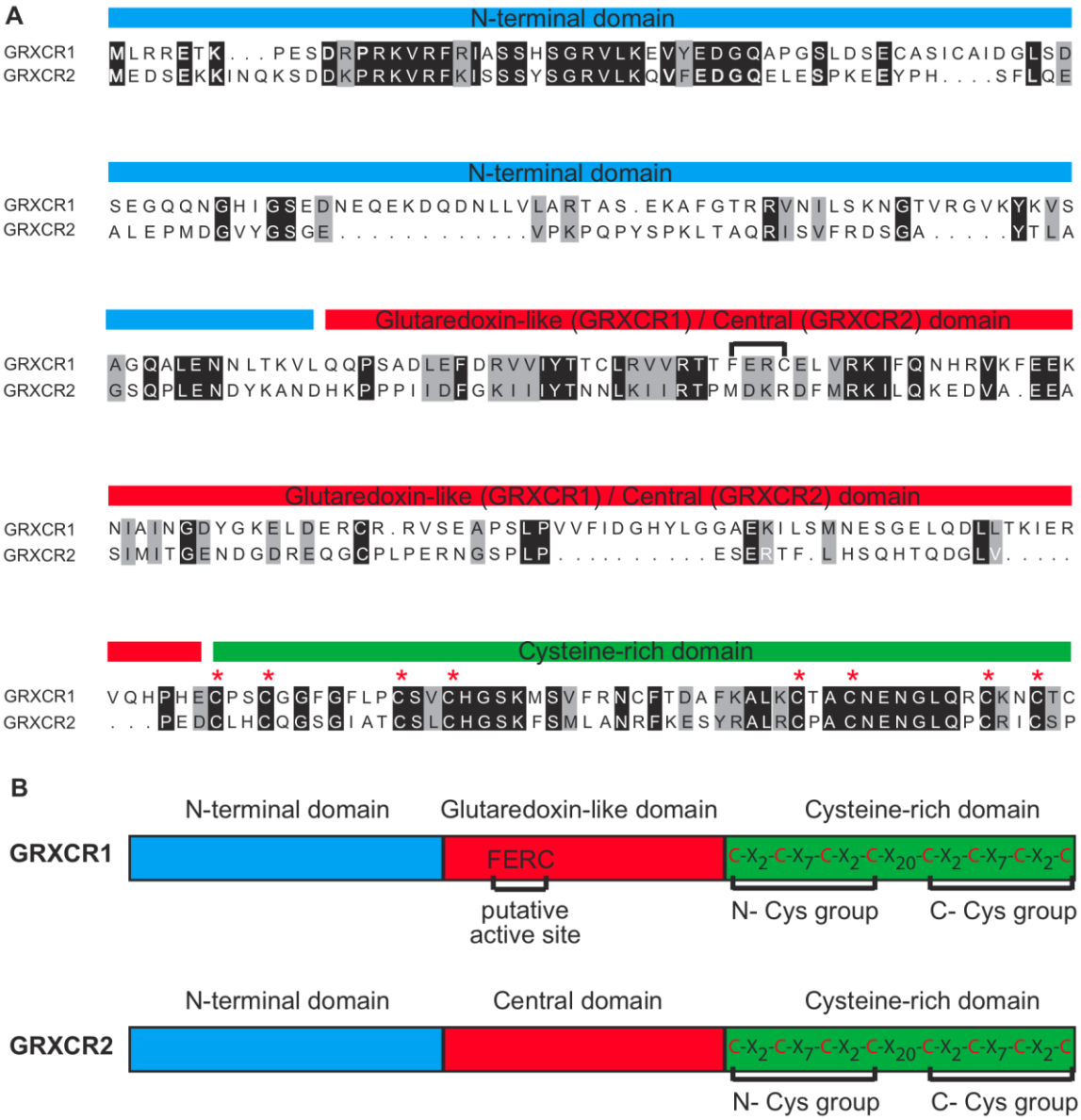

Figure 5.1 Primary sequence features of GRXCR1 and GRXCR2. A.) Amino acid sequence comparison of mouse GRXCR1 and GRXCR2. Putative domains are demarcated by: blue bar = N-terminal domain, red bar = glutaredoxin-like (GRXCR1) / central domain (GRXCR2), green bar = cysteine-rich domain. The red asterisks denote the conserved bipartite arrangement of cysteine residues, bracket indicates putative monothiol active site of GRXCR1; black boxes denote, identical residues and gray boxes denote biochemically similar residues. B.) Schematic representation of GRXCR1 and GRXCR2. The structural features are color coded to match the alignment presented in A.)

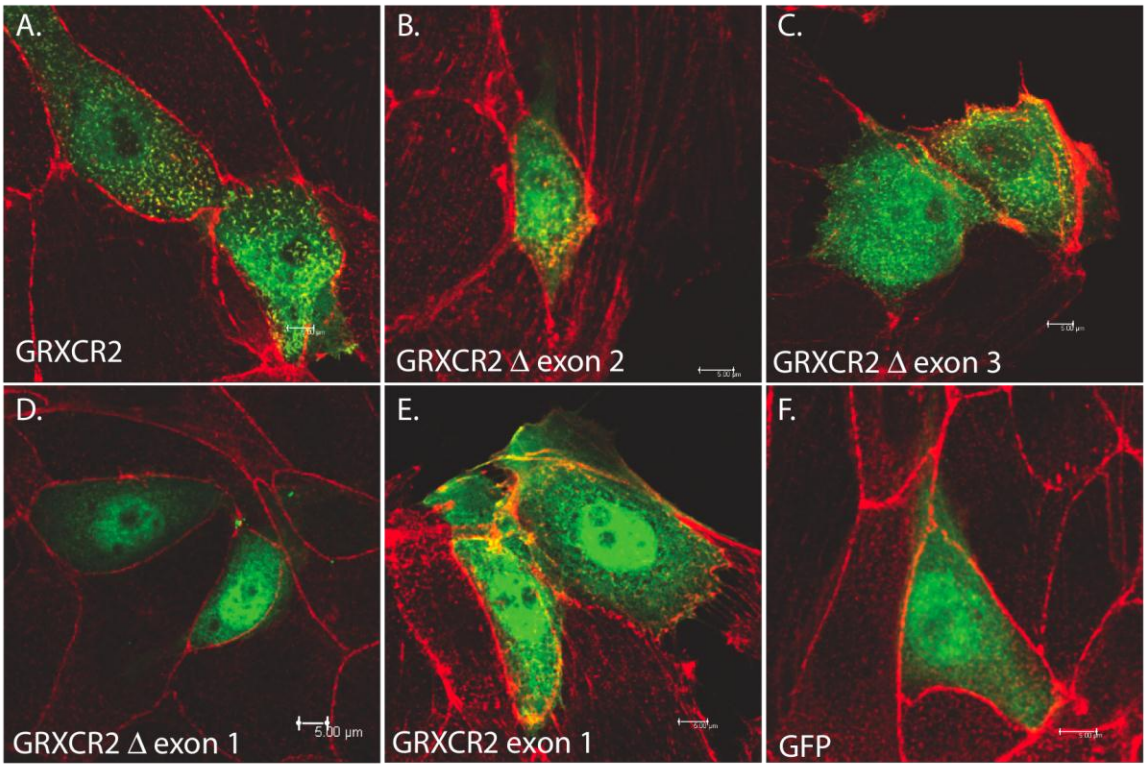

Figure 5.2 The N-terminal domain of GRXCR2 is necessary and sufficient for localization to apical microvilli. Wild type GRXCR2-GFP (green) co-localizes with actin filaments (red) in the apical microvilli of transfected CL4 epithelial cells (A). Similar localization in microvilli was observed with mutant versions lacking the central domain (B) and the C-terminal Cys-rich domain (C). A fusion protein lacking the N-terminus of GRXCR2 (D) localized mainly in the cytoplasm and nucleus, while the N-terminal domain was sufficient to drive localization to microvilli (E). GFP alone localized diffusely in the nuclear and cytoplasm (F).

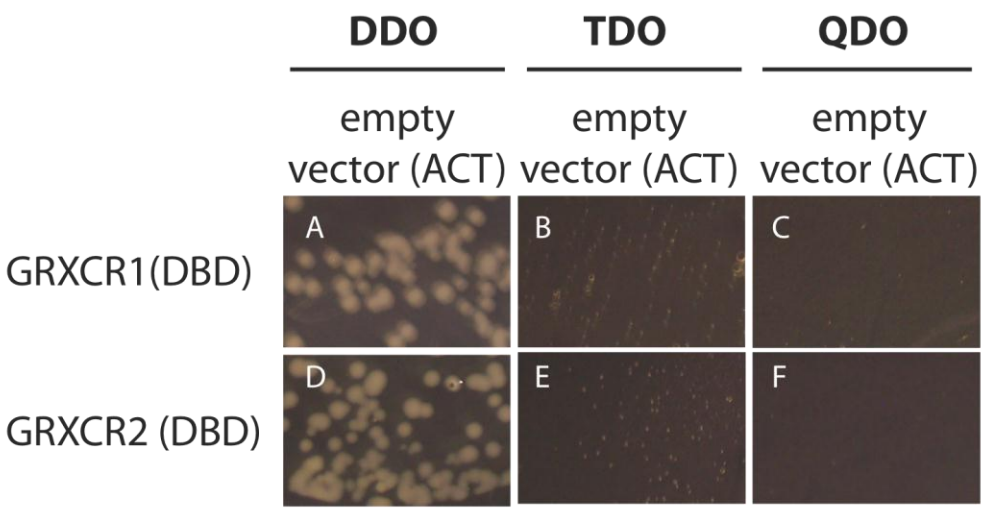

Figure 5.3 Full-length GRXCR1 and GRXCR2 do not autoactivate yeast-two-hybrid reporter genes. Yeast expressing either the GAL4 binding domain (DBD) - GRXCR1 fusion construct or the GAL4 binding domain (DBD) - GRXCR2 fusion constructs were mated with yeast expressing the GAL4 activation domain (ACT) empty vector to test for autoactivation. A & D). The presence of colonies on double drop out media (DDO) indicated successful mating. B & E) Only petite colonies were observed on triple drop out media (TDO), consistent with little or no autoactivation of reporter genes by either GRXCR1 or GRXCR2 fusions. C & F) No colonies were observed on quadruple drop out media (QDO), also indicating lack of autoactivation by the GRXCR1 or GRXCR2 fusions.

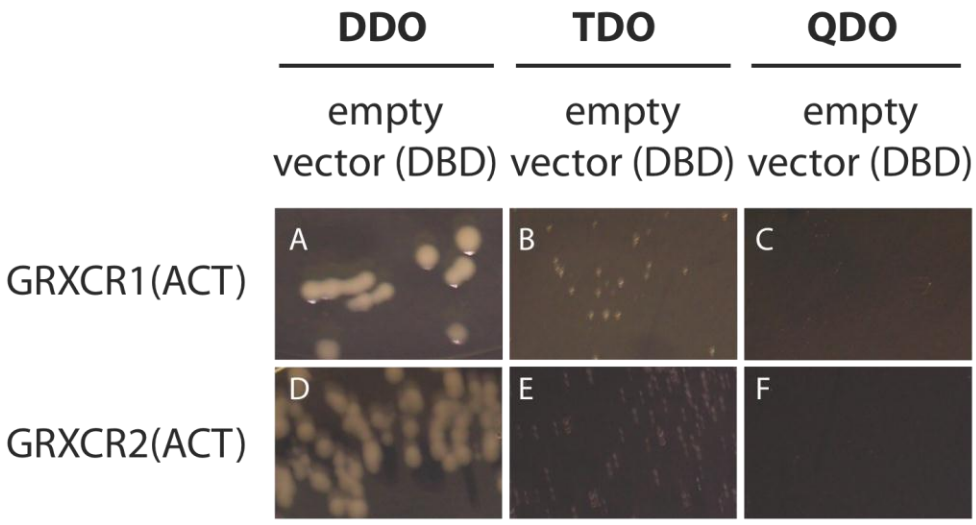

Figure 5.4 Full length GRXCR1 and GRXCR2 do not autoactivate yeast-two-hybrid reporter genes. Yeast either expressing the GAL4 activation domain (ACT) - GRXCR1 fusion construct or the GAL4 activation domain (ACT) - GRXCR2 fusion constructs were mated with yeast expressing the GAL4 binding domain (DBD) alone to test for autoactivation. A & D). The presence of colonies on double drop out media (DDO) is evidence of successful mating. B & E) Petite colonies were observed on triple drop out media (TDO) does not indicate an authentic interaction and is consistent with neither the GRXCR1 or the GRXCR2 construct autoactivating the reporter genes. C & F) No colonies were apparent on quadruple drop out media (QDO) indicating that the reporter genes were not autoactivated by the GRXCR1 or GRXCR2 constructs.

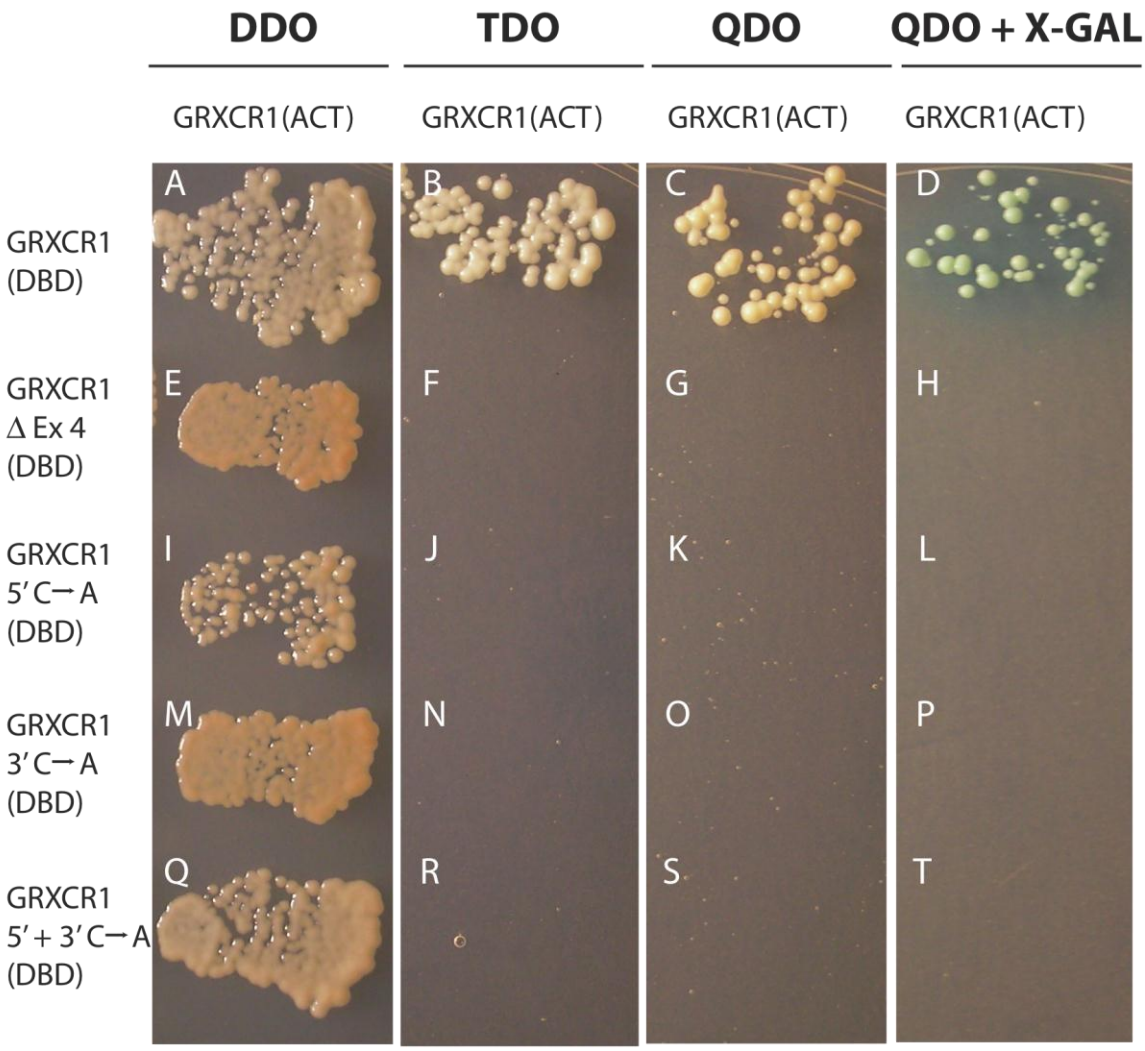

Figure 5.5 GRXCR1 exhibits homotypic interactions in yeast. Yeast expressing the GAL4 activation domain (ACT) - GRXCR1 fusion proteins were mated to yeast expressing the GAL4 binding domain (DBD) fused to wild type or mutant versions of GRXCR1. A.) Growth on DDO media indicated successful mating between strains expressing wild type GRXCR1 fusion proteins. B,C,D) Growth of the diploid strains expressing wild type GRXCR1 fusion proteins on selective media of increasing stringencies is consistent with GRXCR1 self-interactions. E,I, M, Q) Growth on DDO media indicated successful mating between strains expressing GAL4 (ACT) - GRXCR1 and GAL4 (DBD) fusion proteins carrying a deletion of the C-terminal Cys-rich domain of GRXCR1 or Cys-Ala missense mutations in this domain. F-H, J-L, N-P, R-T) Lack of growth on selective media in any of the diploids expressing mutant GRXCR1 hybrids is consistent with the dependence of GRXCR1 self-interactions on the conserved Cys residues in the C-terminus of GRXCR1.

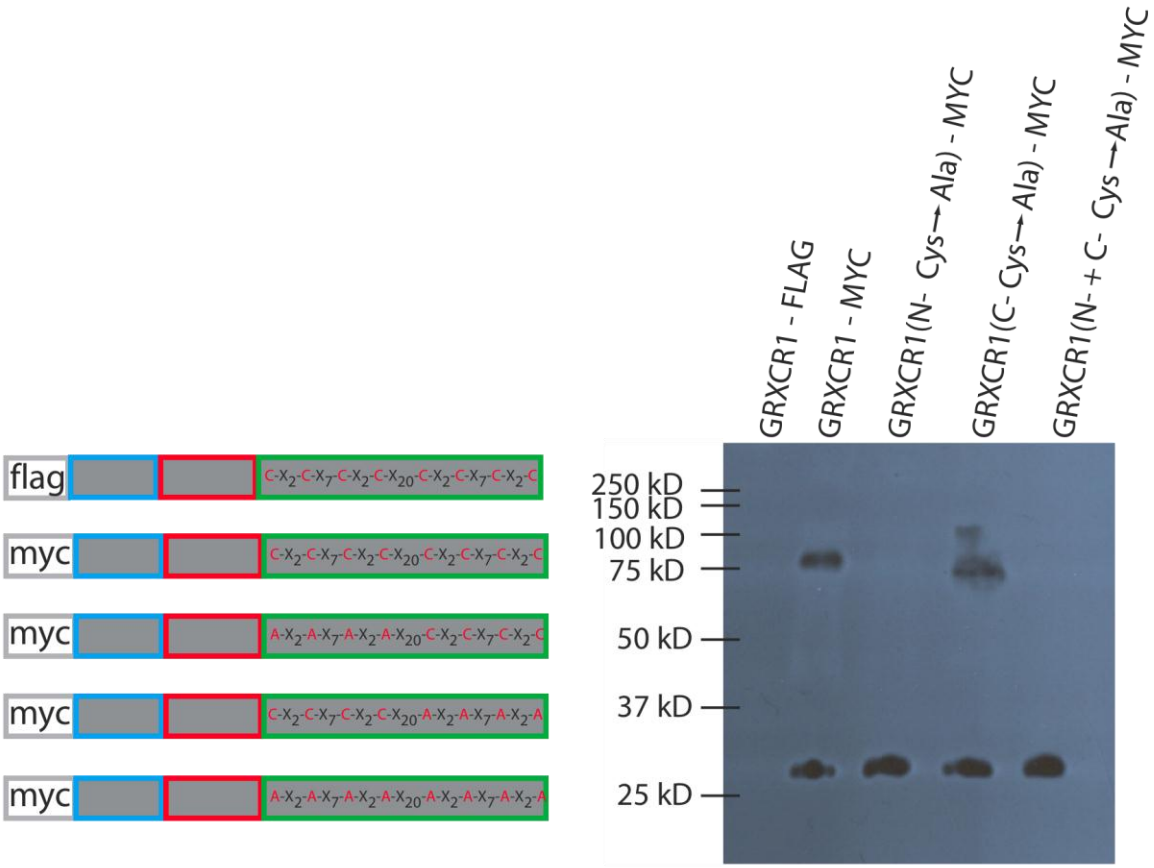

Figure 5.6. Putative dimer formation by GRXCR1. A) Using PCR-based cloning approaches, myc and FLAG epitopes were added to wild type GRXCR1 and versions carrying Cys-Ala missense mutations in the conserved C-terminus. B.) Whole cell protein lysates prepared from COS7 cells transfected with the epitope-tagged GRXCR1 fusion proteins were separated by native polyacrylamide gel electrophoresis, transferred to membranes and incubated with an anti-myc antibody. Immunoreactive signals at approximately 30 kD and 75 kD in the lysate containing the myc-GRXCR1 wild type protein is consistent with the expected positions of monomeric and dimeric forms of the fusion protein. Lack of the putative dimeric signal in lysates containing the N-Cys-Ala and the N+C Cys-Ala mutants indicates that the N- group of conserved cysteines is necessary for putative dimer formation. The lack of myc immunoreactivity in the lysates containing FLAG-tagged GRXCR1 indicates the specificity of the anti-myc antibody.

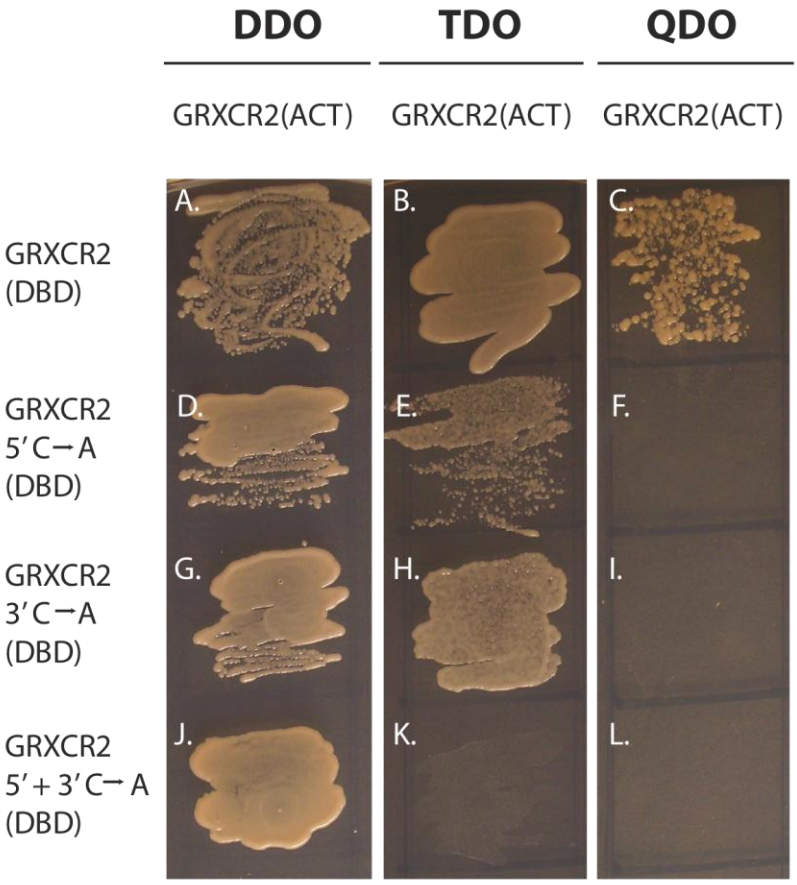

Figure 5.7 GRXCR2 exhibits homotypic interactions in yeast. Yeast expressing the GAL4 activation domain (ACT) - GRXCR2 fusion proteins were mated to yeast expressing the GAL4 binding domain (DBD) fused to wild type or mutant versions of GRXCR2. A,D,G,J) Growth on DDO media indicated successful mating between GRXCR2 expressing strains. B,C) Growth on TDO and QDO selective media of diploid strains expressing the wild type GRXCR2 fusion proteins is consistent with GRXCR2 self interactions. E,H,K) Mutation of both N+C conserved Cys residues prevented growth of the diploids on TDO selective media, although the single set N or C-Cys-Ala mutants were capable of growth. F,I,L) None of the Cys-Ala mutants were able to induce reporter gene activation under QDO selective conditions, indicating the importance of these conserved residues for self interactions of GRXCR2

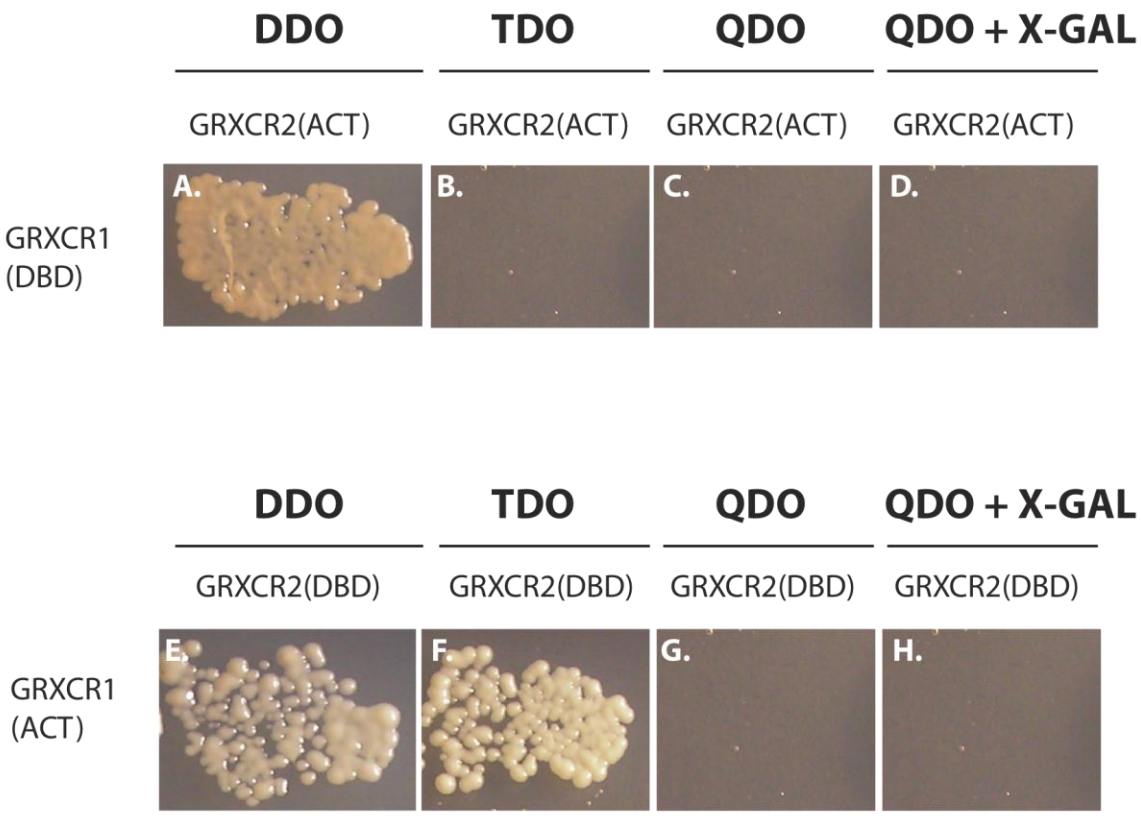

Figure 5.8 Evidence for the formation of GRXCR1-GRXCR2 heterodimers in yeast. Yeast expressing the GAL4 binding domain (DBD) - GRXCR1 fusion protein were mated to yeast expressing the GAL4 activation domain (ACT) - GRXCR2 fusion protein. A.) Growth on double drop-out media (DDO) demonstrates successful mating between strains. B-D) The absence of growth is consistent with no interaction between GRXCR1 and GRXCR2 and therefore no reporter gene activation. E-H) Yeast expressing the GAL4 binding domain (DBD) - GRXCR2 fusion proteins were mated to yeast expressing the GAL4 activation domain (ACT) - GRXCR1 fusion proteins. E.) Growth on double drop-out media (DDO) demonstrates successful mating between strains. F.) The reporter gene that allows growth on triple drop-out media was activated indicative of an interaction between GRXCR1 and GRXCR2. G-H.) The absence of growth on quadruple drop-out (QDO) or QDO + X-gal suggests that GRXCR1 and GRXCR2 did not interact to active the essential reporter genes.

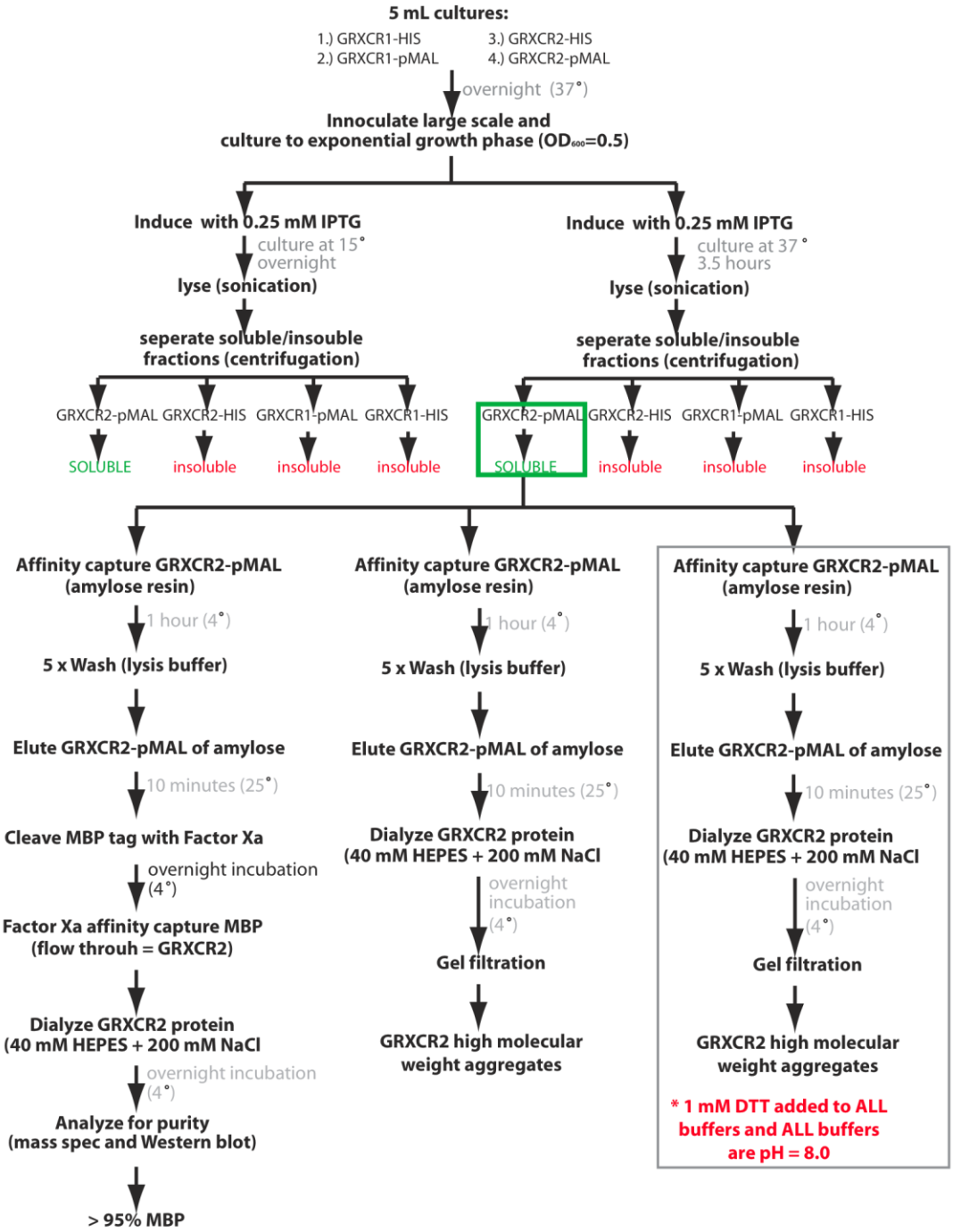

Figure 5.9 Summary of GRXCR1 and GRXCR2 protein purification strategies. Flow chart detailing attempts to purify GRXCR1 and GRXCR2 recombinant protein by affinity capture and gel filtration methodologies.

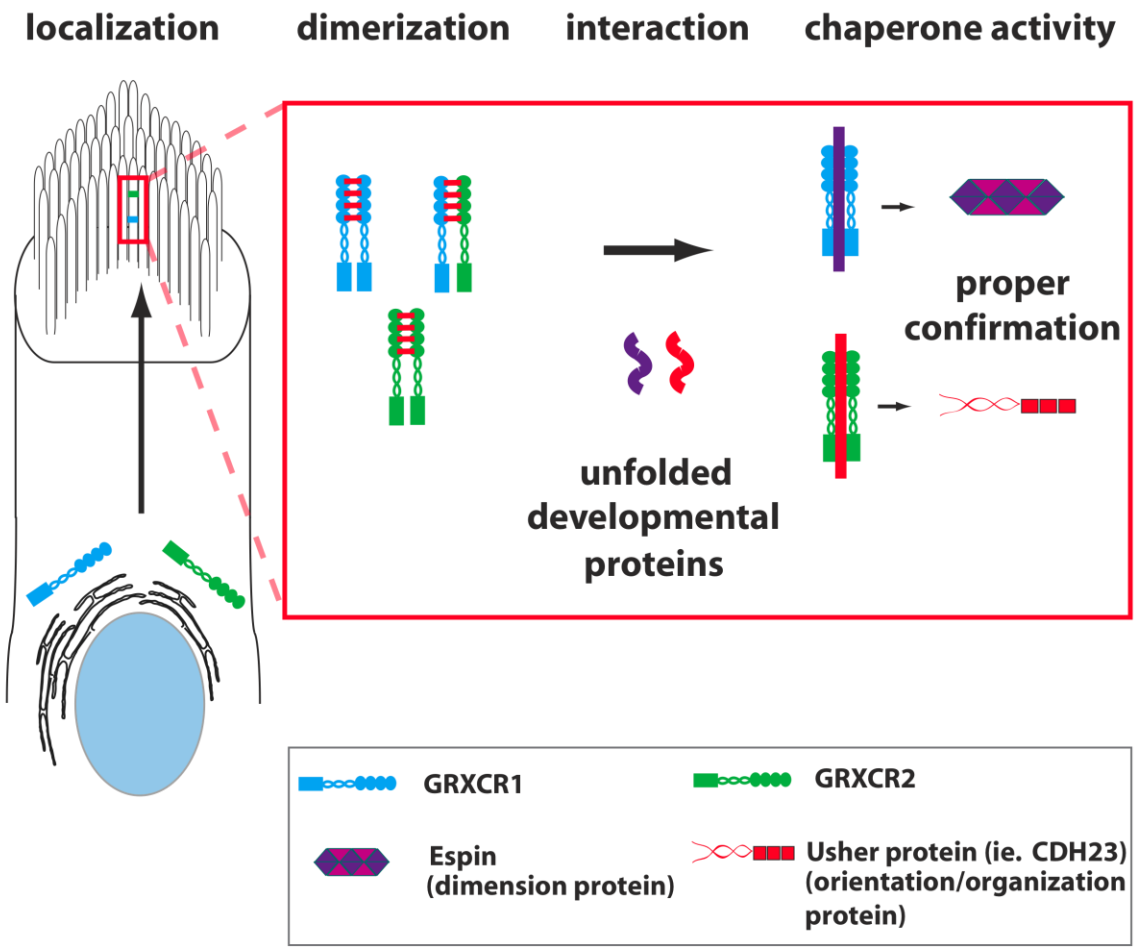

Figure 6.1 Theoretical model for function of GRXCR1 and GRXCR2 in the stereocilia of sensory hair cells. Sequence analysis and experimental data obtained from our mouse models and structure-function analysis supports a model whereby the N- terminal domain of GRXCR1 and GRXCR2 localize the proteins to the stereocilia at early developmental time points. The proteins may dimerize in order to carry out their biochemical function which based upon sequence similarity to the thioredoxin family of proteins may interact with stereocilia developmental proteins and perform chaperone related functions like other non-redox thioredoxins to confer proper confirmation. It may likely be the case that GRXCR1 and GRXCR2 act upon a relatively distinct set of substrates whereby GRXCR1 primarily functions to chaperone dimension proteins and GRXCR2 primarily functions to chaperone orientation/organization proteins. The theoretical difference in chaperone activity on distinct substrates may account for the difference in stereocilia phenotype seen in mouse models of *Grxcr1* and *Grxcr2*.

Bibliography

1. Adato, A. et al. Interactions in the network of Usher syndrome type 1 proteins. Hum Mol Genet 14, 347-56 (2005).

2. Ahmed, Z.M. et al. The tip-link antigen, a protein associated with the transduction complex of sensory hair cells, is protocadherin-15. J Neurosci 26, 7022-34 (2006).

3. Ahmed, Z.M. et al. PCDH15 is expressed in the neurosensory epithelium of the eye and ear and mutant alleles are responsible for both USH1F and DFNB23. Hum Mol Genet 12, 3215-23 (2003).

4. Altschul, S.F. et al. Gapped BLAST and PSI-BLAST: a new generation of protein database search programs. Nucleic Acids Res 25, 3389-402 (1997).

5. Amsler, K. & Cook, J.S. Linear relationship of phlorizin-binding capacity and hexose uptake during differentiation in a clone of LLC-PK1 cells. J Cell Physiol 122, 254-8 (1985).

6. Arany, Z.P. High-throughput quantitative real-time PCR. Curr Protoc Hum Genet Chapter 11, Unit 11 10 (2008).

7. Avenarius M, G.G., Hunker KL, Gong TZ, Gagnon, LH, Johnson KR, Kohrman DC. . Expression and functional analysis of sensory hair cells in Grxcr1 deafness mutants. in preparation - Mammalian Genome (2011).

8. Avenarius M, H.K., Zheng L, Gong TW, Raphael Y, Bartles J, Kohrman D. Determinants of Localization and Induction of Actin Filament-Rich Structures by the Stereocilia Protein GRXCR1. submitted to PloS ONE (2011).

9. Avenarius M, J.J., Kabara L, Askew C, Jones S, Geleoc G, Dolan DF, Raphael Y, Kohrman D. A targeted mutation of Grxcr2 results in hearing loss associated with defects in stereocilia development. . in preparation - Journal of Neuroscience (2011).

10. Avraham, K.B. Mouse models for deafness: lessons for the human inner ear and hearing loss. Ear Hear 24, 332-41 (2003).

11. Ballana, E. et al. Efficient and specific transduction of cochlear supporting cells by adeno-associated virus serotype 5. Neurosci Lett 442, 134-9 (2008).

12. Bartles, J.R., Wierda, A. & Zheng, L. Identification and characterization of espin, an actin-binding protein localized to the F-actin-rich junctional plaques of Sertoli cell ectoplasmic specializations. J Cell Sci 109 (Pt 6), 1229-39 (1996).

13. Belyantseva, I.A., Boger, E.T. & Friedman, T.B. Myosin XVa localizes to the tips of inner ear sensory cell stereocilia and is essential for staircase formation of the hair bundle. Proc Natl Acad Sci U S A 100, 13958-63 (2003).

14. Belyantseva, I.A. et al. Myosin-XVa is required for tip localization of whirlin and differential elongation of hair-cell stereocilia. Nat Cell Biol 7, 148-56 (2005).

15. Belyantseva, I.A., Labay, V., Boger, E.T., Griffith, A.J. & Friedman, T.B. Stereocilia: the long and the short of it. Trends Mol Med 9, 458-61 (2003).

16. Belyantseva, I.A. et al. Gamma-actin is required for cytoskeletal maintenance but not development. Proc Natl Acad Sci U S A 106, 9703-8 (2009).

17. Berndt, C., Lillig, C.H. & Holmgren, A. Thioredoxins and glutaredoxins as facilitators of protein folding. Biochim Biophys Acta 1783, 641-50 (2008).

18. Beyer, L.A. et al. Hair cells in the inner ear of the pirouette and shaker 2 mutant mice. J Neurocytol 29, 227-40 (2000).

19. Boeda, B. et al. Myosin VIIa, harmonin and cadherin 23, three Usher I gene products that cooperate to shape the sensory hair cell bundle. EMBO J 21, 6689-99 (2002).

20. Bork, J.M. et al. Usher syndrome 1D and nonsyndromic autosomal recessive deafness DFNB12 are caused by allelic mutations of the novel cadherin-like gene CDH23. Am J Hum Genet 68, 26-37 (2001).

21. Buchner, J., Grallert, H. & Jakob, U. Analysis of chaperone function using citrate synthase as nonnative substrate protein. Methods Enzymol 290, 323-38 (1998).

22. Catchen, J.M., Conery, J.S. & Postlethwait, J.H. Automated identification of conserved synteny after whole-genome duplication. Genome Res 19, 1497-505 (2009).

23. Chacon-Heszele, M.F. & Chen, P. Mouse models for dissecting vertebrate planar cell polarity signaling in the inner ear. Brain Res 1277, 130-40 (2009).

24. Chow, L.M. et al. Inducible Cre recombinase activity in mouse cerebellar granule cell precursors and inner ear hair cells. Dev Dyn 235, 2991-8 (2006).

25. Curtin, J.A. et al. Mutation of Celsr1 disrupts planar polarity of inner ear hair cells and causes severe neural tube defects in the mouse. Curr Biol 13, 1129-33 (2003).

26. Dallos, P. The Auditory Periphery: Biophysics and Physiology, 548 (Academic PR, 1973).

27. Daudet, N. & Lebart, M.C. Transient expression of the t-isoform of plastins/fimbrin in the stereocilia of developing auditory hair cells. Cell Motil Cytoskeleton 53, 326-36 (2002).

28. Davis, R.R. et al. Genetic basis for susceptibility to noise-induced hearing loss in mice. Hear Res 155, 82-90 (2001).

29. Dehal, P. & Boore, J.L. Two rounds of whole genome duplication in the ancestral vertebrate. PLoS Biol 3, e314 (2005).

30. Deol, M.S. The anatomy and development of the mutants pirouette, shaker-1 and waltzer in the mouse. Proc R Soc Lond B Biol Sci 145, 206-13 (1956).

31. Dickie, M.M. & Woolley, G.W. Linkage studies with the pirouette gene in the mouse. J Hered 37, 335-7 (1946).

32. Dror, A.A. & Avraham, K.B. Hearing loss: mechanisms revealed by genetics and cell biology. Annu Rev Genet 43, 411-37 (2009).

33. Du, X. et al. A catechol-O-methyltransferase that is essential for auditory function in mice and humans. Proc Natl Acad Sci U S A 105, 14609-14 (2008).

34. Erven, A. et al. A novel stereocilia defect in sensory hair cells of the deaf mouse mutant Tasmanian devil. Eur J Neurosci 16, 1433-41 (2002).

35. Fanto, M. & McNeill, H. Planar polarity from flies to vertebrates. J Cell Sci 117, 527-33 (2004).

36. Flock, A., Bretscher, A. & Weber, K. Immunohistochemical localization of several cytoskeletal proteins in inner ear sensory and supporting cells. Hear Res 7, 75-89 (1982).

37. Flock, A. & Cheung, H.C. Actin filaments in sensory hairs of inner ear receptor cells. J Cell Biol 75, 339-43 (1977).

38. Fritzsch, B., Pauley, S. & Beisel, K.W. Cells, molecules and morphogenesis: the making of the vertebrate ear. Brain Res 1091, 151-71 (2006).

39. Geleoc, G.S. & Holt, J.R. Developmental acquisition of sensory transduction in hair cells of the mouse inner ear. Nat Neurosci 6, 1019-20 (2003).

40. Geller, S.F. et al. CLRN1 is nonessential in the mouse retina but is required for cochlear hair cell development. PLoS Genet 5, e1000607 (2009).

41. Gibson, F. et al. A type VII myosin encoded by the mouse deafness gene shaker-1. Nature 374, 62-4 (1995).

42. Gillespie, P.G. & Muller, U. Mechanotransduction by hair cells: models, molecules, and mechanisms. Cell 139, 33-44 (2009).

43. Goodyear, R.J., Marcotti, W., Kros, C.J. & Richardson, G.P. Development and properties of stereociliary link types in hair cells of the mouse cochlea. J Comp Neurol 485, 75-85 (2005).

44. Grillet, N. et al. Harmonin mutations cause mechanotransduction defects in cochlear hair cells. Neuron 62, 375-87 (2009).

45. Grimsley-Myers, C.M., Sipe, C.W., Geleoc, G.S. & Lu, X. The small GTPase Rac1 regulates auditory hair cell morphogenesis. J Neurosci 29, 15859-69 (2009).

46. Halsey, K., Skjonsberg, A., Ulfendahl, M. & Dolan, D.F. Efferent-mediated adaptation of the DPOAE as a predictor of aminoglycoside toxicity. Hear Res 201, 99-108 (2005).

47. Hoffmann, B. et al. The multidomain thioredoxin-monothiol glutaredoxins represent a distinct functional group. Antioxid Redox Signal 15, 19-30.

48. Holme, R.H., Kiernan, B.W., Brown, S.D. & Steel, K.P. Elongation of hair cell stereocilia is defective in the mouse mutant whirler. J Comp Neurol 450, 94-102 (2002).

49. Holmgren, A. Antioxidant function of thioredoxin and glutaredoxin systems. Antioxid Redox Signal 2, 811-20 (2000).

50. Holmgren, A., Soderberg, B.O., Eklund, H. & Branden, C.I. Three-dimensional structure of Escherichia coli thioredoxin-S2 to 2.8 A resolution. Proc Natl Acad Sci U S A 72, 2305-9 (1975).

51. Jagger, D. et al. Alstrom Syndrome protein ALMS1 localizes to basal bodies of cochlear hair cells and regulates cilium-dependent planar cell polarity. Hum Mol Genet 20, 466-81.

52. Jeong, D. et al. PICOT attenuates cardiac hypertrophy by disrupting calcineurin-NFAT signaling. Circ Res 102, 711-9 (2008).

53. Johnson, K.R. et al. Mouse models of USH1C and DFNB18: phenotypic and molecular analyses of two new spontaneous mutations of the Ush1c gene. Hum Mol Genet 12, 3075-86 (2003).

54. Johnson, K.R., Zheng, Q.Y. & Noben-Trauth, K. Strain background effects and genetic modifiers of hearing in mice. Brain Res 1091, 79-88 (2006).

55. Jones, C. et al. Ciliary proteins link basal body polarization to planar cell polarity regulation. Nat Genet 40, 69-77 (2008).

56. Kadota, A. et al. Short actin-based mechanism for light-directed chloroplast movement in Arabidopsis. Proc Natl Acad Sci U S A 106, 13106-11 (2009).

57. Kaltenbach, J.A., Falzarano, P.R. & Simpson, T.H. Postnatal development of the hamster cochlea. II. Growth and differentiation of stereocilia bundles. J Comp Neurol 350, 187-98 (1994).

58. Karolyi, I.J. et al. Myo15 function is distinct from Myo6, Myo7a and pirouette genes in development of cochlear stereocilia. Hum Mol Genet 12, 2797-805 (2003).

59. Kazmierczak, P. et al. Cadherin 23 and protocadherin 15 interact to form tip-link filaments in sensory hair cells. Nature 449, 87-91 (2007).

60. Keen, J.A. A note on the comparative size of the cochlear canal in mammals. J Anat 73, 592-6 (1939).

61. Kemp, D.T. Stimulated acoustic emissions from within the human auditory system. J Acoust Soc Am 64, 1386-91 (1978).

62. Kern, R., Malki, A., Holmgren, A. & Richarme, G. Chaperone properties of Escherichia coli thioredoxin and thioredoxin reductase. Biochem J 371, 965-72 (2003).

63. Khan, S.Y. et al. Mutations of the RDX gene cause nonsyndromic hearing loss at the DFNB24 locus. Hum Mutat 28, 417-23 (2007).

64. Kitajiri, S. et al. Radixin deficiency causes deafness associated with progressive degeneration of cochlear stereocilia. J Cell Biol 166, 559-70 (2004).

65. Kochhar, A., Hildebrand, M.S. & Smith, R.J. Clinical aspects of hereditary hearing loss. Genet Med 9, 393-408 (2007).

66. Lagziel, A. et al. Spatiotemporal pattern and isoforms of cadherin 23 in wild type and waltzer mice during inner ear hair cell development. Dev Biol 280, 295-306 (2005).

67. Lagziel, A. et al. Expression of cadherin 23 isoforms is not conserved: implications for a mouse model of Usher syndrome type 1D. Mol Vis 15, 1843-57 (2009).

68. Laity, J.H., Lee, B.M. & Wright, P.E. Zinc finger proteins: new insights into structural and functional diversity. Curr Opin Struct Biol 11, 39-46 (2001).

69. Lane, P.W. Linkage groups 3 and XVII in the mouse and the position of the light-ear locus. J Hered 58, 21-4 (1967).

70. Lefevre, G. et al. A core cochlear phenotype in USH1 mouse mutants implicates fibrous links of the hair bundle in its cohesion, orientation and differential growth. Development 135, 1427-37 (2008).

71. Les Erickson, F., Corsa, A.C., Dose, A.C. & Burnside, B. Localization of a class III myosin to filopodia tips in transfected HeLa cells requires an actin-binding site in its tail domain. Mol Biol Cell 14, 4173-80 (2003).

72. Levasseur, A. & Pontarotti, P. The role of duplications in the evolution of genomes highlights the need for evolutionary-based approaches in comparative genomics. Biol Direct 6, 11.

73. Lillig, C.H., Berndt, C. & Holmgren, A. Glutaredoxin systems. Biochim Biophys Acta 1780, 1304-17 (2008).

74. Lim, D.J. & Anniko, M. Developmental morphology of the mouse inner ear. A scanning electron microscopic observation. Acta Otolaryngol Suppl 422, 1-69 (1985).

75. Lin, H.W., Schneider, M.E. & Kachar, B. When size matters: the dynamic regulation of stereocilia lengths. Curr Opin Cell Biol 17, 55-61 (2005).

76. Liu, X.Z. et al. Autosomal dominant non-syndromic deafness caused by a mutation in the myosin VIIA gene. Nat Genet 17, 268-9 (1997).

77. Loomis, P.A. et al. Espin cross-links cause the elongation of microvillus-type parallel actin bundles in vivo. J Cell Biol 163, 1045-55 (2003).

78. Lou, X., Bao, R., Zhou, C.Z. & Chen, Y. Structure of the thioredoxin-fold domain of human phosducin-like protein 2. Acta Crystallogr Sect F Struct Biol Cryst Commun 65, 67-70 (2009).

79. Machold, R. & Fishell, G. Math1 is expressed in temporally discrete pools of cerebellar rhombic-lip neural progenitors. Neuron 48, 17-24 (2005).

80. Maly, I.V. & Borisy, G.G. Self-organization of a propulsive actin network as an evolutionary process. Proc Natl Acad Sci U S A 98, 11324-9 (2001).

81. Manor, U. et al. Regulation of stereocilia length by myosin XVa and whirlin depends on the actin-regulatory protein Eps8. Curr Biol 21, 167-72 (2011).

82. Mburu, P. et al. Defects in whirlin, a PDZ domain molecule involved in stereocilia elongation, cause deafness in the whirler mouse and families with DFNB31. Nat Genet (2003).

83. Mburu, P. et al. Gelsolin plays a role in the actin polymerization complex of hair cell stereocilia. PLoS One 5, e11627 (2010).

84. McCormack, E.A., Altschuler, G.M., Dekker, C., Filmore, H. & Willison, K.R. Yeast phosducin-like protein 2 acts as a stimulatory co-factor for the folding of actin by the chaperonin CCT via a ternary complex. J Mol Biol 391, 192-206 (2009).

85. McGee, D.J. et al. Helicobacter pylori thioredoxin is an arginase chaperone and guardian against oxidative and nitrosative stresses. J Biol Chem 281, 3290-6 (2006).

86. McHugh, R.K. & Friedman, R.A. Genetics of hearing loss: Allelism and modifier genes produce a phenotypic continuum. Anat Rec A Discov Mol Cell Evol Biol 288, 370-81 (2006).

87. Meyer, A. & Schartl, M. Gene and genome duplications in vertebrates: the one-to-four (-to-eight in fish) rule and the evolution of novel gene functions. Curr Opin Cell Biol 11, 699-704 (1999).

88. Meyer, Y., Buchanan, B.B., Vignols, F. & Reichheld, J.P. Thioredoxins and glutaredoxins: unifying elements in redox biology. Annu Rev Genet 43, 335-67 (2009).

89. Michel, V. et al. Cadherin 23 is a component of the transient lateral links in the developing hair bundles of cochlear sensory cells. Dev Biol 280, 281-94 (2005).

90. Mitchem, K.L. et al. Mutation of the novel gene Tmie results in sensory cell defects in the inner ear of spinner, a mouse model of human hearing loss DFNB6. Hum Mol Genet 11, 1887-98 (2002).

91. Mogensen, M.M., Rzadzinska, A. & Steel, K.P. The deaf mouse mutant whirler suggests a role for whirlin in actin filament dynamics and stereocilia development. Cell Motil Cytoskeleton 64, 496-508 (2007).

92. Montcouquiol, M. et al. Identification of Vangl2 and Scrb1 as planar polarity genes in mammals. Nature 423, 173-7 (2003).

93. Muller, U. Cadherins and mechanotransduction by hair cells. Curr Opin Cell Biol 20, 557-66 (2008).

94. Mustapha, M. et al. Deafness and permanently reduced potassium channel gene expression and function in hypothyroid Pit1dw mutants. J Neurosci 29, 1212-23 (2009).

95. Nagy, A. et al. Dissecting the role of N-myc in development using a single targeting vector to generate a series of alleles. Curr Biol 8, 661-4 (1998).

96. Nayak, G.D., Ratnayaka, H.S., Goodyear, R.J. & Richardson, G.P. Development of the hair bundle and mechanotransduction. Int J Dev Biol 51, 597-608 (2007).

97. Naz, S. et al. Mutations in a novel gene, TMIE, are associated with hearing loss linked to the DFNB6 locus. Am J Hum Genet 71, 632-6 (2002).

98. Nei, M. Probability of fixation of nonfunctional genes at duplicate loci. Am. Nat. 107, 362-372 (1973).

99. Noben-Trauth, K. & Johnson, K.R. Inheritance patterns of progressive hearing loss in laboratory strains of mice. Brain Res 1277, 42-51 (2009).

100. Noben-Trauth, K., Zheng, Q.Y. & Johnson, K.R. Association of cadherin 23 with polygenic inheritance and genetic modification of sensorineural hearing loss. Nat Genet 35, 21-3 (2003).

101. Odeh, H. et al. Characterization of two transgene insertional mutations at pirouette, a mouse deafness locus. Audiol Neurootol 9, 303-14 (2004).

102. Odeh, H. et al. Mutations in Grxcr1 are the basis for inner ear dysfunction in the pirouette mouse. Am J Hum Genet 86, 148-60 (2010).

103. Osborne, M.P. & Comis, S.D. Preparation of inner ear sensory hair bundles for high resolution scanning electron microscopy. Scanning Microsc 5, 555-64 (1991).

104. Pan, J.L. & Bardwell, J.C. The origami of thioredoxin-like folds. Protein Sci 15, 2217-27 (2006).

105. Park, T.J., Haigo, S.L. & Wallingford, J.B. Ciliogenesis defects in embryos lacking inturned or fuzzy function are associated with failure of planar cell polarity and Hedgehog signaling. Nat Genet 38, 303-11 (2006).

106. Peng, A.W., Belyantseva, I.A., Hsu, P.D., Friedman, T.B. & Heller, S. Twinfilin 2 regulates actin filament lengths in cochlear stereocilia. J Neurosci 29, 15083-8 (2009).

107. Perrin, B.J., Sonnemann, K.J. & Ervasti, J.M. beta-actin and gamma-actin are each dispensable for auditory hair cell development but required for Stereocilia maintenance. PLoS Genet 6, e1001158 (2010).

108. Petit, C. & Richardson, G.P. Linking genes underlying deafness to hair-bundle development and function. Nat Neurosci 12, 703-10 (2009).

109. Pickles, J.O., Billieux-Hawkins, D.A. & Rouse, G.W. The incorporation and turnover of radiolabelled amino acids in developing stereocilia of the chick cochlea. Hear Res 101, 45-54 (1996).

110. Pickles, J.O. et al. The organization of tip links and stereocilia on hair cells of bird and lizard basilar papillae. Hear Res 41, 31-41 (1989).

111. Pickles, J.O., Comis, S.D. & Osborne, M.P. Cross-links between stereocilia in the guinea pig organ of Corti, and their possible relation to sensory transduction. Hear Res 15, 103-12 (1984).

112. Probst, F.J. et al. Correction of deafness in shaker-2 mice by an unconventional myosin in a BAC transgene. Science 280, 1444-7. (1998).

113. Prosser, H.M., Rzadzinska, A.K., Steel, K.P. & Bradley, A. Mosaic complementation demonstrates a regulatory role for myosin VIIa in actin dynamics of stereocilia. Mol Cell Biol 28, 1702-12 (2008).

114. Pujol-Carrion, N. & de la Torre-Ruiz, M.A. Glutaredoxins Grx4 and Grx3 of Saccharomyces cerevisiae play a role in actin dynamics through their Trx domains, which contributes to oxidative stress resistance. Appl Environ Microbiol 76, 7826-35 (2010).

115. Revenu, C., Athman, R., Robine, S. & Louvard, D. The co-workers of actin filaments: from cell structures to signals. Nat Rev Mol Cell Biol 5, 635-46 (2004).

116. Rida, P.C. & Chen, P. Line up and listen: Planar cell polarity regulation in the mammalian inner ear. Semin Cell Dev Biol 20, 978-85 (2009).

117. Ross, A.J. et al. Disruption of Bardet-Biedl syndrome ciliary proteins perturbs planar cell polarity in vertebrates. Nat Genet 37, 1135-40 (2005).

118. Rzadzinska, A., Schneider, M., Noben-Trauth, K., Bartles, J.R. & Kachar, B. Balanced levels of Espin are critical for stereociliary growth and length maintenance. Cell Motil Cytoskeleton 62, 157-65 (2005).

119. Rzadzinska, A.K., Derr, A., Kachar, B. & Noben-Trauth, K. Sustained cadherin 23 expression in young and adult cochlea of normal and hearing-impaired mice. Hear Res 208, 114-21 (2005).

120. Rzadzinska, A.K., Nevalainen, E.M., Prosser, H.M., Lappalainen, P. & Steel, K.P. MyosinVIIa interacts with Twinfilin-2 at the tips of mechanosensory stereocilia in the inner ear. PLoS One 4, e7097 (2009).

121. Schneider, M.E., Belyantseva, I.A., Azevedo, R.B. & Kachar, B. Rapid renewal of auditory hair bundles. Nature 418, 837-8 (2002).

122. Schraders, M. et al. Homozygosity mapping reveals mutations of GRXCR1 as a cause of autosomal-recessive nonsyndromic hearing impairment. Am J Hum Genet 86, 138-47.

123. Schwander, M., Kachar, B. & Muller, U. Review series: The cell biology of hearing. J Cell Biol 190, 9-20 (2010).

124. Schwander, M. et al. A mouse model for nonsyndromic deafness (DFNB12) links hearing loss to defects in tip links of mechanosensory hair cells. Proc Natl Acad Sci U S A 106, 5252-7 (2009).

125. Sekerkova, G., Richter, C.P. & Bartles, J.R. Roles of the espin actin-bundling proteins in the morphogenesis and stabilization of hair cell stereocilia revealed in CBA/CaJ congenic jerker mice. PLoS Genet 7, e1002032 (2011).

126. Senften, M. et al. Physical and functional interaction between protocadherin 15 and myosin VIIa in mechanosensory hair cells. J Neurosci 26, 2060-71 (2006).

127. Shin, J.B., Pagana, J. & Gillespie, P.G. Twist-off purification of hair bundles. Methods Mol Biol 493, 241-55 (2009).

128. Shin, J.B. et al. Hair bundles are specialized for ATP delivery via creatine kinase. Neuron 53, 371-86 (2007).

129. Siemens, J. et al. Cadherin 23 is a component of the tip link in hair-cell stereocilia. Nature 428, 950-5 (2004).

130. Sipe, C.W. & Lu, X. Kif3a regulates planar polarization of auditory hair cells through both ciliary and non-ciliary mechanisms. Development 138, 3441-9.

131. Sobkowicz, H.M., Slapnick, S.M. & August, B.K. The kinocilium of auditory hair cells and evidence for its morphogenetic role during the regeneration of stereocilia and cuticular plates. J Neurocytol 24, 633-53 (1995).

132. Stepanyan, R., Belyantseva, I.A., Griffith, A.J., Friedman, T.B. & Frolenkov, G.I. Auditory mechanotransduction in the absence of functional myosin-XVa. J Physiol 576, 801-8 (2006).

133. Stepanyan, R. & Frolenkov, G.I. Fast adaptation and Ca2+ sensitivity of the mechanotransducer require myosin-XVa in inner but not outer cochlear hair cells. J Neurosci 29, 4023-34 (2009).

134. Stone, I.M., Lurie, D.I., Kelley, M.W. & Poulsen, D.J. Adeno-associated virus-mediated gene transfer to hair cells and support cells of the murine cochlea. Mol Ther 11, 843-8 (2005).

135. Suetsugu, N. et al. Two kinesin-like proteins mediate actin-based chloroplast movement in Arabidopsis thaliana. Proc Natl Acad Sci U S A 107, 8860-5.

136. Sun, S.X. & Walcott, S. Actin crosslinkers: repairing the sense of touch. Curr Biol 20, R895-6.

137. Tilney, L.G. & DeRosier, D.J. Actin filaments, stereocilia, and hair cells of the bird cochlea. IV. How the actin filaments become organized in developing stereocilia and in the cuticular plate. Dev Biol 116, 119-29 (1986).

138. Tilney, L.G. & Tilney, M.S. Functional organization of the cytoskeleton. Hear Res 22, 55-77 (1986).

139. Tilney, L.G., Tilney, M.S., Saunders, J.S. & DeRosier, D.J. Actin filaments, stereocilia, and hair cells of the bird cochlea. III. The development and differentiation of hair cells and stereocilia. Dev Biol 116, 100-18 (1986).

140. Tyska, M.J. & Mooseker, M.S. MYO1A (brush border myosin I) dynamics in the brush border of LLC-PK1-CL4 cells. Biophys J 82, 1869-83 (2002).

141. Van Laer, L., Cryns, K., Smith, R.J. & Van Camp, G. Nonsyndromic hearing loss. Ear Hear 24, 275-88 (2003).

142. van Wijk, E. et al. A mutation in the gamma actin 1 (ACTG1) gene causes autosomal dominant hearing loss (DFNA20/26). J Med Genet 40, 879-84 (2003).

143. Vos, M.J., Hageman, J., Carra, S. & Kampinga, H.H. Structural and functional diversities between members of the human HSPB, HSPH, HSPA, and DNAJ chaperone families. Biochemistry 47, 7001-11 (2008).

144. Wang, J. et al. Reversible glutathionylation regulates actin polymerization in A431 cells. J Biol Chem 276, 47763-6 (2001).

145. Weil, D. et al. Usher syndrome type I G (USH1G) is caused by mutations in the gene encoding SANS, a protein that associates with the USH1C protein, harmonin. Hum Mol Genet 12, 463-71 (2003).

146. Whippo, C.W. et al. THRUMIN1 is a light-regulated actin-bundling protein involved in chloroplast motility. Curr Biol 21, 59-64.

147. Woolley, G.W. & Dickie, M.M. Pirouetting mice. Journal of Heredity 36, 281-284 (1945).

148. Yamamoto, S. et al. Cthrc1 selectively activates the planar cell polarity pathway of Wnt signaling by stabilizing the Wnt-receptor complex. Dev Cell 15, 23-36 (2008).

149. Zheng, L. et al. The deaf jerker mouse has a mutation in the gene encoding the espin actin-bundling proteins of hair cell stereocilia and lacks espins. Cell 102, 377-85 (2000).

150. Zheng, L., Zheng, J., Whitlon, D.S., Garcia-Anoveros, J. & Bartles, J.R. Targeting of the hair cell proteins cadherin 23, harmonin, myosin XVa, espin, and prestin in an epithelial cell model. J Neurosci 30, 7187-201 (2010).

151. Zhou, Q., Gedrich, R.W. & Engel, D.A. Transcriptional repression of the c-fos gene by YY1 is mediated by a direct interaction with ATF/CREB. J Virol 69, 4323-30 (1995).

152. Zhu, M. et al. Mutations in the gamma-actin gene (ACTG1) are associated with dominant progressive deafness (DFNA20/26). Am J Hum Genet 73, 1082-91 (2003).

153. Zine, A. & Romand, R. Development of the auditory receptors of the rat: a SEM study. Brain Res 721, 49-58 (1996).